IN-VIVO MULTIPHOTON EXCITED FLUORESCENCE MICROSCOPY OF THE SPINAL CORD

A Dissertation

Presented to the Faculty of the Graduate School

of Cornell University

In Partial Fulfillment of the Requirements for the Degree of

Doctor of Philosophy

by

Sally Anne Lenore DeNotta

December 2018

IN-VIVO MULTIPHOTON EXCITED FLUORESCENCE MICROSCOPY OF THE SPINAL CORD

Sally Anne Lenore DeNotta, Ph. D., DVM

Cornell University 2018

Spinal cord disorders are frequent causes of morbidity and mortality in human and veterinary medicine alike. Despite spinal cord disease affecting nearly every vertebrate species on earth, the pathophysiological mechanisms of central nervous system (CNS) disease remain poorly understood, largely due to failure of traditional ex-vivo imaging methods to capture the dynamic nature of complex neurophysiologic interactions. To address this, we have developed novel optical techniques for high-resolution, in-vivo imaging of the spinal cord in rodent models. This dissertation details novel methods for two-photon excited fluorescence (2PEF) microscopy of the spinal cord that enable direct observation of the cellular interactions occurring during health and disease. Specifically, we have developed surgical procedures that allow long term optical access in multiple regions of the mouse spinal cord, optimized labeling strategies for multicolor fluorescent *in vivo* imaging of cellular interactions, demonstrated successful recording of real-time calcium transients and neural activity from populations of sensory and motor neurons in the rodent spinal cord, explored and refined established models of SCI and neuropathic pain to make them suitable for serial imaging of axonal dynamics,

inflammatory responses, and alterations in neural circuitry, designed and custom built a treadmill system on which a mouse can walk and run while spine-fixed under a multiphoton microscope, and implemented a recording system for capturing video of spine-fixed, running mice from which 3D spatiotemporal positioning of limbs can be measured and ultimately integrated into a comprehensive kinematic gait analysis system. Finally, we discuss the current capabilities and limitations of 2PEF microscopy for spinal cord imaging, and introduce ongoing initiatives and the inevitable transition to the next generation of multiphoton microscopy, three-photon excited fluorescence (3PEF), as a way to overcome the current challenges to 2PEF and further drive spinal cord research into the future.

BIOGRAPHICAL SKETCH

Sally grew up on the rural Oregon coast and received her veterinary degree from Oregon State University in 2005. After completing an internship at Littleton Equine Medicine Center in Colorado, she spent time in private practice in Oregon before moving to New York for an internal medicine residency at the Cornell University College of Veterinary Medicine. She became board-certified by the American College of Veterinary Internal Medicine in 2013, after which she served on the clinical faculty at Cornell and conducted clinical research in coagulation, neonatology, infectious disease, and colic. In 2014, through a Morris Animal Health Fellowship for Advanced Study, she joined the Schaffer Laboratory to pursue a PhD within the college of Biological and Biomedical Sciences. Within the Schaffer Lab, her graduate work focused on developing novel in-vivo imaging techniques for elucidating mechanisms of spinal cord disease and repair. Following her PhD, Sally will relocate to Gainesville, Florida to join the College of Veterinary Medicine faculty as a Clinical Assistant Professor of Large Animal Medicine and Equine Veterinary Extension Coordinator.

For Alan,

Who has reminded me a thousand times; through research you don't just help one patient, you help them all.

Or maybe he just said that clinics eventually get bloody boring and one should strive to make a bigger impact on the world than just an endless string of sick horses

I can't remember.

ACKNOWLEDGMENTS

First and foremost, I would like to thank the Morris Animal Foundation for their tremendous support of my graduate program. The advanced training I have received through their fellowship in scientific design, critical thinking, grantsmanship, and research technique will be invaluable to my career as an academic veterinarian and clinician scientist.

I would like to thank Chris Schaffer for his mentorship and guidance throughout my program. The transition from clinician to graduate student was not without difficulty, and Chris's willingness to introduce a horse vet to the world of optics provided me a whole new skill set and level of appreciation for the countless labs that day-in and day-out work to push science forward. More than anything, I will take with me lessons learned by observing Chris in his roles as an administrator and leader, and will emulate his methods in management, professionalism, and negotiation throughout my career.

The "Spinal Cord Project" has in no way been a solitary effort, and Yu Ting Cheng, my fellow graduate student and spinal cord team member, deserves much recognition for his contributions to the work presented here. His countless hours, perpetually heightened stress level, and ability to see the humor in spending all hours of the day in a basement chasing after mice with lasers, will in no doubt make him an excellent researcher and scientist, and I was dang lucky to have known and worked with him for the past 4 years. Thanks YT, and high-five. Best of luck in all that you do.

I would like to thank my committee members, Andrew Miller, Robin Dando, and Sergiy Libert, for their input on my research topic as well as their availability and flexibility throughout my graduate program.

Lastly, I need to thank my family, for without their support the last 4 years simply would not have happened. Dad, Julia, Joe, Anthony, Charlie; for so many reasons on so many days, thank you so, so much.

TABLE OF CONTENTS

Biographical sketch……..…….iii

Acknowledgements…….……...….v

Table of Contents……...…vii

List of Figures…….…x

List of Abbreviations……...…xiii

CHAPTER 1: INTRODUCTION AND DISSERTATION ORGANIZATION…..1

Introduction…….2

Dissertation Organization……...3

CHAPTER 2: THE SPINAL CORD IN HEALTH AND DISEASE……...…7

The Spinal Cord: Structure and Function……...……8

Mechanisms of Spinal Cord Injury…….……..13

Therapeutic Options and Clinical Outcomes in Spinal Cord Injury Patients...20

Neuropathic Pain……...22

Clinical Management of Neuropathic Pain……...…23

Questions in Spinal Cord Repair and the Need for *In Vivo* Imaging...…..……23

References……...……..25

CHAPTER 3: TWO-PHOTON EXCITED FLUORESCENCE MICROSCOPY……...28

Fluorescent Microscopy……..…….…….29

Two-Photon Excitation……...……..31

Two-Photon Excited Fluorescence Microscope Set Up……..…….37

References……..……41

CHAPTER 4: *IN VIVO* TWO-PHOTON EXCITED FLUORESCENCE MICROSCOPY OF THE INJURED SPINAL CORD……42

Spinal Cord Injury Research in Mice: Models of Injury and Traditional Research Tools…….…….43

Spinal Cord Fluorescent Labeling Strategies ……..…….47

Implanted Imaging Chambers Provide Long Term Optical Access to the Spinal Cord……...50

In Vivo Two-Photon Excited Fluorescence Imaging of The Injured Spinal Cord Reveals Real-Time Cellular Interactions…….…….59

References……...…..73

CHAPTER 5: *IN VIVO* TWO-PHOTON EXCITED FLUORESCENCE MICROSCOPY IN A NEUROPATHIC PAIN MODEL……74

Neuropathic Pain Research in Mice: Models of Injury and Assessment…..…75

In Vivo Two-Photon Excited Fluorescence Imaging in a Model of Neuropathic Pain Reveals Microglial-Mediated Inflammation……..…79

References……...……..86

CHAPTER 6: FUNCTIONAL SPINAL CORD IMAGING……...……87

Spinal Cord Circuitry……...….89

Genetically-Encoded Calcium Indicators Enable Imaging of Neural Activity 90

Treadmill-Based System Enables 2PEF Microscopy in Awake, Locomoting Mice……..……96

References…….……..105

CHAPTER 7: THE FUTURE OF MULTIPHOTON IN VIVO IMAGING…...107

Limitations to Two-Photon Excited Fluorescence Microscopy in the Spinal Cord……109

Into the Future: Three-Photon Excited Fluorescence Microscopy for Deeper, Higher Resolution *In Vivo* Imaging of the Spinal Cord……..……113

References…….……..121

LIST OF FIGURES

CHAPTER 2

Fig. 2.1 Cross sectional anatomy of the spinal cord.……...……11

Fig. 2.2 Functional organization of the spinal cord……..…….…..12

Fig. 2.3 Mechanisms and phases of spinal cord injury (SCI)..……15

Fig. 2.4 Astrogliosis in response to SCI……...19

CHAPTER 3

Fig. 3.1 Nonlinear absorption and excitation……...34

Fig. 3.2 Localization of excitation by two-photon excitation…….…….35

Fig. 3.3 Schematic of a multi-photon microscopy system.……...……40

CHAPTER 4

Fig. 4.1 2PEF Spectral Diagram.……..……..……..49

Fig. 4.2 Implanted optical imaging chamber …….…….51

Fig. 4.3 Lumbar chamber surgery.……53

Fig. 4.4 Mouse vertebral formula……....54

Fig. 4.5 Chamber plate attachment to lumbar spine ……..…….56

Fig. 4.6 Lumbar chamber placement……..…….58

Fig. 4.7 2PEF microscopy image enables in vivo imaging of spinal cord structure…….60

Fig. 4.8 2PEF microscopy image demonstrates widespread post-operative

microglial influx ……..……62

Fig. 4.9 2PEF microscopy image of axonal dynamics…….……63

Fig. 4.10 2PEF microscopy of dorsal roots and spinocerebellar tracts……64

Fig. 4.11 Crush injury induces hemorrhage and bruising.……66

Fig. 4.12 2PEF microscopy following crush injury……..…67

Fig. 4.13: Axonal fragmentation and prolonged die back following unilateral dorsal hemisection.…….……69

Fig. 4.14 Cellular interactions mediating thrombus formation, phagocytosis and angiogenesis following unilateral dorsal hemisection.……71

CHAPTER 5

Fig. 5.1 Models of peripheral nerve injuries in rodents……..……77

Fig. 5.2 Spared nerve injury (SNI) surgical procedure……..…. 78

Fig. 5.3 Assessment for neuropathic pain following SNI……..…….81

Fig. 5.4 Microglial inflammation in the dorsal spinal cord following SNI….82

Fig. 5.5 Microglial activation and dendritic morphology in response to SNI 85

CHAPTER 6

Fig. 6.1 Crystal structure of GCaMP…….. 92

Fig. 6.2 2PEF microscopy of spontaneous excitatory neural activity……..94

Fig. 6.3 2PEF microscopy reveals altered spinal cord neural activity in a mouse model of neuropathic pain.……95

Fig. 6.4 Treadmill system for awake 2PEF imaging.……97

Fig. 6.5 Mouse treadmill training.……..…….100

Fig. 6.6 Behavioral parameters in spine-fixed mice……..……101

Fig. 6.7 Minimal motion artifact is observed in running mice during 2PEF imaging.……..……..102

Fig. 6.8 Gait analysis system.……104

CHAPTER 7

Fig 7.1 Optical impedance in chronically implanted mice spinal cords…....110

Fig 7.2 Generalized microglial-mediated inflammation following spinal imaging chamber implantation.……..…..112

Fig. 7.3 3PEF microscopy enables deeper imaging of the spinal cord ….....116

Fig. 7.4 3PEF microscopy enables deeper imaging of the spinal cord ……..117

Fig. 7.5 RCaMP calcium transients in an awake, locomoting mouse……119

LIST OF ABBREVIATIONS

2PEF	two-photon excited fluorescence
3PEF	three-photon excited fluorescence
AAV	adeno-associated virus
BBB	Basso, Beattie and Bresnahan
BMS	Basso Mouse Scale
CaM	calmodulin
CaMKII	Ca^{+}/calmodulin-dependent protein kinase II
CNS	central nervous system
CPG	central pattern generator
CSF	cerebrospinal fluid
CSPG	chondroitin sulfate proteoglycans
DRG	dorsal root ganglion
GECI	Genetically encoded calcium indicator
GFP	green fluorescent protein
IR	infrared
PNS	peripheral nervous system
RFP	red fluorescent protein
SCI	spinal cord injury
SNI	spared nerve injury
YPF	yellow fluorescent protein

CHAPTER 1

INTRODUCTION AND DISSERTATION ORGANIZATION

INTRODUCTION

Spinal cord disorders are frequent causes of morbidity and mortality in human and veterinary medicine alike. Despite spinal cord disease affecting nearly every vertebrate species on earth, the cellular interactions and neural circuitry that govern the central nervous system (CNS) in health and disease remain very poorly understood. As a consequence, humans and animals affected by spinal cord disease have limited therapeutic options and frequently suffer permanent loss of function.

In my career as an equine veterinarian, I am continually frustrated by the grim prognosis faced by my patients with neurologic disease; most of whom will ultimately be euthanized. I have been similarly dissatisfied by the poor diagnostic yield provided by clinical imaging techniques and post-mortem histology, which offer little information regarding the dynamic neurophysiologic processes occurring in our patients. In the research setting, traditional ex-vivo imaging methods similarly fail to capture the dynamic nature of complex neurophysiologic processes. Novel methods capable of capturing these complex cellular and electrophysiological interactions are crucial for gaining a deeper understanding of spinal cord pathophysiology and provide a foundation from which targeted therapeutic modalities can be developed.

To address this, in the Schaffer Lab we are developing novel optical techniques for high-resolution, in-vivo imaging of the spinal cord in rodent models. My graduate work has focused primarily on developing methods for two-photon excited fluorescence (2PEF) microscopy of the spinal cord to enable direct observation of the cellular interactions occurring during health and disease. Specifically, we have developed

surgical procedures that allow long term optical access in multiple regions of the mouse spinal cord, optimized labeling strategies for multicolor fluorescent *in vivo* imaging of cellular interactions, demonstrated successful recording of real-time calcium transients and neural activity from populations of sensory and motor neurons in the rodent spinal cord, explored and refined established models of SCI and neuropathic pain to make them suitable for serial imaging of axonal dynamics, inflammatory responses, and alterations in neural circuitry, designed and custom built a treadmill system on which a mouse can walk and run while spine-fixed under a multiphoton microscope, and implemented a recording system for capturing video of spine-fixed, running mice from which 3D spatiotemporal positioning of limbs can be measured and ultimately integrated into a comprehensive kinematic gait analysis system.

Looking ahead to my future in education and clinical veterinary medicine, I will take with me skills in optics and research garnered in the Schaffer Lab and apply them to a career bolstered by evidence-based medicine and relevant clinical research. I look forward to watching the ongoing research conducted in the Schaffer Lab continue to improve our understanding of central nervous system physiology and hopefully, in the near future, lead to improved treatment options and better outcomes for veterinary and human patients alike.

DISSERTATION ORGANIZATION

The work described in this dissertation includes the development of *in vivo,* high spatio-temporal resolution imaging technique to study the spinal cord in normal and

pathological states. We utilized these methods to examine the cellular dynamics of spinal cord injury as well as the neuroinflammatory response in a neuropathic pain model. In addition, we have ongoing development of methods for functional spinal cord imaging to enable observation of real-time neural activity in the spinal cord of awake, locomoting mice.

Chapter 2: Spinal cord disease represents a devastating spectrum of medical disorders for which there are few therapeutic options and frequently poor prognoses. This chapter provides an overview of spinal cord structure and function and a summary of two important clinical spinal cord disorders: SCI and neuropathic pain. Current knowledge regarding mechanisms of disease are provided, as well as a discussion of current therapeutic modalities and clinical outcomes.

Chapter 3: Nonlinear microscopy has become the technique of choice for imaging with sub-cellular resolution deep into scattering tissue in live animals, and has enabled immense progress to be made in studies of complex biological systems such as the brain and spinal cord. This chapter provide an overview of two-photon excited fluorescence (2PEF) by briefly reviewing fluorescence microscopy, two-photon excitation, and describing the 2PEF microscope setup.

Chapter 4: A fundamental challenge in the development of effective treatments for spinal cord injury is incomplete understanding of spinal cord pathophysiology, largely due to inability to study cellular mechanisms *in vivo*. This chapter details a suite of imaging tools in ongoing development that together enable deep, high resolution, in-vivo imaging of structure, cellular dynamics, and neural activity in the spinal cord and allow for longitudinal studies of spinal cord response to injury and disease. Examples of longitudinal imaging studies in rodent models of SCI are presented.

Chapter 5: Neuropathic pain represents a clinical conundrum for which there are few effective treatments and little consensus on underlying cellular mechanisms. In vivo imaging will be crucial for elucidating the complicated interplay between the acute inflammatory response and chronic spinal sensitization that work in concert to ultimately result in sensory dysfunction and neuropathic pain. This chapter reviews rodent models of neuropathic pain and demonstrates novel imaging methods for capturing the dynamic cellular responses occurring at the level of the spinal cord following peripheral nerve injury.

Chapter 6: Unravelling the functional organization of neuronal networks and linking cellular activity to behavioral outcomes are among the biggest challenges in contemporary neuroscience. Despite the importance of understanding how these circuits work and how they fail after spinal cord injury or in disease, there is no existing approach to directly measure the patterns of activity across a large ensemble

of spinal cord neurons in awake, moving animals. In this chapter, the currently knowledge gap in spinal cord circuitry is introduced, followed by novel imaging approaches we are developing that will enable neural activity to be directly visualized in the spinal cord of awake mice that are spine fixed under the microscope and able to move on a treadmill.

Chapter 7: Multiphoton excited fluorescence microscopy is providing insight into the fundamental mechanisms of spinal cord physiology in ways never before possible. This final chapter summarizes our broad findings thus far and discusses current capabilities and limitations of 2PEF microscopy for spinal cord imaging. Ongoing initiatives and the inevitable transition to the next generation of multiphoton microscopy, three-photon excited fluorescence (3PEF), are proposed as a way to overcome the current challenges to 2PEF and further drive spinal cord research into the future.

CHAPTER 2

THE SPINAL CORD IN HEALTH AND DISEASE

Figure acknowledgements:

Fig. 2.1 Cross section anatomy of the spinal cord
https://sensoryandnervous.files.wordpress.com/2013/05/12-30b_spinalcord_1.jpg
Copyright © 2004 Pearson Education, Inc., publishing as Benjamin Cummings

Fig. 2.2 General scheme of the human spinal cord
http://www.daviddarling.info/encyclopedia/S/spinal_cord.html
Copyright © 2016 Dorling-Kindersley

Fig. 2.3 The mechanism of spinal cord injury (SCI). Demonstration of various phases of SCI after trauma to the spinal cord
Quadri, S.A., Farooqui, M., Ikram, A. et al. Recent update on basic mechanisms of spinal cord injury. Neurosurg Rev (2018). https://doi-org.proxy.library.cornell.edu/10.1007/s10143-018-1008-3.

Fig. 2.4 Glial scar formation after the spinal cord injury at the site of impact, leading to recruitment of immune cells
Quadri, S.A., Farooqui, M., Ikram, A. et al. Recent update on basic mechanisms of spinal cord injury. Neurosurg Rev (2018). https://doi-org.proxy.library.cornell.edu/10.1007/s10143-018-1008-3.

Spinal cord injury (SCI) affects between 250,000 and 500,000 people each year and an estimated 2-3 million people are living with SCI worldwide. In the United States alone, the the economic impact of SCI is estimated to be more than 4 billion dollars annually (Varma 2013). Motor vehicle accidents represent the primary cause of SCI in the western world, whereas violence is a primary cause of SCI in developing countries. Males are at 2-5 times greater risk for incurring SCI, as are young adults of both sexes. The regenerative capacity of the spinal cord is poor and complete recovery from SCI is rare, with the majority of patients suffering some degree of neurologic impairment for the remainder of their lives (Quadri 2018). In addition to the sensory and motor deficits frequently observed in SCI patients, many will additionally develop some degree of neuropathic pain, a poorly understood disorder characterized by chronic, aberrant painful sensation poorly responsive to traditional analgesics.

This chapter provides an overview of spinal cord structure and function and a summary of two important clinical spinal cord disorders: SCI and neuropathic pain. Current knowledge regarding mechanisms of disease are provided, as well as a discussion of current therapeutic modalities and clinical outcomes.

THE SPINAL CORD: STRUCTURE AND FUNCTION

The spinal cord represents the portion of the central nervous system (CNS) caudal to the brain, and runs within the vertebral canal from the first cranial vertebrae to the lumbar spine in most species. The spinal cord functions as the conduit from the brain to the rest of the body, and is responsible for transmitting sensory, motor, and autonomic

information between the brain and peripheral nervous system (PNS). Unlike the brain, the spinal cord core is made up of gray matter (primarily neuronal cell bodies) surrounded circumferentially by layers of white matter myelinated axonal tracks running bidirectionally up and down the cord (**Fig. 2.1**). Organization of the spinal cord is similar across mammalian species and is functionally divided into the cervical, thoracic, lumbar, and sacral sections, based on the regions of the body innervated (**Fig. 2.2**). Intumescences (enlargements) within the thoracic and lumbar sections supply innervation to the thoracic and pelvic limbs, respectively. Surrounding the spinal cord are three outer membranes, the dura mater, arachnoid, and innermost pia mater. Cerebrospinal fluid produced by the choroid plexus within the ventricular system of the brain flows cranially to caudally within the subarachnoid space. At the center of the spinal cord runs the ependymal (central) canal, a cerebrospinal fluid-filled structure continuous with the cerebral ventricles.

The spinal cord white matter is further divided into the dorsal, dorsolateral, lateral, ventral and ventrolateral funiculi. Within these funiculi are organized ascending (afferent) tracts of axons supplying sensory information to the brain as well as descending (efferent) tracts supplying motor input to the body. The gray matter is divided into the dorsal horn, intermediate grey, ventral horn, and a centromedial region surrounding the central canal. Dorsal roots exit the dorsal horn and dorsolateral white matter and enter the dorsal root ganglion (DRG), after which they unite with ventral roots originating from the ventral grey and white matter layers to coalesce and form a trunk that becomes the spinal nerve. Spinal nerves exit the vertebral column via the

intervertebral foramena and go on to form the peripheral nervous system (PNS), a large network of plexuses and nerves that supply sensory, autonomic, and motor innervation to the body.

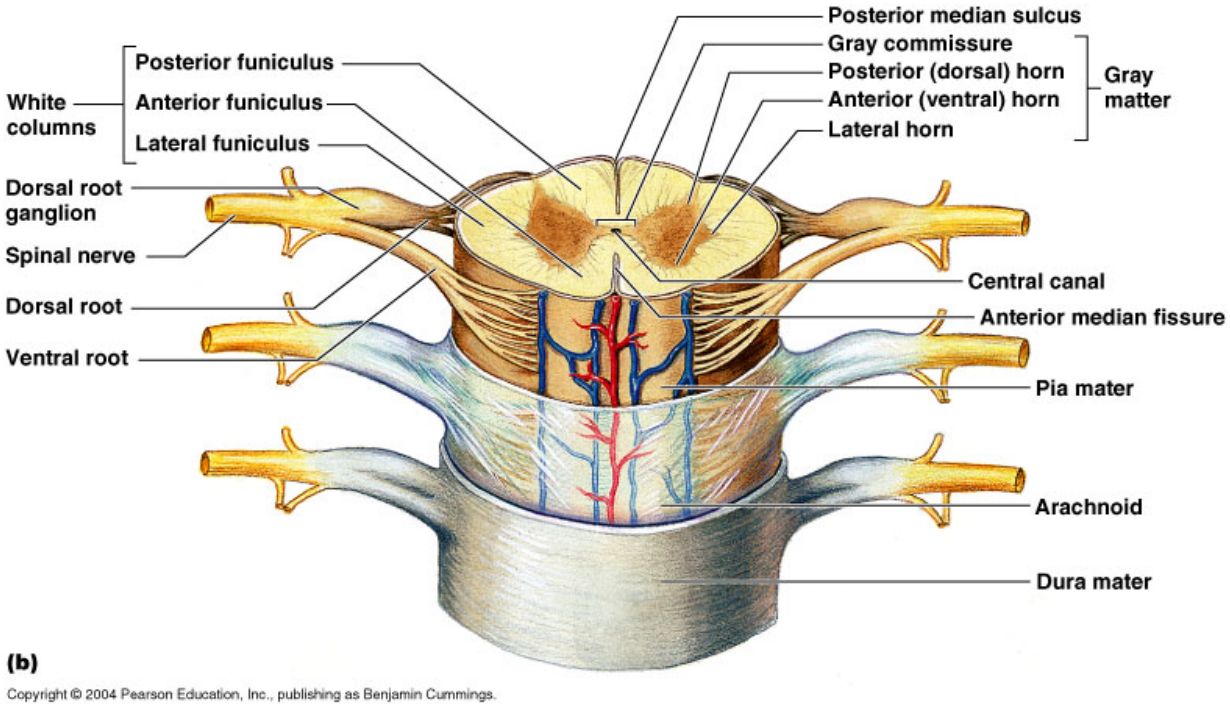

Fig. 2.1 Cross sectional anatomy of the spinal cord.

Source: https://sensoryandnervous.files.wordpress.com/2013/05/12-30b_spinalcord_1.jpg

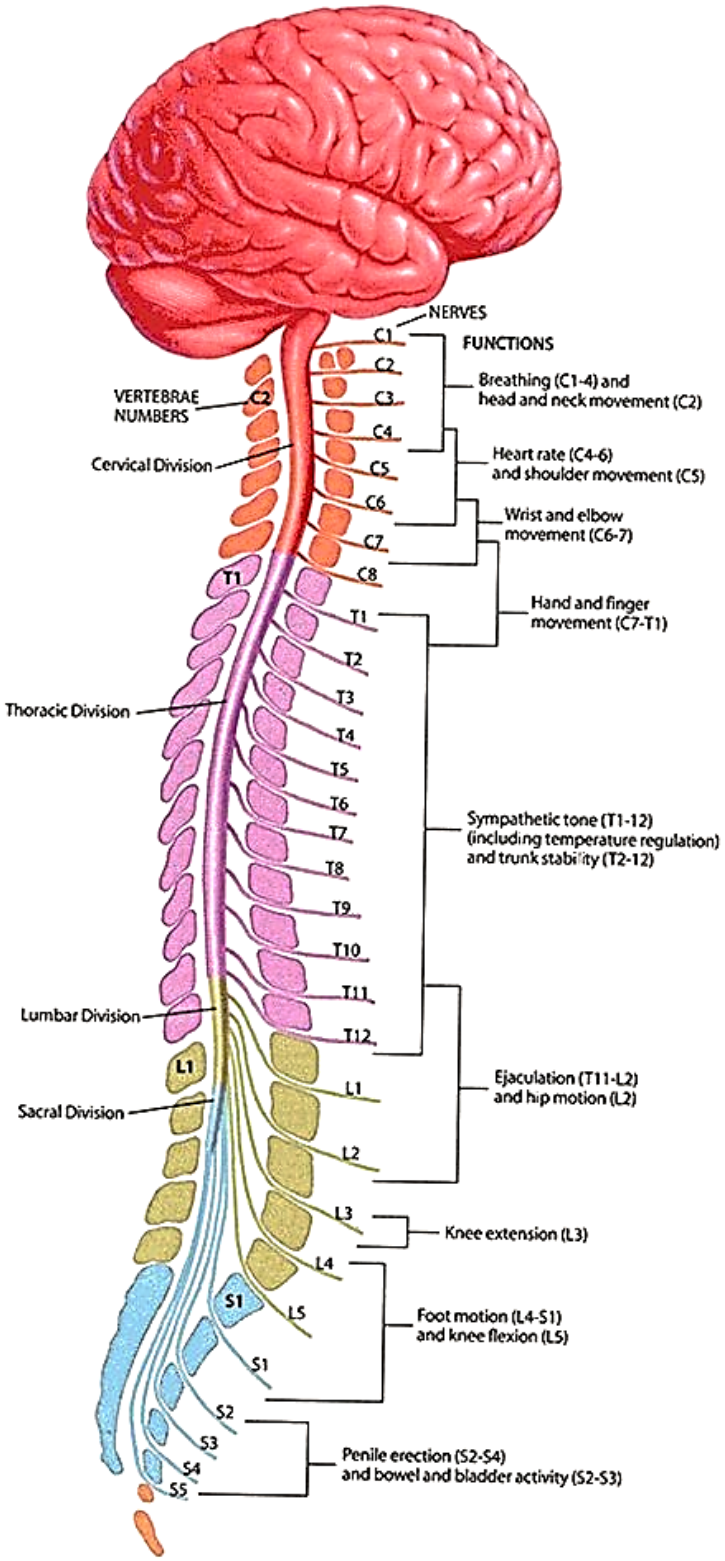

Fig. 2.2

General scheme of the human spinal cord

Source:
http://www.daviddarling.info/encyclopedia/S/spinal_cord.html

The primary cell type of the spinal cord is the neuron, a highly specialized, excitable cell capable of transmitting, processing, and receiving information through electrochemical signals. Neurons propagate signals via connections with other neurons called synapses. Within the spinal cord, there are sensory neurons that transmit information from the periphery to the brain and motor neurons that convey signals originating in the brain down to the muscles of the limbs and body. Interneurons are specialized neurons that act to transmit signals, often inhibitory, between other neurons. Together, neurons form circuits that conduct all proprioceptive, autonomic, sensory and motor information between the brain and body.

In addition to neurons, the spinal cord contains populations of non-neuronal, non-excitable cells termed glial cells. The main types of glial cells are astrocytes, oligodendrocytes, and microglia. Astrocytes are a structural cell and form scaffolds for other CNS cells. Oligodendrocytes produce myelin, which wraps around the long, tail-like axons of neurons and speeds up impulse conduction. Microglia are the primary immune cell of the CNS, and are similar to macrophages elsewhere in the body. These antigen-presenting cells migrate to regions of inflammation and/or injury to become activated and carry out phagocytic roles, sometimes concurrently with blood-origin monocytes.

MECHANISMS OF SPINAL CORD INJURY

The pathophysiology of SCI occurs in multiple stages: an acute injury phase initiated by physical insult to the spinal cord via compression, contusion, and/or transection,

followed by a delayed secondary phase characterized by inflammation and neurotoxic biochemical changes that potentiate further cell death and spinal cord dysfunction (**Fig. 2.3)**. The acute phase is immediate, while the secondary phase can occur over hours to weeks following injury (Quadri 2018). Damaged neurons at the site of injury with axons traveling proximally and distally through ascending and descending white matter tracks eventually die, resulting in cellular damage that extends above and below the actual site of physical insult.

Immediately following physical impact to the spinal cord, local hemorrhage, edema, and ischemia can be observed as the hallmarks of the primary injury phase. Direct trauma disrupts the structural integrity of the cord causing immediate damage to both gray and white matter, while disruption of local vasculature leads to hemorrhage into surrounding tissues. Interstitial fluid and blood rapidly accumulate within the confined space of the vertebral canal, creating additional pressure and worsening existing compressive and ischemic injury.

The secondary phase of injury is a prolonged event during which cells that survived the initial insult phase undergo delayed damage and death, largely mediated by cellular membrane breakdown with subsequent ionic dysregulation and neurotoxicity. Calcium influx across compromised cellular membranes leads to intracellular calcium accumulation, resulting in protease activation, dysfunctional mitochondria, free radical production, and activation of pro-apoptotic pathways. Excessive intracellular calcium also triggers the over-release of glutamate, an excitatory

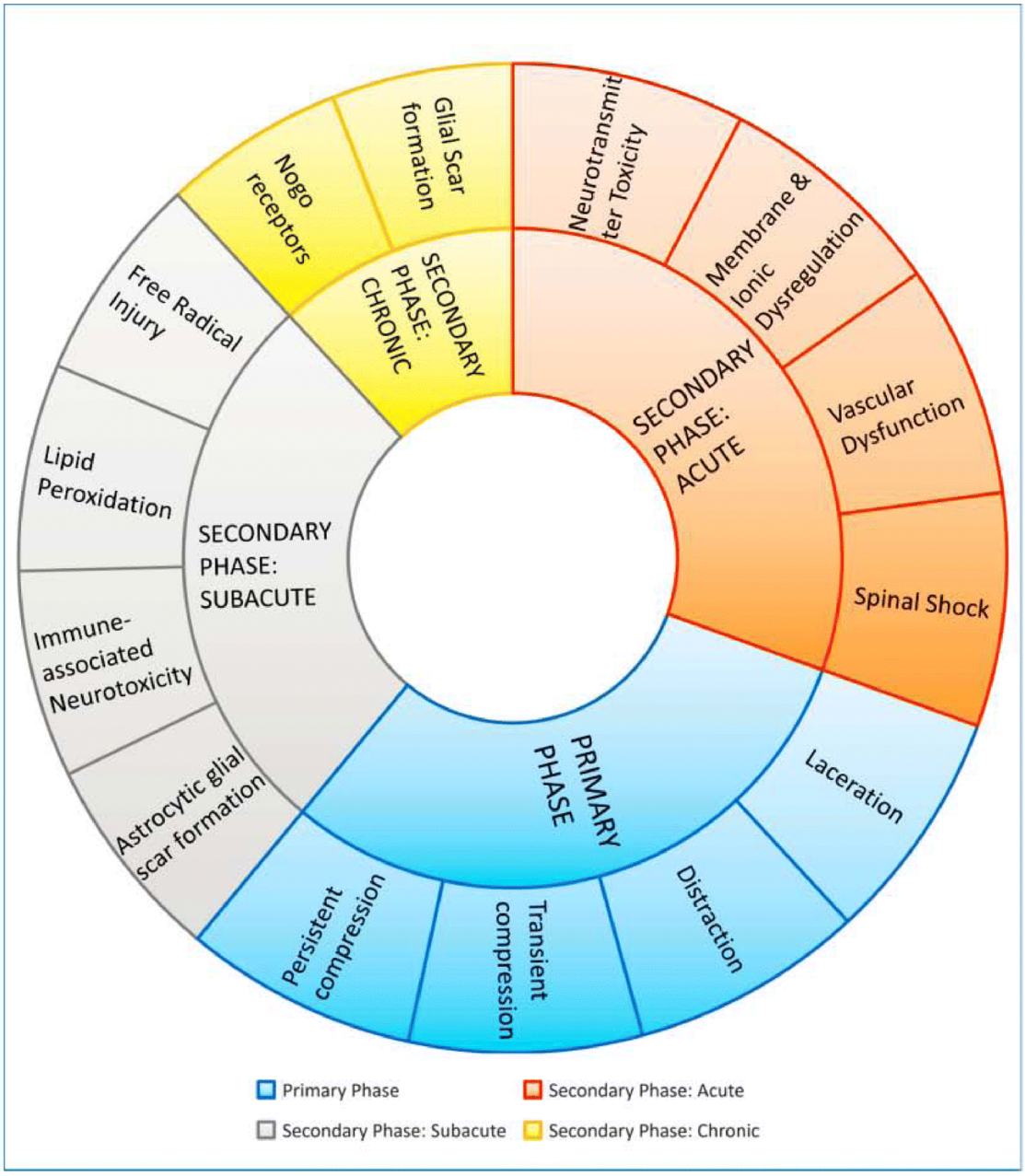

Fig. 2.3 The mechanism of spinal cord injury (SCI). Demonstration of various phases of SCI after trauma to the spinal cord.

Source: Quadri, S.A., Farooqui, M., Ikram, A. et al. Recent update on basic mechanisms of spinal cord injury. Neurosurg Rev (2018). https://doi-org.proxy.library.cornell.edu/10.1007/s10143-018-1008-3.

neurotransmitter usually stored in axon terminal vesicles and released upon calcium influx into the synaptic cleft. Extracellular glutamate accumulation activates voltage-gated calcium channels and further exacerbates calcium influx and neurotoxicity, a process known as excitatory cell death. Reperfusion of previously ischemic regions circulate oxygen-derived free radicals and other toxic by-products of hypoxia, leading to oxidative stress and free radical damage, further exacerbating endothelial damage, vascular permeability, and edema.

The immune response to SCI is an area of much research and controversy, as there is evidence that inflammation at the site of injury is both beneficial and detrimental to recovery following insult. Release of pro-inflammatory mediators and cytokines blood-derived neutrophils and monocytes initiate the inflammatory response. Microglia migrate to the site of injury, assume an activated state and release IL-1, IL-6, and TNF, a process that initiates the formation of a glial scar. While their phagocytic properties are essential for removing cellular debris following injury, the cytokines, free radicals and proteases they release into the local environment are toxic and further damage adjacent neurons and glial cells. Even specific cell types appear to have dual degenerative-regenerative roles in their response to SCI. Activated microglia at the site of injury assume either an M1 or M2 phenotype. While this classification system is still being defined, it appears that M1 microglia are generally pro-inflammatory and responsible for secretion of cytokines and chemokines that ramp up the inflammatory response, while M2 microglia are considered anti-inflammatory; secreting cytokines that actually suppress the local immune response and promote tissue regeneration. The

exact interplay and significance of these dueling roles remains poorly understood, and an area of current research and debate (David 2011).

The eventual fate of most spinal cord lesions is the formation of a glial scar through a process called astrogliosis. Following injury, microglia-secreted chemokines activate nearby astrocytes and initiate their migration to the epicenter of the lesion and form a glial scar, which is characterized by a central fluid-filled cyst surrounded by an outer layer of astrocytes and other inflammatory cells (**Fig. 2.4**). It remains unclear whether this process is neuroprotective or neurotoxic. While it protects the surrounding CNS by isolating and containing harmful cellular by-products at the site of injury, this shielding layer of astrocytes also acts as a prohibitive physical barrier that blocks axonal regrowth and regeneration of functional neural conduits.

In addition to the physical barrier effects of the glial scar, various cellular mechanisms contribute to poor axonal regrowth during the secondary phase of SCI. Several molecules known to prevent axonal growth and regeneration are produced by the extracellular matrix within the glial scar environment. These inhibitory molecules include tenascin, semaphoring 3A, keratin sulfate proteoglycan, myelin-associated glycoprotein, Nogo, and oligodendrocyte-myelin glycoprotein. Additionally, a family of sulfated glycosaminoglycan-protein chain molecules called chondroitin sulfate proteoglycans (CSPGs), work to inhibit axonal regrowth by creating physical barriers around axons through the formation of perineuronal nets. There are also inhibitory mechanisms inherent to the axons themselves that further prevent regeneration and repair after injury. Nogo receptors are myelin transmembrane proteins shown to

collapse growth cones and stop neurite elongation, and their targeted inhibition has recently garnered much research interest and progression through to clinical trials (Quadri 2018).

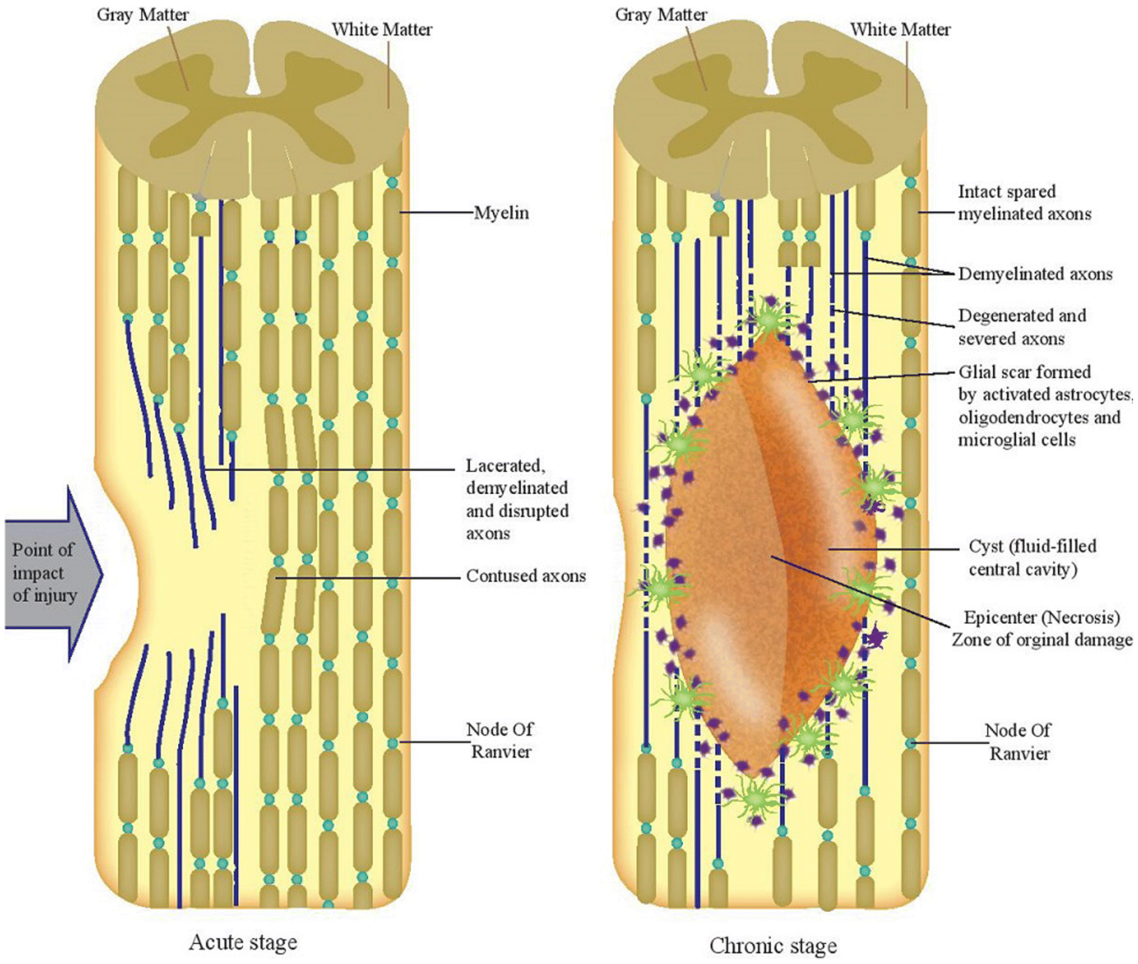

Fig. 2.4 Astrogliosis in response to SCI

Glial scar formation after the spinal cord injury at the site of impact, leading to recruitment of immune cells.

Source: Quadri, S.A., Farooqui, M., Ikram, A. et al. Recent update on basic mechanisms of spinal cord injury. Neurosurg Rev (2018). https://doi-org.proxy.library.cornell.edu/10.1007/s10143-018-1008-3.

THERAPEUTIC OPTIONS AND CLINICAL OUTCOMES IN SPINAL CORD INJURY PATIENTS

It is estimated that approximately 11,000 new spinal cord injuries occur in the United States each year. Of these, 45% are associated with a complete transection of the spinal cord and roughly half of all injuries result in quadriplegia and functional paralysis of both arms and legs (SCI-info-pages: *https://www.sci-info-pages.com/facts.html*). The physical sequelae to spinal cord trauma is dependent on the location and severity of injury. In addition to loss of function of areas innervated by the region of injury, spinal cord sections distal to the injury site are also often dysfunctional. In the case of spinal cord transection, complete loss of all sensory and motor function distal to the injury site is observed. For patients with cervical spinal cord injury, this often translates to loss of sensory and motor to the arms and legs, urinary and bowel incontinence, and sexual dysfunction. Patients with proximal cervical injuries additionally suffer loss of motor input to the respiratory musculature, and require external ventilator support for life.

There are currently no known curative therapies for SCI. While initial insult to the spinal cord is generally accidental and unavoidable, treatment generally focuses on mitigating the prolonged secondary phase of injury and restoring as much function as possible in the long term. In the acute phase, minimizing inflammation of the spinal cord as well as adjacent traumatized soft tissues is crucial for preventing further swelling and subsequent compression and ischemia to the cord. The use of steroids remains very controversially but widely practiced and prescribed (Silva 2014). Perfusion of the injury

site is supported by maintaining mean arterial pressures via intravenous fluid therapy and vasopressor support. Minocycline, a tetracycline antimicrobial, has received much research interest in recent years as an acute treatment for SCI due to its anti-inflammatory properties in the CNS via suppression of microglial activation (Wells 2003, Cox 2015).

In recent years, studies have shown variable success using regenerative modalities to encourage spinal cord repair. Direct transplantation of Schwann cells, embryonic stem cells, mesenchymal stem cells, and neural stem cells have been evaluated in basic research studies as well as pre-clinical trials. While some of these therapies have demonstrated some degree of success, the most effective cell type and mode of delivery is yet to be determined. Furthermore, substantial safety concerns exist regarding the use of allogeneic biologics, graft versus host disease, and risk of tumor formation following transplantation (Mariano 2015).

Long term rehabilitative care for SCI focuses on physical therapy through the use of body-weight-supported treadmill training and robotic-assisted gait training. This treatment modality helps maintain strength and muscular tone, and encourages functional recovery through the development of compensatory neural circuits (Ma 2017) Psychological support is also very important, as many SCI suffer depression as a consequence of their condition. Ongoing management of physical comorbidities such as pneumonia, decubital pressure sores, and urinary and dermatological infections are also an integral part of managing SCI long term, and these non-spinal cord specific comorbidities largely contribute to the shortened expected lifespan of SCI patients.

Despite much research in the area of spinal cord injury, overall recovery rates are less than 1%, and most patients will suffer life-long neurologic impairment.

NEUROPATHIC PAIN

Neuropathic pain is defined as an abnormal pain state arising from a damaged central or peripheral nervous system (PNS). Inciting causes include direct trauma and/or injury to the spinal cord or peripheral nerves, viral or bacterial infection, degenerative conditions, metabolic and endocrine disorders, toxicities and autoimmune disease.

Patients with neuropathic pain suffer from a myriad of symptoms including poorly localized relentless pain, tingling or burning sensation, and paroxysmal stabbing or shooting pain. Often times the pain is distant to the original site of injury. The so-called "phantom limb" pain experienced by amputees is a form of neuropathic pain, as is diabetic neuropathy syndrome (Jay 2014).

Several mechanisms of neuropathic pain have been proposed, including synaptic remodeling, excessive upregulation of neuronal calcium and sodium channels, enhanced excitatory and reduced inhibitory drive, morphologic and electrophysiologic changes to dorsal horn neurons – all ultimately leading to circuit-level rewiring, altered connectivity, and aberrant nociceptive signal processing at the level of the spinal cord (Campbell 2006). The theories are corroborated by studies demonstrating abnormal spontaneous neural firing activity in the spinal cord dorsal horn in ex-vivo mouse models of PNS injury (West 2015). More recently, glial cells have been implicated in

the development of neuropathic pain, and research has focused on the potential role that activated microglia play in altering neural activity and circuitry in the dorsal horn following CNS and/or PNS injury (Vallejo 2010, Peng 2015, Gu 2016).

CLINICAL MANAGEMENT OF NEUROPATHIC PAIN

Clinical management is frustrating and difficult, and a hallmark of neuropathic pain is its overall poor response to conventional analgesic therapies. This is likely due to our relatively incomplete understanding of the true mechanisms of neuropathic pain, and as a consequence, inability to develop targeted treatment modalities that address and mitigate those mechanisms. Diagnosis is made by exclusion of all other possible causes of the patient's symptoms of pain. Treatment focuses on a combination of pharmacotherapeutics including opioids, anti-inflammatories, targeted neural blockade, anti-convulsants, and anti-depressants. In most cases, clinical symptoms may be lessened in quality and intensity but are rarely completely ablated. The addition of adjuvent therapies such as electroacupuncture, massage, and targeted neurolysis are often attempted with variable success (Finnerup 2012, Jay 2014).

QUESTIONS IN SPINAL CORD REPAIR AND THE NEED FOR *IN VIVO* IMAGING

Clearly much remains to be learned about how the spinal cord responds to insult and how we can bolster that response and improve functional recovery in human and animal

patients following injury and disease. Traditional approaches to SCI research with electrophysiology and immunohistochemistry are performed on isolated tissues and provide only a static snapshot of cellular structure at one point in time. Many of the most important questions in spinal cord research could be answered with optical techniques capable of capturing cell-resolved events serially over time. Are all axons created equally, or do some have greater regenerative capacity when compared to others? If microglia and the local inflammatory responses are both helpful and harmful to axonal regrowth, at what phases following injury do they exert these effects? Can we identify time points in the recovery phase when targeted immune suppression may mitigate the inhibitory environment of the glial scar while still preserving its ability to protect the surrounding environment from toxic byproducts cellular damage? Can we induce axonal behavioral changes through the introduction of growth factors and or stem cells, and if so, what is the optical time point after injury to implement such regenerative therapies? How, and when, do changes in cellular populations within the CNS ultimately lead to alterations in neural activity? Are the partial recoveries observed in SCI patients the result of restored cellular architecture and neural infrastructure, or an adaptive neuroplasticity response allowing the body to regain old functions through the development of entirely new circuits? And most importantly, how do changes at the cellular level lead to alterations in neural activity and signaling patterns, and ultimately define the final output of the motor and sensory systems: the ability to move and feel.

REFERENCES

- Campbell J, Meyer R. Mechanisms of neuropathic pain. Neuron (2006) 52:77-92.
- David S, Kroner A. Repertoire of microglial and macrophage responses after spinal cord injury. Nature Reviews: Neuroscience (2011) 12: 388-400).
- Finnerup NB, Baastrup C. Spinal cord injury pain: mechanisms and management. Curr Pain Headache Rep 2012;16:207-16.
- Gu N, Eyo U, Murugan M, Peng J, Matta S, Dong H, Wu L. Microglial P2Y12 receptors regulate microglial activation and surveillance during neuropathic pain. Brain Behav Immun (2016) 55:82-92.
- Jay G, Barkin R. Neuropathic Pain: Etiology, pathophysiology, mechanisms and evaluations. Disease-a-month (2014)60:6-47. https://doi.org/10.1016/j.disamonth.2013.12.001.
- Jenson T, Finnerup N. Allodynia and hyperalgesia in neuropathic pain: clinical manifestations and mechanisms. The Lancet: Neurology (2014)13:924-935.
- Ma D, Zhang X, Ying J, Chen Z, Li L. Efficacy and safety of 9 nonoperative regimens for the treatment of spinal cord injury. Systemic Review and Meta-Analysis (2017)96. https://insights-ovid-com.proxy.library.cornell.edu/pubmed?pmid=29381946
- Mariano E, Batista C, Barbosa B, Marie S, Teixeiera M, Margalla M, Tatagiba M, Li J, Lepski G. Current perspectives in stem cell therapy for spinal cord

repair in humans: a review of work from the past 10 years. Views and Reviews (2015)451-457.

- Nógrádi A, Vrbová G. Anatomy and Physiology of the Spinal Cord. In: Madame Curie Bioscience Database. Austin (TX): Landes Bioscience; 2000-2013. Available from: https://www.ncbi.nlm.nih.gov/books/NBK6229/.
- Peng J, Gu N, Zhou L, Eyo U, Murugan M, Gan W, Wu L. Microglia and monocytes synergistically promote the transition from acute to chronic pain after nerve injury. Nature Communications 2015.
- Quadri, S.A., Farooqui, M., Ikram, A. et al. Recent update on basic mechanisms of spinal cord injury. Neurosurg Rev (2018). https://doi-org.proxy.library.cornell.edu/10.1007/s10143-018-1008-3.
- SCI-info-pages: Quadriplegic, Paralegic and Caregiver Resources. https://www.sci-info-pages.com/facts.html
- Silva NA, Sousa N, Reis RL, et al. From basics to clinical: a comprehensive review on spinal cord injury. Prog Neurobiol 2014;114:25-57.
- Vallejo R, Tilley D, Vogel L, Benyamin R. The role of glia and the immune system in the development and maintenance of neuropathic pain. Pain Practice (2010)10: 167-184.
- Varma AK, Das A, Wallace G, et al. Spinal cord injury: a review of current therapy, future treatments, and basic science frontiers. Neurochem Res 2013;38:895-905

- Wells J, Hurlbert R, Fehlings M, Yong. Neuroprotection by minocycline facilitates significant recovery form spinal cord injury in mice. Brain (2003) 126:1628-1637.
- West S, Bannister K, Dickenson A, Bennett D. Circuitry and plasticity of the dorsal horn – toward a better understanding of neuropathic pain. Neuroscience (2015)300:254-75.

CHAPTER 3

TWO-PHOTON EXCITED FLUORESCENCE MICROSCOPY

Figure acknowledgments:

Fig. 3.1 Nonlinear absorption and excitation
https://i.stack.imgur.com/uLMeH.png

Fig. 3.2 Localization of excitation by two-photon excitation
Zipfel W, Williams R, Webb W. Nonlinear magic: multiphoton microscopy in the biosciences. *Nat Biotechnol (2003)* 21:1369.

Fig. 3.3 Schematic of a multi-photon microscopy system
Zipfel W, Williams R, Webb W. Nonlinear magic: multiphoton microscopy in the biosciences. *Nat Biotechnol (2003)* 21:1369.

Nonlinear microscopy has become the technique of choice for imaging with sub-cellular resolution deep into scattering tissue in live animals, and has enabled immense progress to be made in studies of complex biological systems such as the brain and spinal cord. Through 2PEF one can perform real-time in *vivo* imaging of subcellular structures and functions without causing damage to the tissues or host animal. When combined with chronic surgical preparations, structures of interest and biological processes can be serially monitored over days to weeks. This chapter provide an overview of 2PEF by briefly reviewing fluorescence microscopy, two-photon excitation, and describing the 2PEF microscope setup. The imaging techniques described in this chapter were utilized for all imaging described in Chapters 4, 5 and 6.

FLUORESCENCE MICROSCOPY

Fluorescence microscopy utilizes fluorophores to visualize biological structures. Fluorophores are compounds that absorb energy, become excited (absorbed energy leads to electron transitions from the ground state to high energy, excited state) and emit light upon relaxation back to ground state. They are endogenous to some cellular structures, and can be exogenously introduced to label specific structures of interest inside live animals through genetic manipulation and/or injection of fluorescent dyes. For example, we frequently utilize transgenic mice that constitutively express yellow fluorescent protein (YFP) in neurons and green fluorescent protein (GFP) in microglia, then transiently label blood plasma via intravenous injection of a Texas-Red-tagged dextran.

In order to excite a fluorophore, a quantized amount of energy must be introduced to enable electrons to transition from the ground energy state to a higher excitation state. This energy can be delivered by one photon of the correct energy, or multiple photons whose energies add up to the correct amount for that particular kind of fluorophore, if those multiple photons interact with the electron at almost exactly the same time. The energy of a photon is inversely proportional to its wavelength and can be described with the following equation:

$$E = h\,c\,/\,\lambda$$

where h is Planck's constant and c and λ are the speed and wavelength of light in vacuum, respectively.

The amount of energy required to excite a fluorophore depends on the chemical structure of that particular fluorophore compound. Once excited, the electron quickly relaxes to the lowest level excited state through thermal relaxation, then returns to the ground state by emitting a photon that has less energy than what was absorbed due to the thermal relaxation. There is a large selection of fluorophores available that use a wide range of excitation energies and exhibit an equally wide range in the energy/wavelength of emitted photons (Bestvater 2002). Diversity in fluorophore properties, coupled with the use of spectral filters and different excitation wavelengths, allow multiple structures labeled with different fluorophore dyes to be simultaneously distinguished and imaged.

TWO-PHOTON EXCITATION

Challenges of fluorescence imaging in vivo

Biological tissue is an intrinsically turbid medium, with optical properties characterized by strong scattering and a heterogeneous refractive index. This is especially true in the spinal cord, where the dense white matter layer comprised mostly of myelin acts as a highly-scattering optical barrier to excitation light. Excitation light attenuated by scattering can redirect to interact with fluorophores outside of the focus, producing fluorescence from multiple locations and diminishing spatial resolution of individual structures. Additionally, high levels of scattering results in less excitation light reaching the focal area of interest and less ability to excite fluorophores present in the tissues. This deleterious effect increases with depth, thereby limiting depth penetration in highly scattering tissues.

Furthermore, traditional one-photon excited fluorescence microscopy does not allow for imaging at depth, as the individual photons are of high-enough energy to excite fluorophores anywhere along their path within tissues, resulting in fluorescence generation at multiple locations within the excitation beam pathway. While imaging in a single plane is appropriate for single-layer samples such as tissue sections or cell culture, this imaging modality has little utility for *in vivo* imaging of organs and tissues *in situ*.

Two-photon excitation physics

The aforementioned limitations to fluorescent imaging can be overcome using nonlinear optics, such as multiphoton excited fluorescence microscopy. Two photons can provide the same amount of energy as a single photon at half their wavelength (**Fig. 3.1**). For the two-photon nonlinear absorption process to occur, both photons must interact with the fluorophore within about 10-16 s of each other, i.e. essentially simultaneously. The probability of such an interaction depends on the density of photons quadratically, and therefore the probability that two photons will be absorbed simultaneously is quadratically dependent on the light intensity. Therefore, high light intensity is required in order for this absorption to occur. In order to avoid damaging the biological sample, tightly focused, femtosecond duration laser pulses are utilized to achieve a sufficiently high intensity with low average power (Williams 2001).

Advantages of two-photon excited fluorescence microscopy

The use of this nonlinear optical absorption for fluorescence excitation yields several advantages. First, because two photons must be absorbed simultaneously to excite a fluorophore, with the appropriate choice of laser parameters the only location where the intensity of the femtosecond pulses are sufficiently high to cause this excitation is the submicron-sized focal volume. **(Fig. 3.2)** The localization of the fluorescence excitation naturally yields optical sectioning of samples. The focal volume is then scanned in three

dimensions and the fluorescence is collected point-by-point to build a three-dimensional, micrometer resolution image. Second, because fluorescence is only excited in one spatial location, it is not necessary to spatially resolve the fluorescence emission on the detection side of the microscope in order to know where that fluorescence came from.

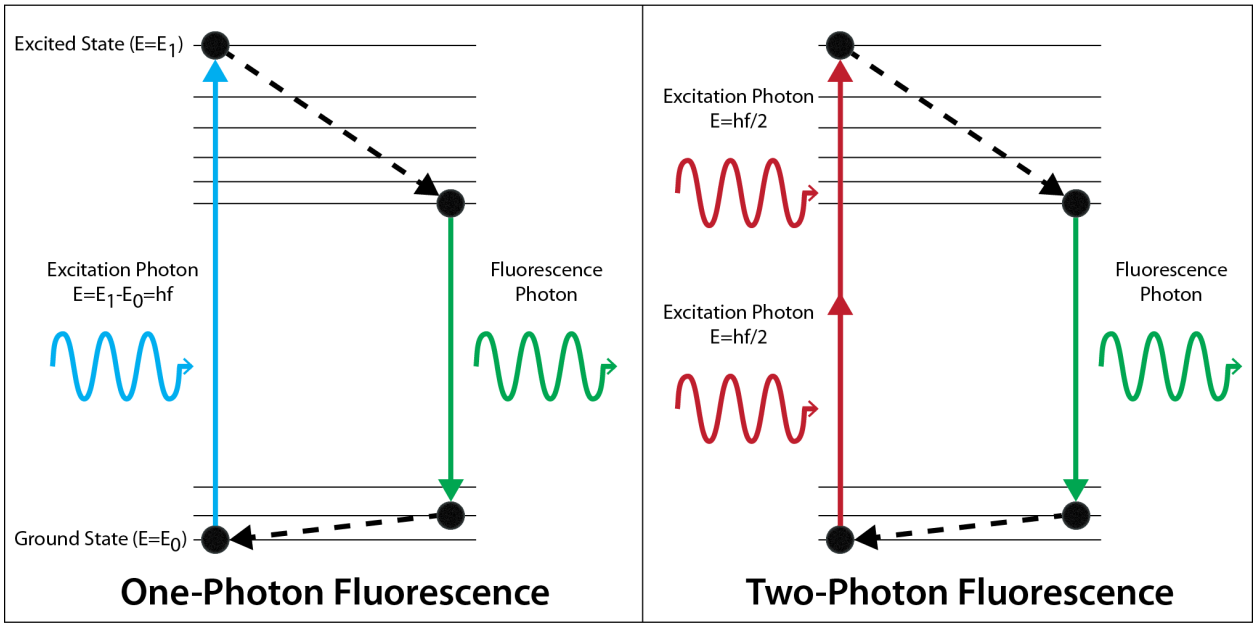

Fig. 3.1 Nonlinear absorption and excitation

Energy level diagram illustrating the one- and two-photon absorption and excitation that enables fluorescence generation.

Source: https://i.stack.imgur.com/uLMeH.png

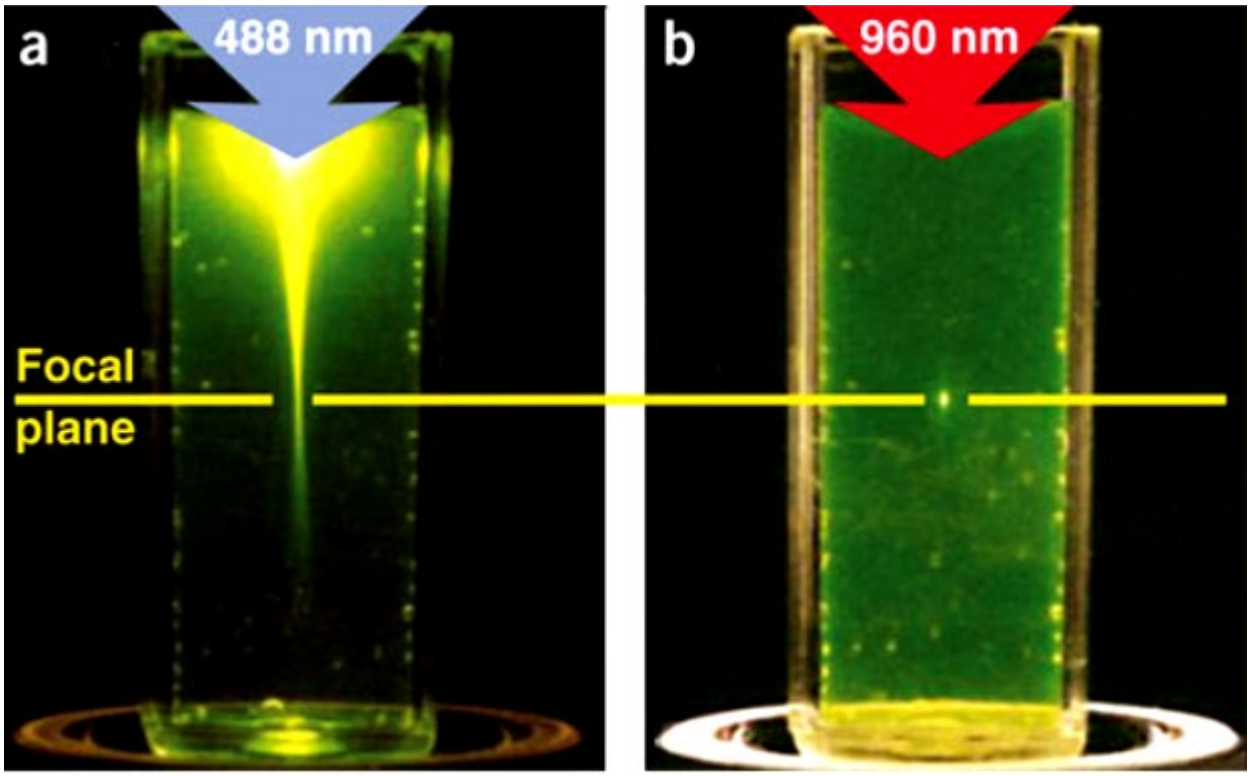

Fig. 3.2 Localization of excitation by two-photon excitation

(a). Single-photon excitation of fluorescein by focused 488-nm light. (b) Two-photon excitation using focused femtosecond pulses of 960-nm light

Source: Zipfel W, Williams R, Webb W. Nonlinear magic: multiphoton microscopy in the biosciences. *Nat Biotechnol (2003)* 21:1369.

This makes the imaging relatively insensitive to optical scattering of the emitted fluorescence. Any emitted fluorescence light that can be collected and detected contributes to image formation and does not degrade the signal to noise. Finally, two photon excitation is relatively tolerant to optically scattering of the excitation beam. The longer excitation wavelengths typically used (800 – 1,300 nm for 2PEF) are less optically scattered by tissue, enhancing penetration depth. In addition, scattered excitation light cannot effectively generate fluorescence, so it does not contribute to background (Zipfel 2003). Instead, the incident laser energy can simply be increased to compensate for laser energy that is scattered away, thereby achieving the laser intensity needed to drive two-photon excitation at the focus.

Ultimately, the limit of depth penetration for two-photon microscopy comes from out-of-focal-plane excitation. When imaging deeper and deeper into tissue, the laser energy must be increased exponentially with depth to compensate for optical scattering losses. The increase in laser intensity due to optical focusing is only geometric with depth, and at some depth the laser intensity near the sample surface becomes high enough to drive two-photon excitation. At this depth, typically around 800 μm for 800 nm excitation light in rodent cortex, image contrast is lost.

TWO-PHOTON EXCITED FLUORESCENCE MICROSCOPE SET UP

Pulse Laser Source

Titanium-sapphire (Ti:S) lasers are the most widely used in two-photon microscopy. Their repetition rate is ~100 MHz, which matches typical fluorescence lifetimes of ~10 ns, resulting in minimum saturation and maximized excitation efficiency. The wavelength can be tuned over a large range (670-1070 nm) to excite many different kinds of fluorophores. In addition, a wide range of laser powers are available, depending on the power of the pump laser and design of the Ti:S laser cavity.

Excitation Pathway

Starting from the laser, the beam is routed through one or more telescopes to adjust the beam size to ultimately overfill the back aperture of the objective. Because the beam intensity profile is Gaussian-shaped, overfilling of the back aperture provides a compromise between maximized power transmission and optimal resolution. When the laser's ultrashort pulses propagate through optical elements in the microscope, dispersion occurs because longer-wavelength components (e.g. red) travel faster through materials than shorter-wavelength components (e.g. blue). In order to compensate for this dispersion, a prism sequence is inserted to spatially separate the different-wavelength components, which are then forced to travel through different path lengths before being recombined. One way to implement this dispersion compensation

is to place a pair of prisms at a point in the system where the laser beam propagates through twice (Tsai 2002). Lastly, the beam intensity at the sample can be controlled using neutral-density (ND) filters or a rotatable waveplate combined with a polarizer.

Beam Scanner

An image from a 2PEF microscope is acquired by detecting fluorescence signals emitted as the laser raster scans over the region of interest. Because fluorescence is produced only in a small focal volume, the focal volume is scanned through the sample, causing fluorescence. The intensity measurement at each focus location becomes a voxel in the final image. Two rotating mirrors are used for XY scanning over the sample. The field of view depends on how far the mirrors can rotate, while the acquisition rate depends on how fast the mirrors can move. Thus, there is a trade-off between spatial and temporal resolution. The sample or the objective is moved to adjust the imaging plane and acquire stacks of 2D images.

Detectors

The photons from sample fluorescence are emitted in all directions, but only the ones that travel back towards the microscope objective are collected. These photons reflect from a dichroic mirror that separates excitation from emission light based on the wavelength. The signal passes through a filter for the particular wavelength range being detected before reaching a photomultiplier tube, where it is then converted into a voltage

measurement. This voltage signal is then digitized and recorded using ScanImage software, which also controls the motion of the scan mirrors and sample translation stage (Pologruto 2003) (**Fig. 3.3)**

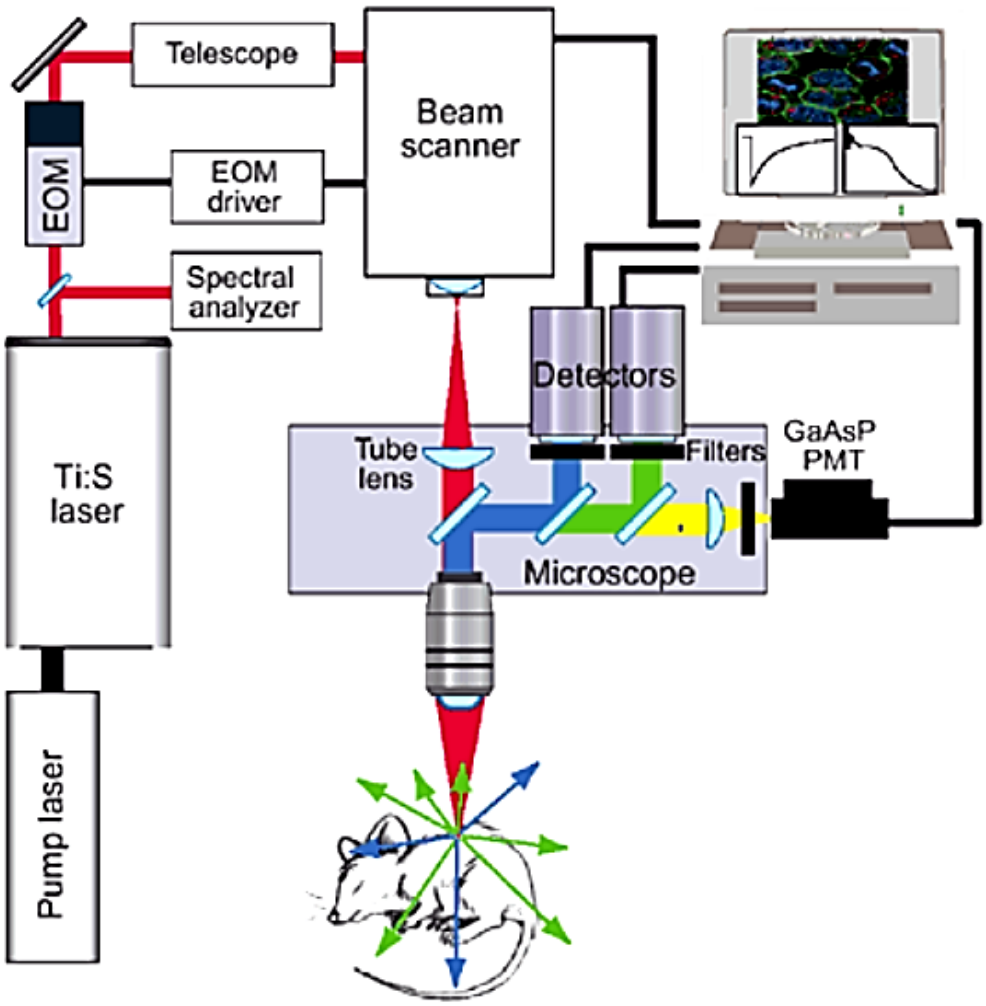

Fig. 3.3 Schematic of a multi-photon microscopy system

Source: Zipfel W, Williams R, Webb W. Nonlinear magic: multiphoton microscopy in the biosciences. *Nat Biotechnol (2003)* 21:1369.

REFERENCES

- Bestvater F, *et al.* Two-photon fluorescence absorption and emission spectra of dyes relevant for cell imaging. *J Microsc* (2002) 208:108.
- Pologruto T, Sabatini B, Svoboda K. ScanImage: flexible software for operating laser scanning microscopes. *Biomed Eng Online (2003)* 2:13.
- Tsai P, *et al.* Principles, design, and construction of a two photon laser scanning microscope for in vitro and in vivo brain imaging. *In vivo optical imaging of brain function*. (2002): 113.
- Williams R, Zipfel W, Webb W. Multiphoton microscopy in biological research. *Curr Opin Chem Biol (2001)* 5:603.
- Zipfel W, Williams R, Webb W. Nonlinear magic: multiphoton microscopy in the biosciences. *Nat Biotechnol (2003)* 21:1369.

CHAPTER 4

IN VIVO TWO-PHOTON EXCITED FLUOROESCENCE MICROSCOPY OF THE INJURED SPINAL CORD

Figure acknowledgements:

Fig. 4.2 Implanted optical imaging chamber

Farrar M, Bernstein I, Schlafer D, Cleland T, Fetcho J, Schaffer B. Chronic in vivo imaging in the mouse spinal cord using an implanted chamber. Nat Methods (2012) 3:297-302.

The ability to image sub-cellular resolution deep into scattering tissue in live animals makes multiphoton fluorescence microscopy the technique of choice for *in vivo* imaging of complex biological systems such as the spinal cord. Never before has there been such exciting potential for shedding light on the poorly understood mechanisms of axonal regeneration, CNS inflammation, and neural circuit plasticity. In order to make this a reality, however, several critical technical aspects of *in vivo* imaging must be adapted for both multiphoton microscopy and the spinal cord, including appropriate rodent injury models, fluorescent labeling of structures of interest, and finally, surgical preparations that enable long term optical access to the spinal cord without the need for repeated surgical procedures. Each representing its own suite of challenges, all of these conditions must work simultaneously if serial, *in vivo*, 2PEF microscopy of the injured spinal cord is to be achieved.

SPINAL CORD INJURY RESEARCH IN MICE: MODELS OF INJURY AND TRADITIONAL RESEARCH TOOLS

Rodent models of SCI are widely used due to their accessibility, ease of care, and ability to manipulate their genome to create specific experimental conditions. Three classes of SCI are generally used in research: transection, contusion, and compression (Rosenzweig 2004). Each injury generates a different physiologic response and closely resemble the most common traumatic injuries observed in human patients.

The transection model involves cutting through the dura and spinal cord using a sharp instrument. Variations of transection injuries include complete transection of the entire cord, lateral hemisections in which only one side of the cord is affected, and dorsal or ventral hemisections in which only the dorsal or ventral aspects of the cord are transected, respectively. Each transection type injures distinct regions within the spinal cord and create sensory and motor deficits specific to the regions affected. Advantages of the transection SCI is the ability to specifically target which spinal cord functions are to be affected; ie, full transection for studying bladder and bowel dysfunction, or dorsal hemisection for investigating the effects of corticospinal tract injury on limb placement and gait. The primary disadvantage of the transection injury models is that it least resembles naturally occurring injuries in human SCI patients when compared to contusion or compression injury.

The contusion model of injury is induced by subjecting the spinal cord to blunt force trauma using an impactor device to deliver a set amount of direct force. Many commercial impactors are available that allow researchers to fine tune the severity of injury with adjustable impulse, velocity, power and energy. The advantages of the contusion model include its biologic similarity to the majority of traumatic human SCI, while the disadvantages include relative difficulty reproducing the exact same contusion injury repeatedly and inability to discern spared tissue from regenerative tissues following injury.

The compression model is created by subjecting the spinal cord to external pressure using a modified aneurysm clip, forceps, or similar instrument. This creates an

injury comparable to intervertebral disk disease or stenotic myelopathy commonly observed in humans and veterinary patients. Similar to the contusion models, the compression model can be adjusted to create an injury of desired severity by altering the degree of pressure and time of compression (Silva 2014).

Assessment following induced injury in mice is achieved via evaluation of motor and sensory function using a myriad of behavioral tests to allow the researcher to correlate the degree of functional deficit with lesion severity and location, as well as assess for recovery from SCI with or without therapeutic intervention. The most widely used test of motor function in mice is The Basso Mouse Scale (BMS), a 9-point scale designed to assess recovery of hindlimb function following injury to the thoracic spinal cord. The test is performed with the animal moving freely about an open-field assessment area, and assigns scores based on ability to spontaneously ambulate, gait coordination, paw placement, joint angles, as well as position and stability of the limbs, truck, and tail. The BMS was designed specifically for mouse studies and was adapted from the BBB Scale, which was primarily intended for use in rats. While the BMS is easy to learn and perform, the assigned scores are somewhat subjective, and variability between assessors can confound results across cohorts of mice. In addition to the BBB locomotor scale, proprioception and motor function is often further assessed through a variety of obstacle or task-based tests, including ladder climbing, swim tests, object grabbing, and rotorod grip tests. Gait quality may also be evaluated by recording paw print patterns on paper walked across by mice with ink-dipped paws, and or a variety of commercially-available limb-tracking systems.

While there exists a plethora of options for assessing behavior and gross motor function following SCI in mice, methods for assessing corresponding cellular changes and alterations in neural functionality, particularly *in vivo*, are extremely limited. Immunohistochemistry is a mainstay of spinal cord research, providing information regarding tissue architecture as well as identification of a variety of cell types *in situ*. The major drawback to immunohistochemical staining is that it can only be performed on ex-vivo tissue sections, thereby providing no information regarding dynamic cellular interaction and/or neural activity. Furthermore, animals providing tissue for immunohistochemistry (IHC) must be euthanized, thereby limiting researchers to data collection at only one single point in time. Longitudinal IHC data, therefore, must be collected from large cohorts of mice grouped into discrete time points for sacrifice and tissue harvest.

Electrophysiology helps to bridge the gap between IHC and the *in vivo* imaging techniques described in this dissertation by providing direct measurements of muscle activation and both somatosensory-evoked and motor-evoked potentials. This technique can be performed *in vivo*, and is based on stimulation of a specific location, transmission of the evoked potential through the injured region of spinal cord, and then recording any impulses that are successfully transmitted through to another point opposite the injury site. This test can be performed bidirectionally across a SCI site, and provides information regarding the integrity and regeneration of motor and sensory pathways following injury. Electrophysiology can also be performed *in vitro*, generally for experiments that utilize freshly-harvested spinal cords placed in artificial cerebrospinal

fluid (CSF) to evaluate the effects of ionic influxes and pharmacologics on impulse transmission across an injury site. The primary disadvantage of electrophysiology is the necessity of general anesthesia, which greatly dampens normal spontaneous spinal cord activity. Furthermore, while electrophysiology can confirm the presence of intact neural connections across which evoked potentials can travel, it provides no information regarding signaling patterns and circuitry across groups of neurons.

SPINAL CORD FLUORESCENT LABELING STRATEGIES

For the experiments described in this dissertation, we utilized genetically modified mouse lines in combination with exogenously delivered injectable dyes to simultaneously image neurons, microglia, and spinal vasculature.

To label neurons and their associated axons, we used a B6.Cg-Tg(Thy1-YFP)16Jrs/J transgenetic mouse line, which express yellow fluorescent protein (YFP) in both sensory and motor neurons of the central and peripheral nervous systems under the control of regulatory sequences of the Thy1 gene. (Josvay 2014). To label microglia, we used a B6.129P-Cx3cr1^{tm1Litt}/J transgenetic mouse line, which express green fluorescent protein (GFP) in brain microglia, monocytes, and dendritic cells under control of the endogenous Cx3cr1 locus. (Jung 2000). The Thy1-YFP and CX_3CR1-GFP lines were crossed to produce double transgenic mice expressing YFP and GFP in neurons and microglia, respectfully. To label spinal vasculature during imaging sessions, a Texas Red labelled dextran was intravenously introduced via retrobulbar

injection. This soluble fluorescent dye distributes throughout blood plasma and remains in circulation for several hours.

Vector-borne delivery of genetic machinery via adeno-associated viruses (AAV) can also be utilized for transfecting specific populations of cells and inducing transcription of specific fluorescent proteins, and was performed for some of the imaging studies discussed in Chapters 6 and 7.

To simultaneously image YFP, GFP, and Texas Red, we used a custom-designed multiphoton microscope and performed 2PEF imaging using 800-nm wavelength excitation from a femtosecond pulse-wave laser source. Emission spectrum was filtered at 645/65 nm, 550/50 nm, and 517/65 nm to isolate fluorescence from Texas Red dextran, YFP, and GFP, respectively (**Fig. 4.1**).

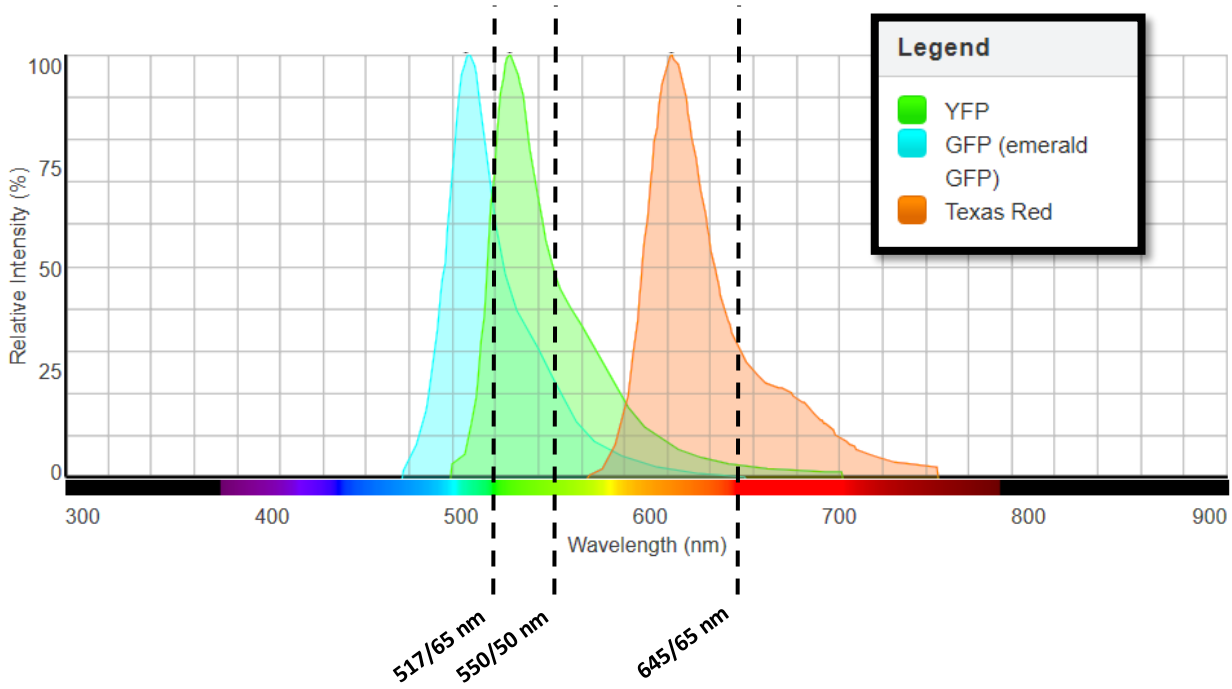

Fig. 4.1 2PEF Spectral Diagram

Diagram of emission spectra from YFP, GFP, and Texas Red. Placement of emission filters (center wavelength/bandwidth) used for 2PEF imaging denoted with black dash lines.

Created using: ThermoFisher Scientific Fluorescence SpectraViewer

https://www.thermofisher.com/us/en/home/life-science/cell-analysis/labeling-chemistry/fluorescence-spectraviewer.html

IMPLANTED IMAGING CHAMBERS PROVIDE LONG TERM OPTICAL ACCESS TO THE SPINAL CORD

Longitudinal studies following cellular interactions over time are needed in order to better understand spinal cord physiology in health and disease. This requires chronic optical access without the need for repeated surgeries. A long-term implantable spinal cord imaging chamber was developed in the Schaffer Lab that allows for serial imaging of the thoracic spinal cord. With careful surgery, there is no injury to the spinal cord and the chamber does not restrict mouse locomotion. The imaging chamber consisted of two metal bars that grip the spine together with a top plate that holds a glass optical window (**Fig. 4.2**). The chamber holds the spine fixed under the microscope and limits respiratory motion artifacts to less than 3 μm and eliminates heartbeat-induced movement (Farrar 2012).

The original chamber implantation surgery describes placement in the mid-thoracic spine due to vertebral accessibility at that site and relatively simple surgical approach. However, in order to study the cellular mechanisms that control limb motion and gait, optical access to the regions of the spinal cord containing the highest density of neurons supplying innervation to the limbs - the spinal intumescences - is required. Most mice have 12-13 thoracic vertebrae (with 12-13 corresponding ribs), and 5-6 lumbar vertebrae. The pelvic intumescence is located between L2 and S2, and holds the majority of the neuronal cell bodies from both efferent and afferent tracts to the limb. To achieve optical access to this region, we modified the original surgical procedure to

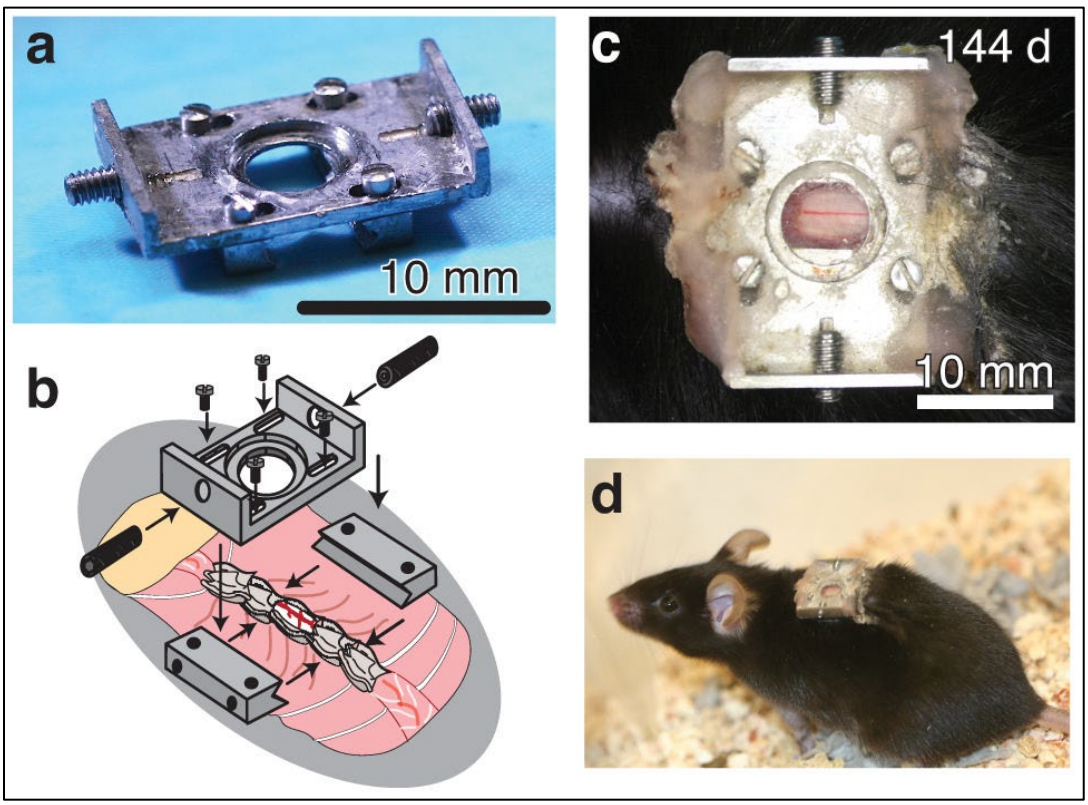

Fig. 4.2 Implanted optical imaging chamber

(a) Photograph of the imaging chamber. Scale bar, 10 mm. **(b)** Schema showing the implantation of the imaging chamber in mice at the T11-T12 vertebra, just below the dorsal fat pad (taupe). **(c)**, Photograph showing the spinal cord imaged through the implanted chamber 144 days after the surgery. Scale bar, 10 mm **(d)** Photograph of a mouse with an implanted chamber (same mouse from panel (c)).

Source: Farrar M, Bernstein I, Schlafer D, Cleland T, Fetcho J, Schaffer B. Chronic in vivo imaging in the mouse spinal cord using an implanted chamber. Nat Methods (2012) 3:297-302.

enable placement of the imaging chamber in the lumbar spine (between L2 and L5) directly over the pelvic intumescence. To implant an imaging chamber in the lumbar spine, an anesthetized mouse is placed in ventral recumbency and the caudal back is clipped and surgically prepped. The wings of the ilium are palpated on either side of the spine and used as caudal landmarks for chamber placement. A 1-2cm linear skin incision is made along the mid to caudal spine, and skin retractors are used to expose underlying epaxial musculature (**Fig 4.3**). Epaxial muscles are bluntly dissected from the dorsal vertebral laminae of 3 consecutive lumbar vertebrae. Lumbar vertebral are identified by their broad, anti-clinal (forward-pointing) dorsal spinous processes (**Fig. 4.4**). Epaxial musculature is much thicker in this region compared to the thoracic spine, and much care must be taken to gently peel and/or rub the musculature from their vertebral attachments to avoid tearing the muscle bellies and causing terminal hemorrhage. Once the dorsal aspects of three vertebrae have been exposed, they are fused together by clamping them on either side with small metal bars held in place by a supporting stereotax. Once the spine is securely clamped into place, vanna scissors are used to transect the dorsal lamina on both the left and right sides of the vertebra in the center of the incision. The dorsal laminar bone is gently lifted to expose the underlying lumbar spinal cord. The dura is left intact.

Because the lumbar vertebral bodies are thicker and broader than those in the thoracic spine, additional pedicle bone must be removed to facilitate chamber placement close enough to the spinal cord to allow imaging. This can be achieved with careful vanna scissor cuts under a dissecting microscope, or through the use of a small

Fig. 4.3 Lumbar chamber surgery

(a) Mouse positioning for lumbar imaging chamber implantation. Caudal back is clipped and prepped. Stars denoted cranial margins of sacrum, which serve as landmarks for chamber placement.

(b) Linear incision over caudal spine

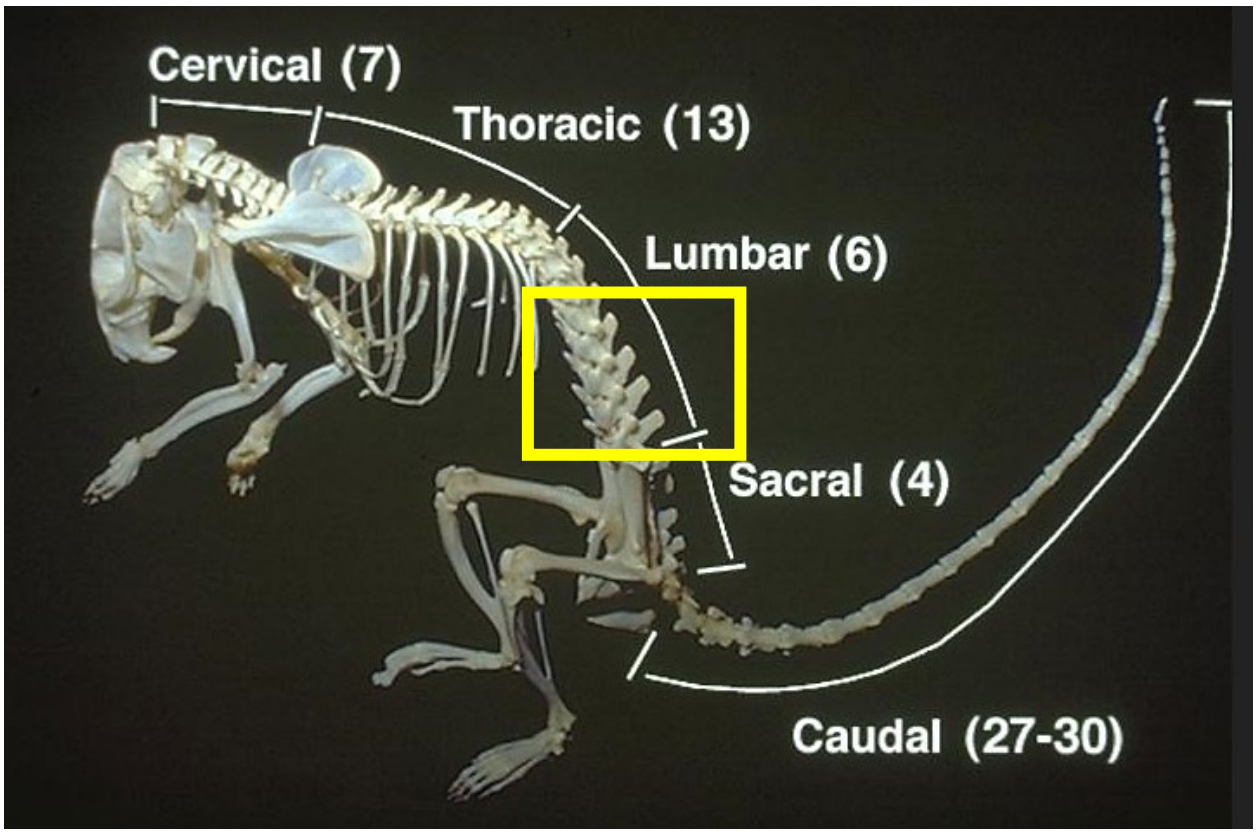

Fig. 4.4 Mouse vertebral formula

Imaging chambers can be implanted in thoracic or lumbar spine. Anti-clinal (forward pointing) dorsal spinous processes in the lumbar vertebrae act as anatomic confirmation of lumbar placement during surgery.

motorized bone burr. In either case, exposed vertebral pedicle bone on either side of the spinal cord is carefully reduced until the spinal cord is laterally exposed on both sides. The remaining exposed pedicle bone is sealed with cyanoacrylate. The top of the chamber is bolted onto the metal clamping bars, thereby fixing the spine to the chamber (**Fig. 4.5**). A minimally optically-scattering silicone elastomer is applied to the spinal cord to fill the space between cord and window, and a glass coverslip is secured into place within the imaging window. The skin is closed around the chamber with tissue glue and dental cement, and the mouse is allowed to recover in a heated cage.

Most imaging chambers remain visibly clear for approximately 1-2 weeks, after which a pale pink haze can be observed obscuring visibility of the underlying spinal cord. We attribute this 'hazy' tissue layer to fibrinous granulation tissues and eventually fibrous scarring. This process occurs more rapidly and more frequently than observed in thoracic chambers, which can often be maintained for weeks to months. Part of the reason for this is likely that compared to thoracic chambers, lumbar chambers are associated with more post-operative hemorrhage under the imaging window, likely due to more the aggressive vertebral bone removal required for implantation. While overt hemorrhage under the imaging window renders a chamber permanently unusable, even a small amount of focal bleeding post operatively delivers a myriad of clotting factors, platelets, and blood-borne immune cells – all of which contribute to local inflammation and rapid development of granulation tissue.

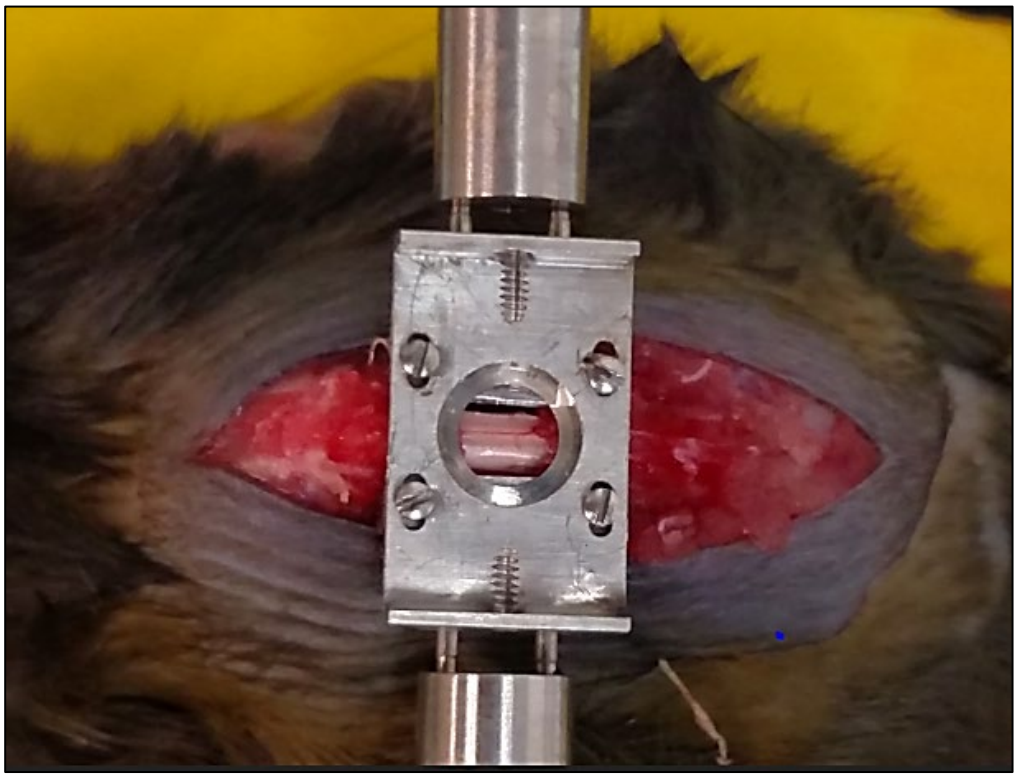

Fig. 4.5 Chamber plate attachment to lumbar spine

Following laminectomy, the top of the chamber is bolted onto the metal clamping bars, thereby fixing the spine to the chamber. Note the exposed spinal cord centered in the imaging window.

With practice, imaging chambers can be successfully implanted in the lumbar spine of juvenile and young-adult mice. Because of the thicker epaxial musculature and larger, denser vertebral bodies in the lumbar spine, chamber placement in older, larger, or obese mice is very challenging, and in our hands associated with excessive hemorrhage and poor chamber attachment to the spine. We have found that surgical access to the lumbar spine in larger animals can be facilitated by placing the animals in a "frog legged" position, in which the hind limbs are drawn as far forward as possible. This extends the spine and tips the pelvis caudally and ventrally, thereby retracting and stabilizing the lumbar spine. Elevating the trunk by draping the mouse over rolled gauze is also helpful. Using the described techniques, we have consistently implanted multiple mice with imaging chambers and confirmed consistent anatomic placement in the L3-L4 region of the spinal cord using post mortem CT imaging (**Fig. 4.6**)

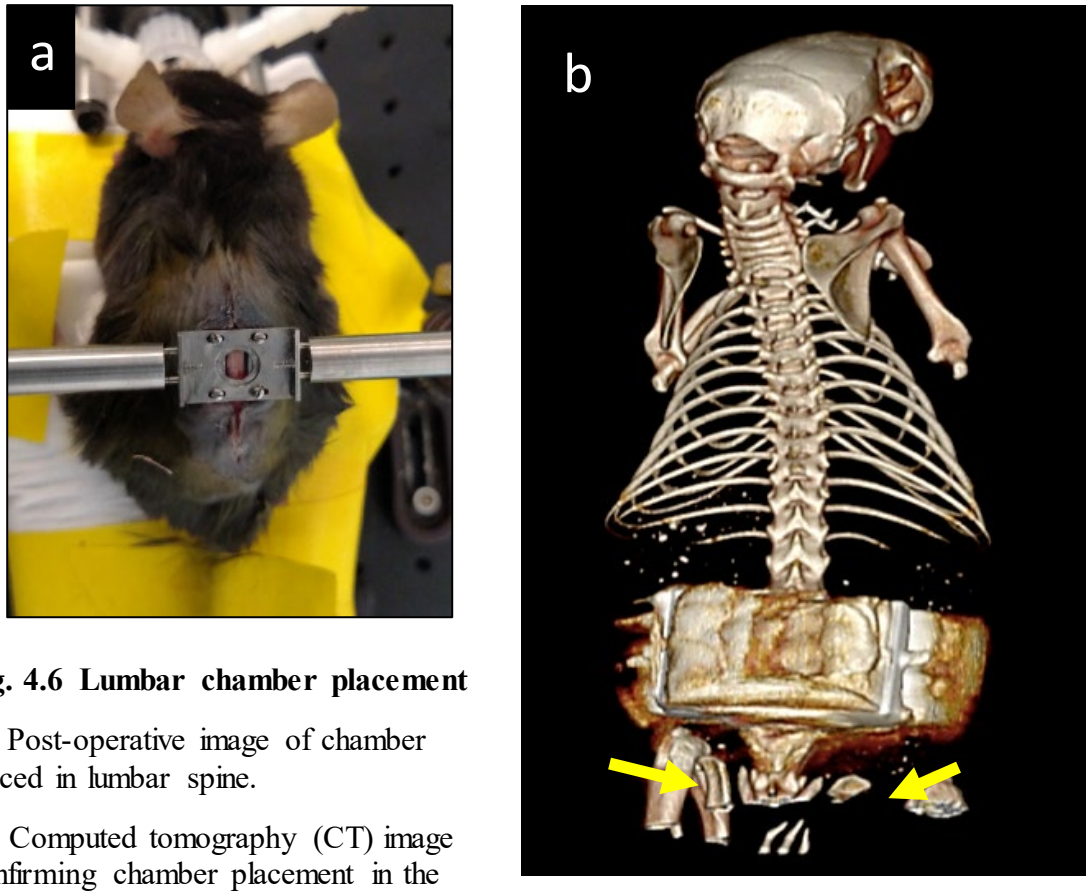

Fig. 4.6 Lumbar chamber placement

(a) Post-operative image of chamber placed in lumbar spine.

(b) Computed tomography (CT) image confirming chamber placement in the caudal lumbar spine. Mice have 12-13 thoracic vertebrae (with corresponding ribs) and 5-6 lumbar vertebrae. The pelvic intumescence is located between L2 and S2. The wings of the ilium (arrows) act as palpable surgical landmarks and form the caudally anatomical limiting structure to chamber placement.

IN VIVO TWO-PHOTON EXCITED FLUORESCENCE IMAGING OF THE INJURED SPINAL CORD REVEALS REAL-TIME CELLULAR INTERACTIONS

A fundamental challenge in the development of treatments for spinal cord injury has been an inability to study dynamic cellular interactions and pathophysiologic mechanisms in live animal models. We have bridged this knowledge gap by developing a suite of imaging tools to enable deep, high resolution, in-vivo imaging of structure, cellular dynamics, and neural activity in the spinal cord and allow for longitudinal studies of spinal cord response to injury and disease.

Using a combination of transgenic mice and exogenous vascular labels, we are able to simultaneously image spinal cord vasculature, axons, and microglia using 2PEF microscopy in the thoracic and/or lumbar spines of live rodents implanted with long-term imaging chambers. Twenty-four hours after chamber implantation windows are generally quite clear and cellular structures can be easily identified at low and high magnification (**Fig. 4.7**). At low magnification (4x) we can observe the dorsal spinous vein and its smaller tributary venules. Some venules course superficially and laterally across the dorsal white matter, while others turn sharply and dive into the spinal cord parenchyma. Compared to the thoracic spine, the lumbar spinal contains a greater number of tributary vessels coursing into the dorsal spinal vein, which likely contributes to the increased propensity for hemorrhage during lumbar chamber placement. Low magnification vascular maps are routinely obtained to serve as a topographical guide for identifying the location of structures during higher magnification imaging. Axons

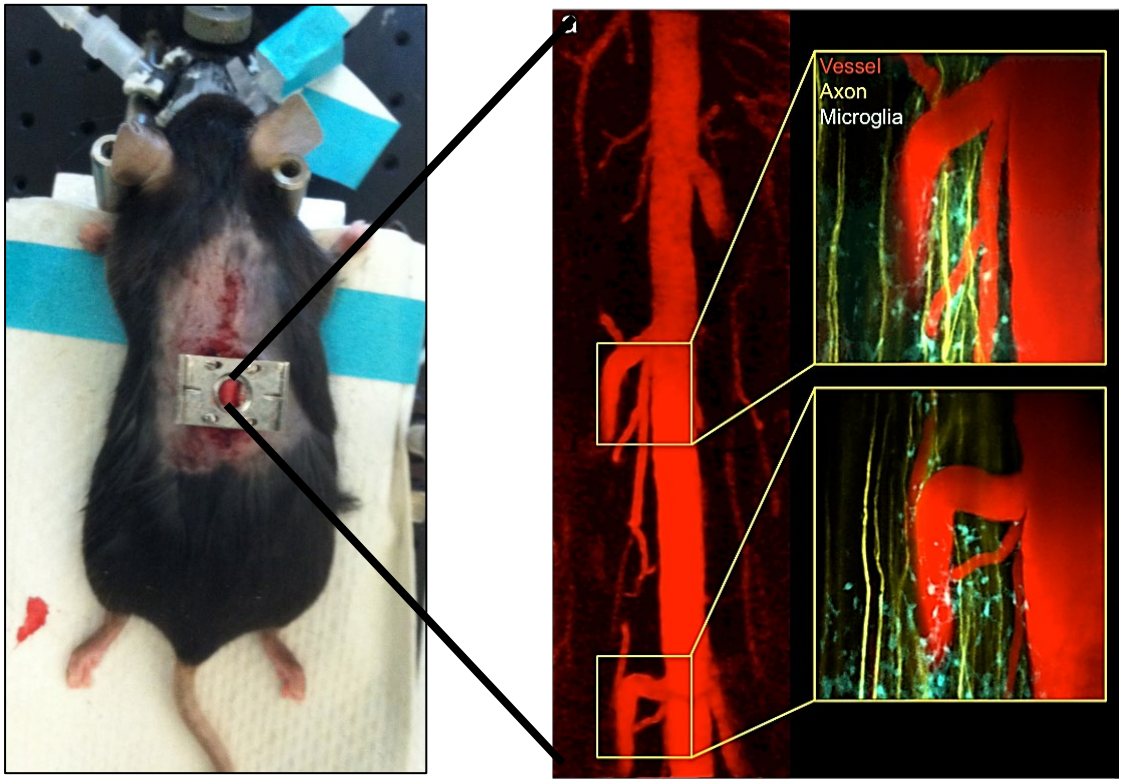

Fig. 4.7 2PEF microscopy image enables in vivo imaging of spinal cord structure

2PEF image from from the lumbar spine in an anesthetized double transgenic mouse obtained 24 hours after chamber implantation. Dorsal spinal vein and its venous tributaries are imaged to create a vascular map (left), while axons and microglia can be observed in higher magnification images (right).

YFP axons (yellow), GFP microglia (green), Texas Red vasculature (red).
4x magnification (left), 20x magnification (right)

comprising the dorsal white matter can be seen coursing parallel along both sides of the dorsal vein, occasionally crossing above or below laterally-traversing venules. There is a predicable microglial response following chamber implantation, characterized by a generalized, homogenous infiltration of the imaging field (**Fig. 4.8**). The density of microglia that migrate to the imaging field is variable, and increases with sloppy surgical technique, surgeries requiring multiple attempts to place the glass coverslip window, and/or hemorrhage necessitating repeated saline flushing of the spinal cord. Similarly, alterations in axonal morphology can indicate damage during surgery, and the presence of axonal blebbing can alert the researcher to potential mechanical or chemical trauma incurred during chamber implantation **(Fig. 4.9)**. Axons are more densely clustered axially near the dorsal spinal vein and grow progressively more sparse laterally in regions where dorsal horn gray matter forms the dorsal root and exits the cord. Axonal tracts become dense again at the lateral aspects of the dorsal white matter, and can be successfully imaged by careful placement of the imaging chamber at a slight angle to preferentially capture the lateral aspects of the spinal cord (**Fig. 4.10**). These laterally positioned axons comprise the spinocerebellar tracts, which supply sensory information from the periphery to the brain via the cerebellum, and represent a potential region of interest for studying proprioception and spatial positioning.

It is important to note that all imaging studies described here are limited to the dorsal aspects of the spinal cord. As mentioned previously, myelinated white matter on the dorsal surface of the spinal cord is highly optically scattering and severely restricts

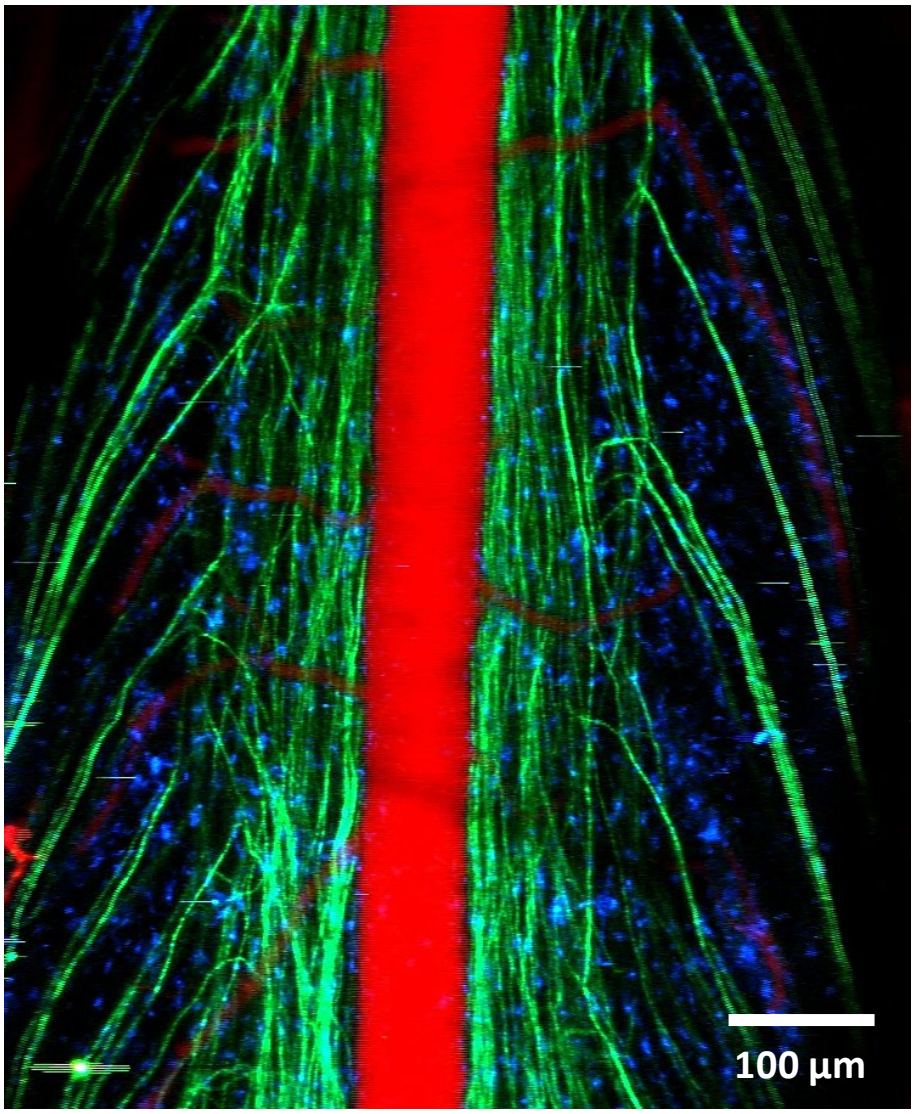

Fig. 4.8 2PEF microscopy image demonstrates widespread post-operative microglial influx

2PEF microscopy image obtained from the lumbar spinal cord 36 hours after chamber implantation. Generalized post-operative microglial infiltration is observed throughout the imaging window. Axonal morphology appears normal, with no visible evidence of surgically-induced trauma.

YFP axons (green), GFP microglia (blue), Texas Red vasculature (red).
4x magnification

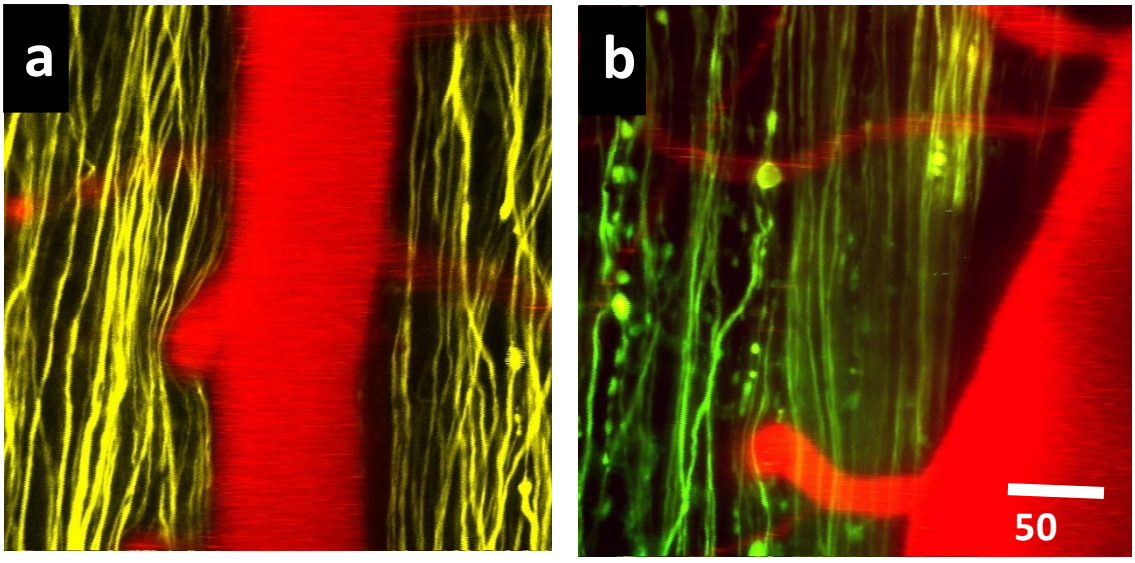

Fig. 4.9 2PEF microscopy image of axonal dynamics

2PEF microscopy images obtained from the lumbar spinal cord of two separate mice 1 hour after chamber implantation.
(a) Healthy, intact axons coursing on either side of the dorsal spinal vein are observed in the image on the left, while (b) while axons displaying evidence of physical damage, including 'blebbing' and fragmentation following inadvertent trauma during chamber implantation surgery.

YFP axons (yellow/green), Texas Red vasculature (red).
20x magnification

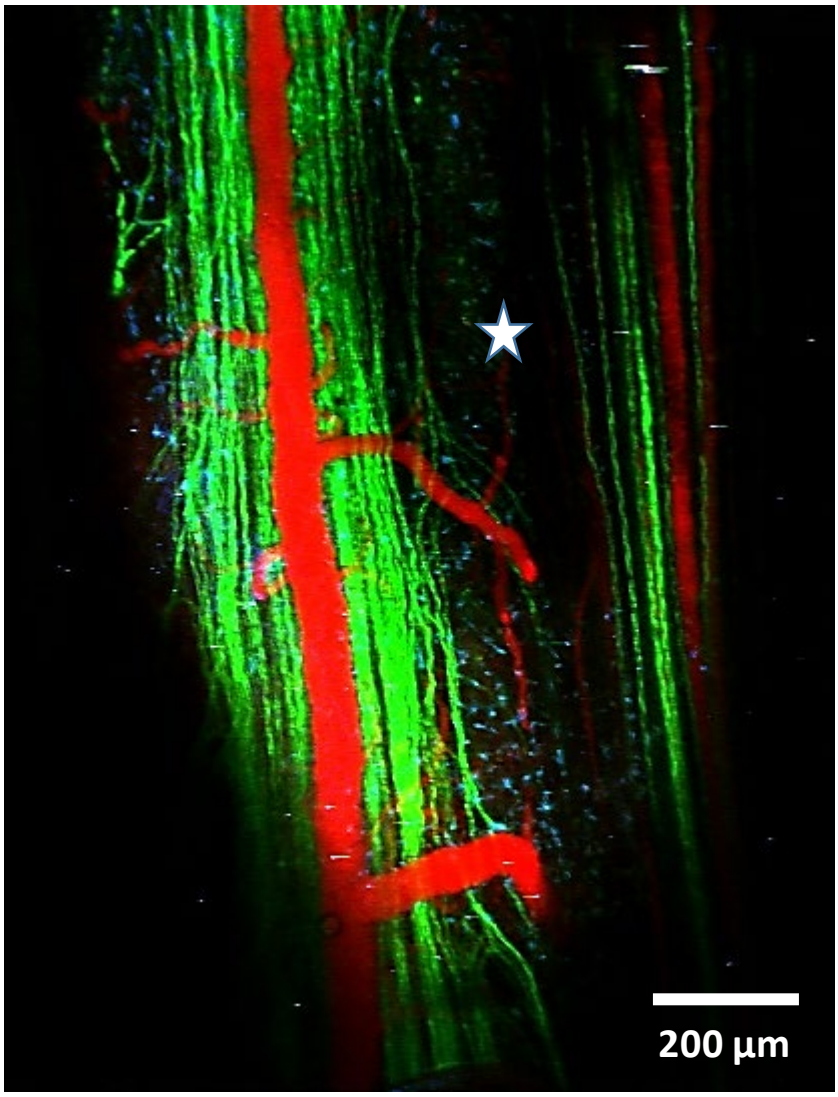

Fig. 4.10 2PEF microscopy of dorsal roots and spinocerebellar tracts

2PEF image from the lumbar spine in an anesthetized double transgenic mouse obtained 24 hours after chamber implantation. The imaging chamber was placed on the spine at a slight angle to better capture the most lateral aspects of the dorsal white matter. Axonal tracts become sparse (star) where dorsal horn gray matter forms the dorsal roots and exit the cord. Axons of the spinocerebellar tracts can be seen coursing laterally in the right aspect of the image.

YFP axons (yellow), GFP microglia (green), Texas Red vasculature (red).
4x magnification

the imaging depth that can be achieved with 2PEF. In practice, it is rarely possible to see through the dorsal white matter, so imaging studies are restricted to visualizing the behavior of the dorsal axons in the top ~150 μm of the spinal cord. Much of the spinal cord functions relevant to motor and gait occur in the mid to ventral spinal cord, and our ability to investigate those regions is greatly limited by the technical constraints of 2PEF. These limitations will be highlighted throughout this work, as they form the primary driving force behind the ongoing transition to next generation, higher order nonlinear microscopy techniques.

In addition to structural imaging studies of healthy spinal cord, we explored methods for *in vivo* 2PEF imaging in established models of SCI such as contusion, crush and transection. Crush, contusion, and compression models of SCI proved to be technically challenging due to localized bruising and damage to surrounding spinal vasculature. Trauma to the blood brain barrier during each of these injuries created hemorrhage throughout the chamber window, largely obscuring optical access to the underlying spinal cord (**Fig 4.11**). Extravasation of blood-borne immune cells, platelets, and clotting factors further prevented imaging long term by encouraging deposition of fibrin and ultimately fibrous scar tissue in the space between the spinal cord and chamber window. The highly scattering dense white matter layers of the spinal cord, coupled with any degree of fibrinous or fibrous tissue, was enough to prevent 2PEF excitation wavelengths from reaching fluorophores within the spinal cord unscattered, thereby preventing image acquisition (**4.12**)

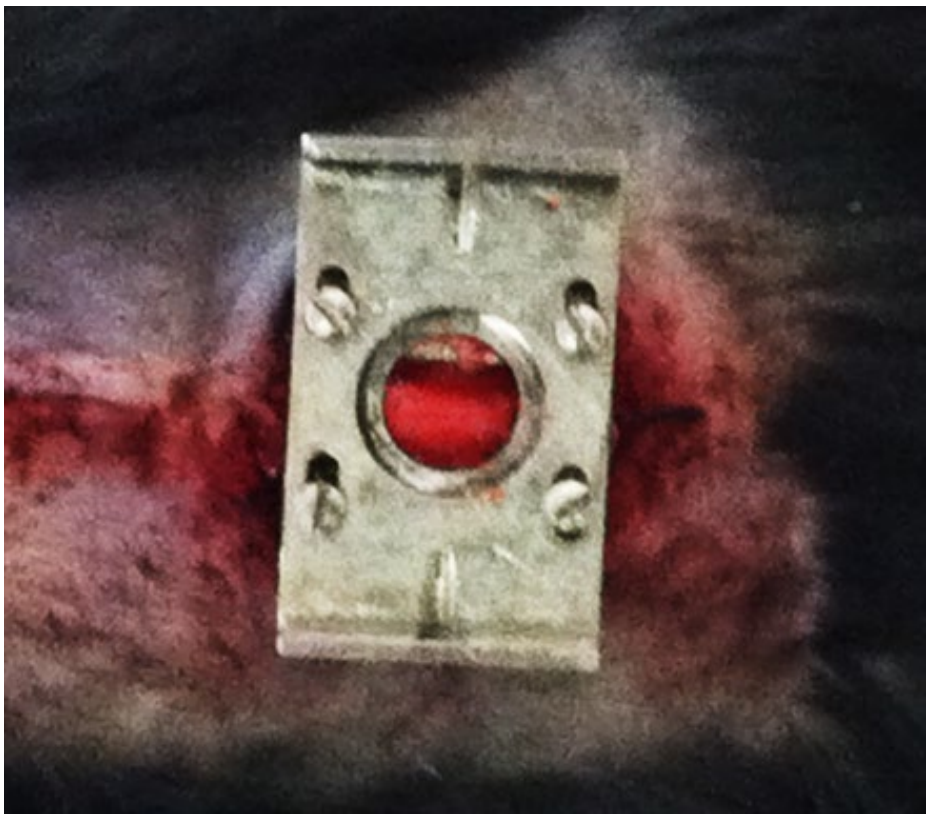

Fig. 4.11 Crush injury induces hemorrhage and bruising

Generalized hemorrhage and bruising observed immediately after crush injury to the lumbar spinal cord.

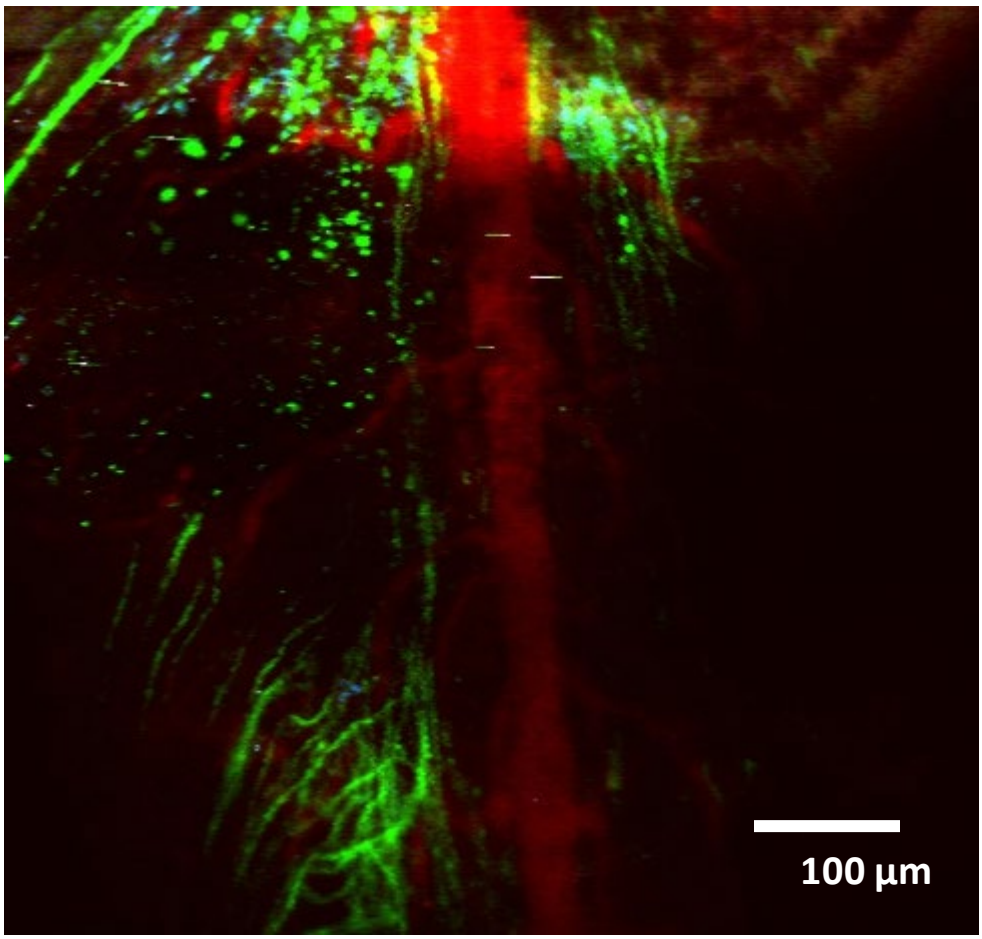

Fig. 4.12 2PEF microscopy following crush injury

2PEF image of lumbar spine obtained from mouse featured in Fig. 4.11. 2PEF imaging immediately after crush injury was largely obscured by optical scattering due to hemorrhage and bruising on the surface of the spinal cord. Extensive axonal fragmentation can be seen proximal to the site of impact. Within 24 hours no structures were visible with the imaging window.

YFP axons (yellow), GFP microglia (green), Texas Red vasculature (red).
4x magnification

In contrast to crush and contusion models, transection of the spinal cord proved to be a viable option for 2PEF SCI imaging. Transection injury was induced during spinal cord chamber implantation surgery, just before placement of the silicone elastomer and cover glass window. Specifically, a 30 ga hypodermic needle was used to create a focal laceration in the dorsal white matter of the spinal cord by inserting the sharp bevel into the cord adjacent to the dorsal vein and pulling it laterally through the spinal cord parenchyma. To prevent excessive hemorrhage, the dorsal spinal vein was avoided, as were any large tributary vessels in the area. We performed unilateral dorsal hemisection injury to enable the contralateral side to be used a comparative control. The white matter tracts severed are superficially located and largely populated with afferent sensory axons, therefore, motor deficits were not observed in our mice following surgery. Using this injury model, both immediate and delayed responses by the vascular and immune systems could be observed. Following unilateral dorsal hemisection to the lumbar spinal cord, we observed immediate local intra-lesional hemorrhage followed by rapid axonal blebbing, die-back, and fragmentation. Damaged axons continued to degenerate for days after injury, sometimes regressing completely out of the imaging window. Uninjured axons on the contralateral side of the cord remained largely unchanged throughout the imaging period, and appeared to be unaffected by the inflammatory processes occurring in the adjacent injured side (**Fig. 4.13**).

Observation of transection injury sites at higher magnification revealed distinct phases of phagocytosis and neovascularization. Immediately following injury, local intralesional hemorrhage was observed. This hemorrhage ceased with the formation of

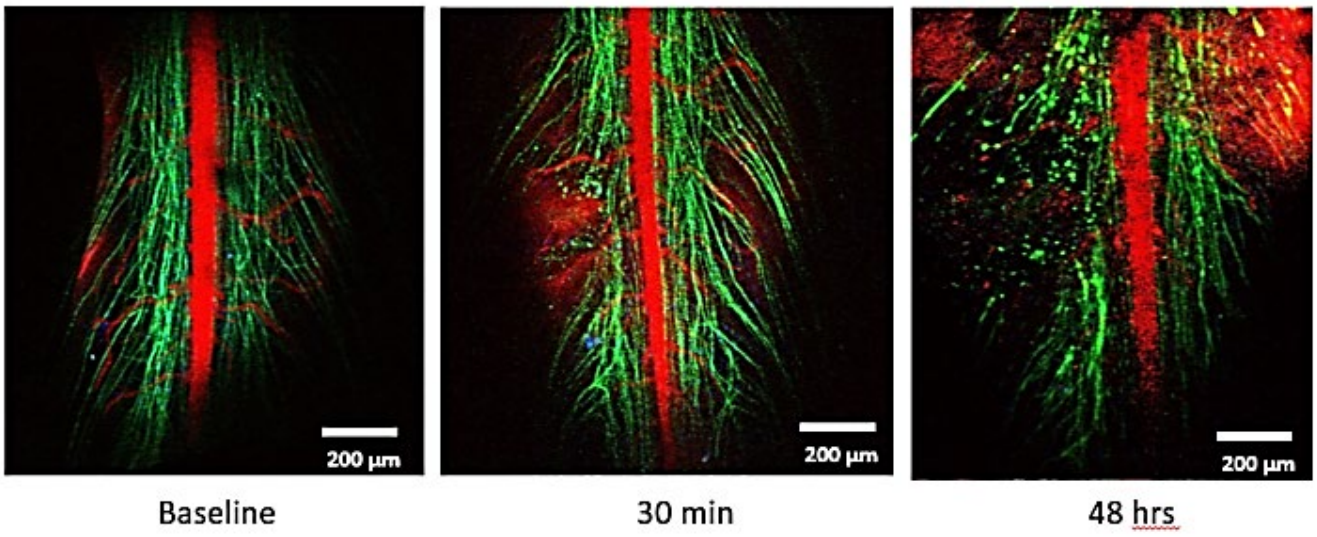

Fig. 4.13: Axonal fragmentation and prolonged die back following unilateral dorsal hemisection

2PEF time-lapse images of a mouse spinal cord before, 30 minutes, and 48 hours after unilateral dorsal hemisection injury. Note axonal blebbing (green), microglial migration (blue), and local hemorrhage at 30 minute time point. At 48 hours extensive axonal dieback and fragmentation was observed. The contralateral side to injury remained largely unaffected throughout the imaging period.

YFP axons (green), GFP microglia (blue), Texas Red vasculature (red).
4x magnification

a stable structure within the transection site, presumably a thrombus. At 24 hours following injury, both hemorrhage and thrombus had resolved and abundant resident microglia were noted at the site of injury. Many of these microglia assumed close proximity to severed and fragmented axons and appeared to phagocytose axonal and cellular debris. Interestingly, within 48 hours of injury signs of neovascularization and early angiogenesis was observed infiltrating the void left behind by axonal die-back (**Fig. 4.14**). This rapid neovascularization is similarly observed in cerebral stroke studies performed in our lab.

Taken together, we have identified and refined an injury model suitable for *in vivo* 2PEF microscopy that allows for direct observation of detailed cellular responses to acute spinal cord injury. The ability to serially observe real-time cellular interactions and axonal dynamics in the presence of active biologic input from the surrounding environment is something not possible prior to the introduction of *in vivo* imaging techniques. Through nonlinear optics, we now have a method for future studies utilizing direct observation as a means to answer questions about efficacy of therapeutic intervention on spinal cord repair following injury. For example, how does microglial inhibition affect axonal dieback? Can growth factors and/or regenerative scaffolds be introduced to stimulate axonal regrowth across the injury site?

While this work represents a monumental improvement over previous ex-vivo and post-mortem imaging techniques, there are substantial limitations and hurdles yet to be overcome. Of primary significance is optical interference from highly-scattering superficial myelination precluding imaging any deeper than dorsal white matter axons.

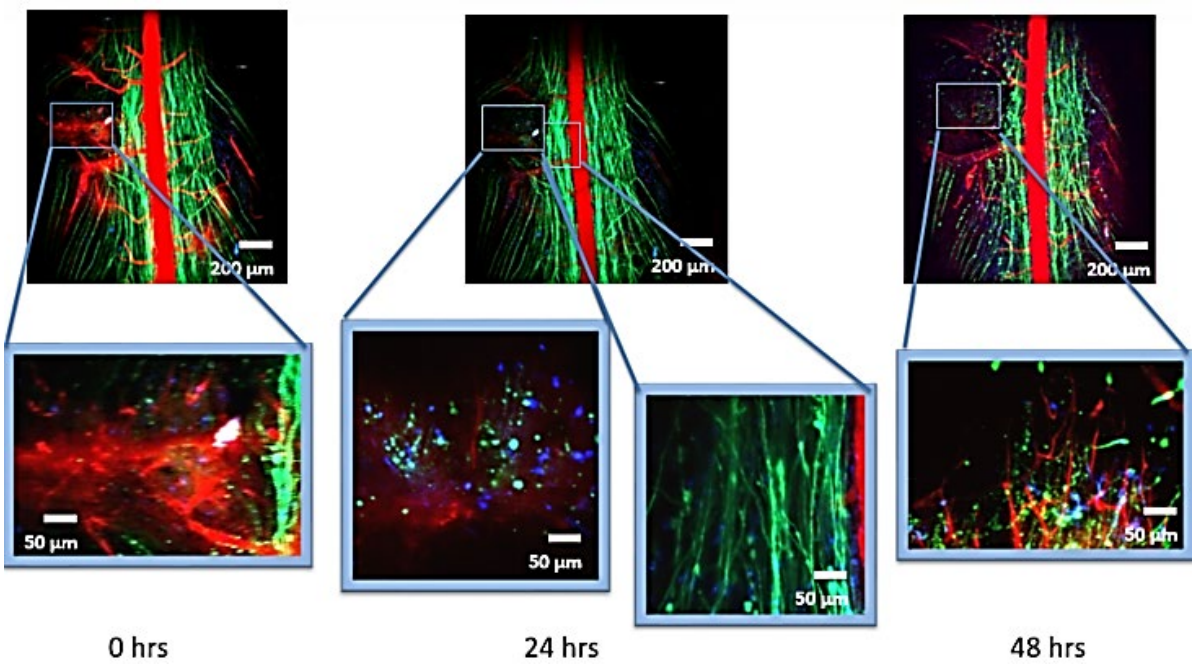

Fig. 4.14 Cellular interactions mediating thrombus formation, phagocytosis and angiogenesis following unilateral dorsal hemisection

2PEF time-lapse images of a mouse spinal cord at time 0, 30 minutes, and 48 hours after dorsal hemisection injury. 4x magnification images are presented in top row with selected 20x magnification images displayed in bottom row. Note hemorrhage and thrombus formation at injury site at time 0, followed by microglial migration (blue) at 24 hrs. Normal appearing, intact axons (green) and few microglia can be seen adjacent to the injury site at 24 hrs. By 48 hours signs of revascularization is noted at the injury site.

YFP axons (green), GFP microglia (blue), Texas Red vasculature (red).

Even in the clearest of surgical preps, 2PEF has only been successful at producing cell-resolved images down to approximately 150 um below the spinal cord surface, leaving the majority of the functional regions of the cord optically inaccessible. Furthermore, the optical scattering introduced by inflammation and hemorrhage at the site of injury precludes imaging multiple injury models throughout the acute and chronic stages. The highly scattering dense white matter layers of the spinal cord, coupled with any degree of post-operative hemorrhage and inflammation, is enough to prevent 2PEF excitation wavelengths from reaching fluorophores within the spinal cord unscattered, thereby preventing image acquisition. While studies of detailed cellular dynamic are still possible, limited depth penetration and loss of resolution greatly limit the types of SCI models that can be used, as well as physiologic questions that can be feasibly answered.

Looking toward the future, the limited imaging depth of 2PEF can be improved by using higher-order nonlinear processes. Using recently developed three-photon processes to excite fluorescent dyes allows high signal to noise imaging at a much greater depth than possible with 2PEF. In chapter 7 we discuss the limitations of 2PEF microscopy and introduce three-photon excited fluorescence (3PEF) as a promising cutting edge technique for overcoming optically scattering superficial tissues layers in the spinal cord.

REFERENCES

- Farrar M, Bernstein I, Schlafer D, Cleland T, Fetcho J, Schaffer B. Chronic in vivo imaging in the mouse spinal cord using an implanted chamber. Nat Methods (2012) 3:297-302.
- Josvay K, Winter Z, Katona R, Pecze L, Marton A, Buhala A, Szakonyi G, Olah Z, Vizler C. Besides neuro-imaging, the Thy1-YFP mouse could serve for visualizing experimental tumours, inflammation and wound-healing. Scientific Reports (2014) 4:6776.
- Jung F, Aliberti J, Graemmel P, Sunshine MJ, Kreutzberg GW, Sher A, Littman DR. Analysis of frackaline receptor CX(3)CR1 function by targeted deletion and green fluorescent protein reporter gene insertion. Mol Cell Biol (2000) 11:4106-14.
- Rosenzweig E, McDonald J. Rodent models for treatment of spinal cord injury: research trends and progress toward useful repair. Curr Opin Neurol (2004) 2:121-31.
- Silva NA, Sousa N, Reis RL, et al. From basics to clinical: a comprehensive review on spinal cord injury. Prog Neurobiol (2014) 114:25-57.

CHAPTER 5

IN VIVO TWO-PHOTON EXCITED FLUORESCENCE MICROSCOPY IN A NEUROPATHIC PAIN MODEL

Figure acknowledgements:

Fig. 5.1 Models of peripheral nerve injuries in rodents
Campbell J, Meyer R. Mechanisms of Neuropathic Pain. Neuron (2006) 52:77-92.

Fig. 5.2 Spared nerve injury (SNI) surgical procedure
Bourquin A, Suveges M, Pertin M, Spahn D, Decosterd. Assessment and analysis of mechanical allodynia-like behavior induced by spared nerve injury (SNI) in the mouse. Pain (2006).

Just as there remain many unanswered questions regarding cellular mechanisms of SCI and repair, the cellular cascade of events that lead to the development of neuropathic pain remain largely unelucidated. Of particular research interest are the mechanisms by which microglial-mediated inflammation in the spinal cord alter dorsal horn neural activity and ultimately lead to chronic pathologic pain. The methodology we have developed for in vivo imaging of SCI has proven to be well suited for observing microglia in the dorsal spinal cord, and with the addition of appropriate rodent models of neuropathic pain, we can begin to build the armamentarium of tools needed to study this complex sensory disorder.

NEUROPATHIC PAIN RESEARCH IN MICE: MODELS OF INJURY AND ASSESSMENT

Neuropathic pain can be experimentally induced in rodents through a variety of central and peripheral nervous system injuries known to create the hallmark signs of spontaneous pain, allodynia and hyperalgesia. Allodynia is defined as a painful response to a normally non-noxious stimulus, while hyperalgesia is defined as an increased sensitivity to pain. Ideally, models of neuropathic pain should be characterized by only sensory dysfunction, which no associated motor impairment.

Peripheral nerve injuries are excellent models for neuropathic pain, and reliably produce repeatable, testable signs of allodynia and hyperalgesia in the limb affected. Surgical variations of peripheral nerve injury include partial sciatic transection, rhizotomy, sciatic nerve ligation, spinal nerve ligation, and spared nerve

injury **(Fig. 5.1)** (Campbell 2006). Of these, the spared nerve injury (SNI) is the most widely used experimental model, due to its relatively simple surgical procedure, straight forward nerve accessibility, and rapid post-operative recovery. To induce this injury, animals are anesthetized and the three terminal branches of the sciatic nerve (the sural, tibial, and common peroneal) are exposed via an incision through the lateral thigh. The tibial and common peroneal nerves are ligated and transected, while the sural nerve is left intact (**Fig. 5.2**). Sparing the sural nerve maintains sensory innervation to the hind paw and contributes to the development of neuropathic pain, particular in its autonomous zone of the lateral plantar paw. Following SNI, animals develop self-protection behaviors and have exaggerated responses to mechanical and thermal stimuli within 4 days after surgery, and these signs persist for several weeks to months following injury (Sousa 2016).

Assessment of neuropathic pain in rodent models involves both qualitative and quantitative measurements. Qualitative assessment documents the presence of hallmark signs of spontaneous pain and over-sensitization to tactile stimuli: repeated lifting of the paw, excessive grooming of the affected paw with or without self-mutilation, reluctance to utilize the affected paw for normal standing/moving behavior.

Quantitative assessment of neuropathic pain is most often achieved using the Von Frey filament test. In this test, a series of small, monofilament hairs are applied to the plantar surface of the paw to assess the mouse's reactivity to tactile stimuli. A series of filaments of varying stiffness (ranging from 0.008g to 4g, measured in grams

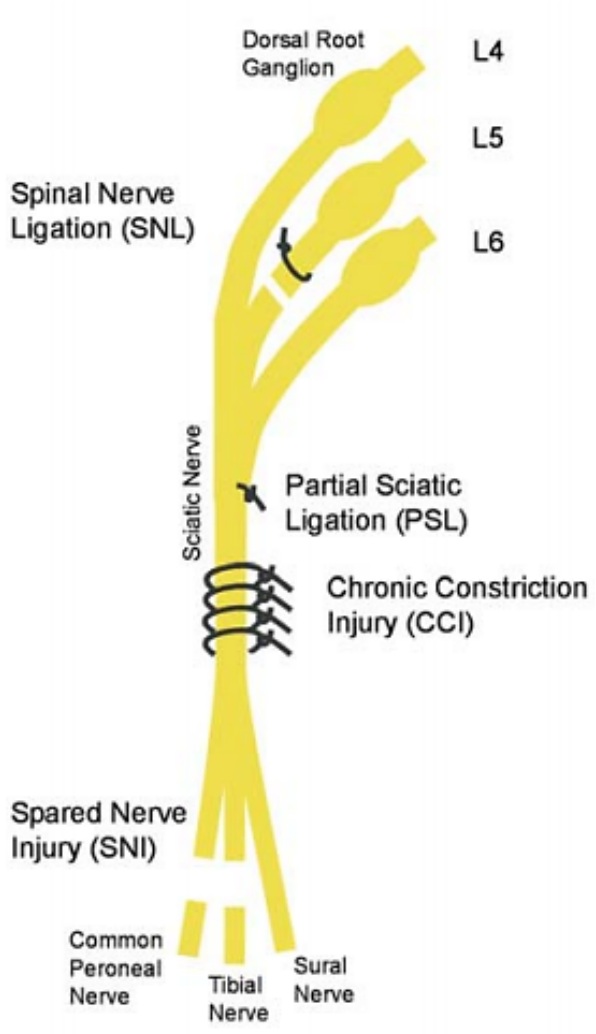

Fig. 5.1: Models of peripheral nerve injuries in rodents

Four different nerve injury models are shown. In the spinal nerve ligation (SNL) model, one or more spinal nerves going to the foot are ligated and cut (Kim and Chung, 1992). In the partial sciatic ligation (PSL) model, a portion of the sciatic nerve is tightly ligated (Seltzer et al., 1990). The chronic constriction injury (CCI) model involves placement of four loose chromic-gut ligatures on the sciatic nerve. An immune response to the sutures leads to nerve swelling and nerve constriction. In the spared nerve injury (SNI) model, the common peroneal and tibial nerves are cut, sparing the sural nerve (Decosterd and Woolf, 2000). In each model, only a portion of the afferents going to the foot are lesioned.

Source: Campbell J, Meyer R. Mechanisms of Neuropathic Pain. Neuron (2006) 52:77-92.

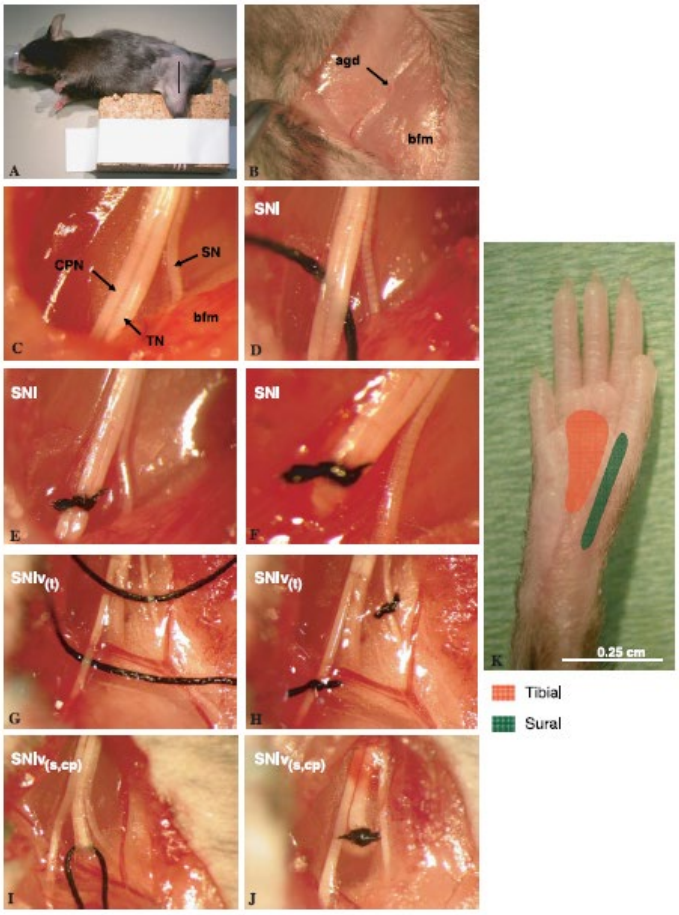

Fig. 5.2: Spared nerve injury (SNI) surgical procedure

(A) Anesthetized mouse positioning and incision mark on left hind thigh. The paw is immobilized in an extended and slightly elevated position. (B) The biceps femoris muscle is exposed and the artery genus descendes is used as a landmark for direction of muscle incision. (C) Exposure of the sciatic nerve and peripheral branches: common peroneal, tibial and sural nerves. (D) The 6.0 silk thread is slipped under the common peroneal and the tibial nerves. The nerve dissection is minimal and any contact with the sural nerve is avoided. (E) Ligature of the common peroneal and the tibial nerves. (F) The ligated nerves are transected distally and a 2 mm section is removed. Care is taken to avoid the sural nerve completely. (G and H) The ligation is placed around the common peroneal and sural nerves, leaving the tibial nerve intact in the SNIv(t). (I and J) The tibial nerve is injured in the SNIv(s,cp), while the sural and common peroneal nerves are spared by the procedure. (K) Plantar view of the left hindpaw. The colored area on the photograph corresponds to the sural/tibial nerve skin territory that is stimulated with the von Frey monofilaments. Notice that glabrous/hairy border is carefully avoided. bfm, biceps femoris muscle; agd, genus descendes artery; CPN, common peroneal nerve; TN, tibial nerve; SN, sural nerve.

Source: Bourquin A, Suveges M, Pertin M, Spahn D, Decosterd. Assessment and analysis of mechanical allodynia-like behavior induced by spared nerve injury (SNI) in the mouse. Pain (2006)

of applied pressure before the filament bends) are applied in ascending order from weakest to strongest stimulus. The 'withdrawal threshold,' is defined as the weakest filament that evokes ≥2 positive paw withdrawal responses. The test is performed on both the injured and non-injured (control) limbs. Mice suffering from neuropathic pain display lower withdrawal thresholds and higher withdrawal frequencies in the affected paws when compared to uninjured control paws (Bourquin 2006). One downside of the Von Frey assessment is the potential for mice to become desensitized to larger diameter filaments, resulting in a reduced pain response to increased force stimuli.

IN VIVO TWO-PHOTON EXCITED FLUORESCENCE IMAGING IN A MOUSE MODEL OF NEUROPATHIC PAIN REVEALS MICROGLIAL-MEDIATED INFLAMMATION

Much controversy exists regarding the complicated interplay of central microglial inflammation following peripheral nerve injury and the development of the chronic spinal cord over-sensitization that characterizes neuropathic pain. Independent studies have demonstrated that, 1. Microglial migration and activation within the dorsal horn of the spinal cord is necessary for the development of neuropathic pain in rodent models (Peng 2015, Gu 2016), and, 2. Dorsal horn neurons from animals with neuropathic pain display aberrant, spontaneous firing patterns of activity (West 2015), yet no study to date has demonstrated the two processes occurring simultaneously, nor have any studies attempted to elucidate the link between these two overlapping

mechanisms *in* vivo. Hypotheses proposing that peripheral nerve injury leads to microglia activation adjacent to afferent tracts of affected sensory neurons within the spinal cord could be confirmed using the *in vivo* 2PEF imaging methods we've developed for studying SCI. Additional hypotheses suggesting that these activated microglia drive rewiring of the local neural network and bias toward an overly excitatory network – and subsequent neuropathic pain disorder - could be investigated using functional neural imaging, which is discussed in the next chapter.

We have attempted to address this paucity of knowledge by developing methods for *in vivo* imaging of rodent models of neuropathic pain using the same 2PEF spinal cord imaging techniques developed for SCI. First, we performed simultaneous SNI surgery and lumbar imaging chamber implantation in juvenile double-transgenic mice expressing YFP and GFP in axons and neurons, respectively. Mice were assesses for the development of neuropathic pain with the Von Frey filament test every 3 days for 21 days post operatively. 2PEF imaging was performed every three days for as long as window clarity allowed.

Mice with unilateral SNI developed signs of allodynia and hyperalgesia within 4 days following surgery, displayed behavioral signs of excessive grooming, self-mutilation, and paw guarding. Lowered withdrawal thresholds were noted in paws ipsilateral to SNI as assessed by the Von Frey filament test beginning at day 3 and continuing throughout the 3 week study period (**Fig. 5.3**). When imaged using 2PEF, mice exhibited microglial migration in the lumbar spinal cord at day 1 following surgery (**Fig. 5.4**). This microglial influx was noted on both the contralateral ipsilateral sides to

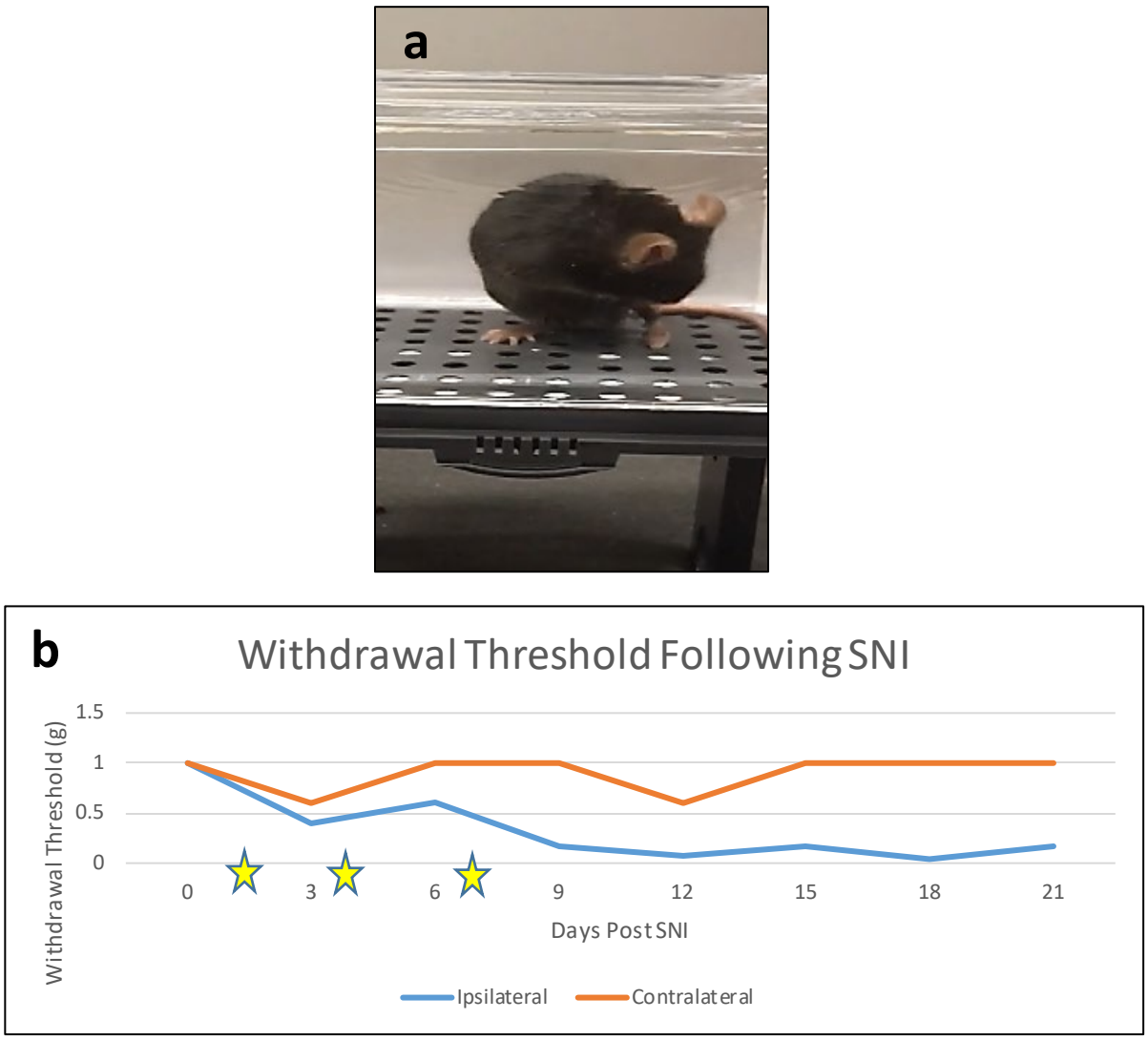

Fig. 5.3 Assessment for neuropathic pain following SNI

(a) Mouse displaying signs of neuropathic pain 16 days post left-sided SNI procedure. Note 'cupped' paw stance and preferential grooming behavior. This mouse licked the affected paw excessively to the point of self-mutilation.

(b) Withdrawal threshold is decreased in ipsilateral paw of a mouse with SNI. Withdrawal threshold was assessed by Von Frey filament test in the ipsilateral and contralateral paws every three days for 21 days following SNI. 2PEF imaging sessions are denoted with stars.

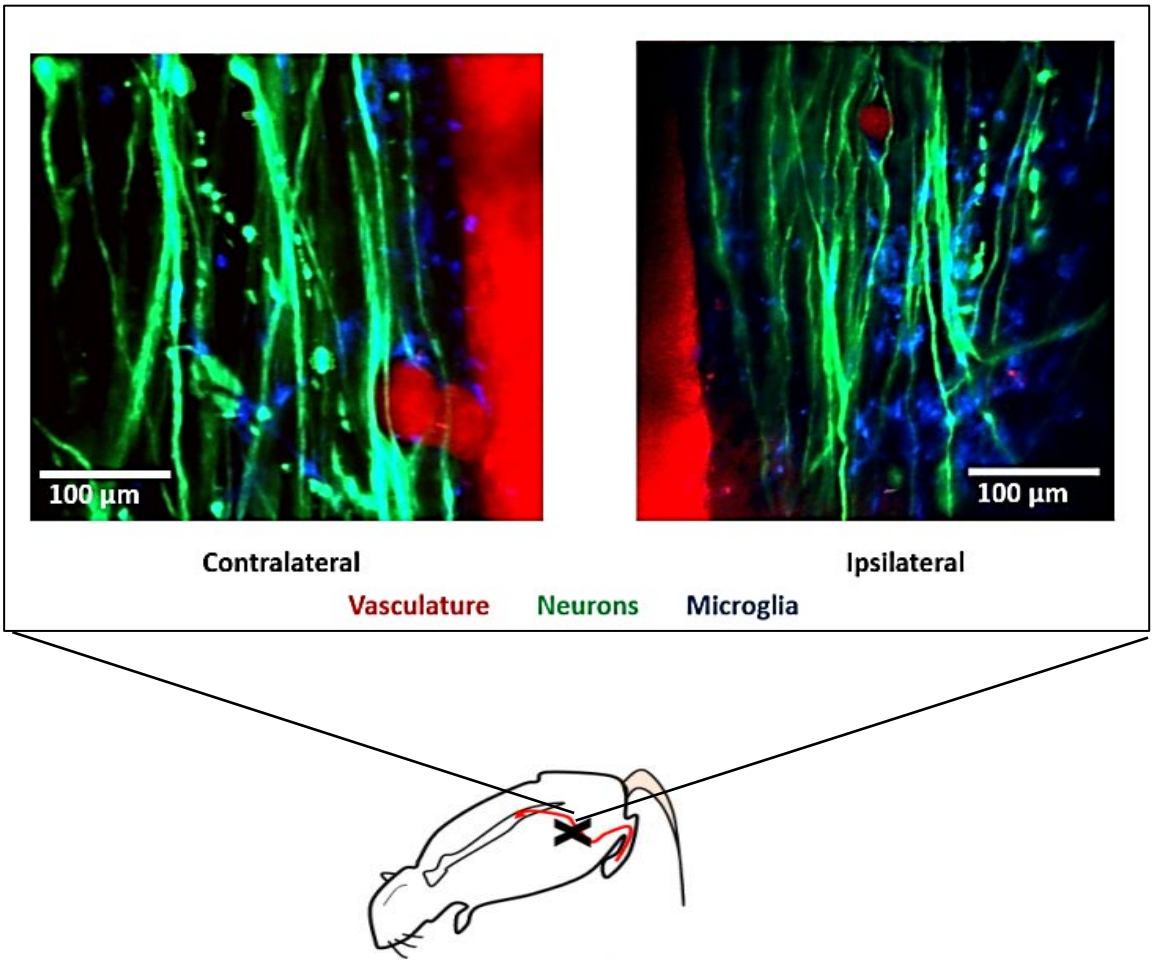

Fig. 5.4 Microglial inflammation in the dorsal spinal cord following SNI

2PEF image from the lumbar spine in an anesthetized mouse demonstrating microglial migration and activation following unilateral spared nerve injury (Marked with X). Microglia can be observed on both the contralateral and ipsilatersal sides to the nerve injury.

YFP axons (green), GFP microglia (blue), Texas Red vasculature (red).
20x magnification

SNI, and persisted beyond when the spinal cord window became optically inaccessible; generally around 5 days post-operatively. After approximately 1 week, the chamber windows became hazy with reactive fibrinous and fibrous tissues, preventing serial imaging long term. While it subjectively appeared that microglial were more densely populated on the side ipsilateral to the SNI procedure, which would corroborate several ex vivo study findings, the generalized inflammatory response that occurred in the days following imaging chamber implantation confounded objective quantification of the microglial response. When observed under higher magnification, migrating microglia closely associate with dorsal column axons and assume an elongated, dendritic morphology indicative of activation (**Fig. 5.5**). This finding has been reported in other studies of neuropathic pain utilizing immunohistochemical stains for markers of microglial activation (Peng 2015).

Clearly there are substantial hurdles yet to be overcome before we can use 2PEF to elucidate the role of microglial inflammation in neuropathic pain. Of primary importance will be the ability to maintain optical access to the spinal cord for weeks to months following chamber implantation. This would enable one to implant the imaging chamber and wait 2-3 weeks for any surgical inflammation to resolve before performing a SNI at a later date, thereby preventing any confounding overlap of the two inflammatory processes. As mentioned previously, higher order nonlinear optical methods, such as 3PEF, have the ability to penetrate deeper into scattering tissues and would likely suffer much less attenuation (and therefore less resolution degradation) from a layer of reactive scar tissue as compared to 2PEF imaging. 3PEF would

additionally enable us to explore the other critical component of neuropathic pain – altered neural activity patterns in the dorsal horn. In the next chapter, the transition to next generation 3PEF imaging will be introduced as a method to overcome many of the optical and technical challenges to 2PEF imaging.

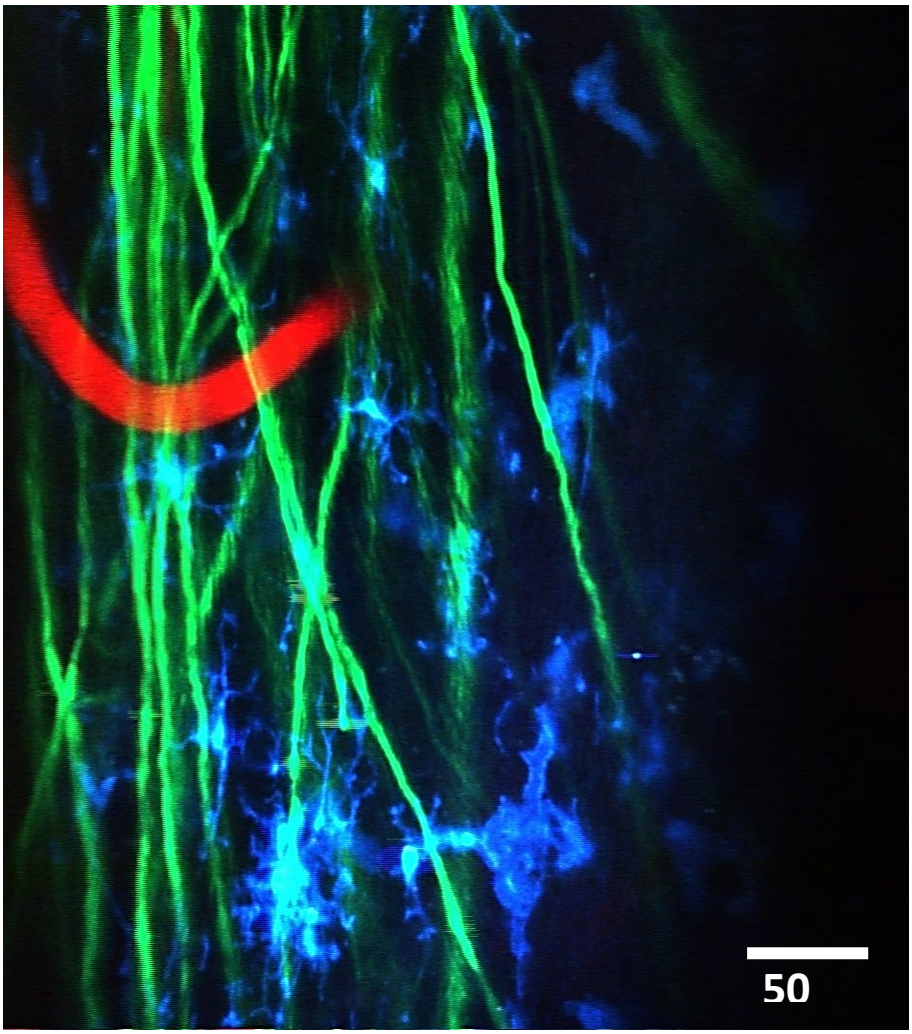

Fig 5.5 Microglial activation and dendritic morphology in response to SNI

2PEF microscopy image from the lumbar spinal cord of a mouse 3 days post-SNI procedure. Note microglia displaying activated, dendritic phenotypes (blue).

YFP axons (green), GFP microglia (blue), Texas Red vasculature (red).
20x magnification

REFERENCES

- Bourquin A, Suveges M, Pertin M, Gilliard N, Sardy S, Davison A, Spahn D, Decosterd. Assessment and analysis of mechanical allodynia-like behavior induced by spared nerve injury (SNI) in the mouse. Pain (2006) 122.
- Campbell J, Meyer R. Mechanisms of neuropathic pain. Neuron (2006) 52:77-92.
- Gu N, Eyo U, Murugan M, Peng J, Matta S, Dong H, Wu L. Microglial P2Y12 receptors regulate microglial activation and surveillance during neuropathic pain. Brain Behav Immun (2016) 55:82-92.
- Peng J, Gu N, Zhou L, Eyo U, Murugan M, Gan W, Wu L. Microglia and monocytes synergistically promote the transition from acute to chronic pain after nerve injury. Nature Communications 2015.
- Sousa A, Lages G, Pereira C, Slullitel A. Experimental models for the study of neuropathic pain. Revista Dor (2016) 17.
- West S, Bannister K, Dickenson A, Bennett D. Circuitry and plasticity of the dorsal horn – toward a better understanding of neuropathic pain. Neuroscience (2015)300:254-75.

CHAPTER 6

FUNCTIONAL SPINAL CORD IMAGING

Figure acknowledgements:

Fig. 6.1: Crystal structure of GCaMP
http://www.jbc.org/content/284/10/6455/F1.large.jpg,
Akerboom J, Rivera JDV, Guilbe MMR, etc al. Crystal structures of the GCaMP calcium sensor reveal the mechanism of fluorescence signal change and aid rational design. J Bio Chem 2009: 284(10): 6455-6464.

Unravelling the functional organization of neuronal networks and linking cellular activity to behavioral outcomes are among the biggest challenges in contemporary neuroscience. Though much correlative work has been done utilizing traditional electrophysiological and behavioral approaches, much remains to be learned about the sensory and locomotor networks that together work in concert to facilitate locomotion, gait, and movement. Similarly, the functional organization of neural circuits underlying nociception, pain modulation, and sensory disorders such as neuropathic pain remain largely unknown.

Despite the importance of understanding how these circuits work and how they fail after spinal cord injury or in disease, there is no existing approach to directly measure the patterns of activity across a large ensemble of spinal cord neurons in awake, moving animals. Electrophysiology has made some progress in this area by enabling one to interrogate action potentials and conductivity across specific regions of interest, but isn't able to access the dense spatiotemporal patterns of activity that likely underlie complex nervous system functions. In this chapter, the currently knowledge gap in spinal cord circuitry is introduced, as well as the promise of newer research tools, such as in vivo calcium imaging, for elucidating the ways in which the spinal cord creates and transmits information.

Finally, a newly developed awake imaging system that enables in vivo imaging to be performed on an awake, spine-fixed mouse while walking or running on a treadmill is described. This set up will build upon all components of in vivo imaging currently available, amalgamating multiphoton imaging, functional calcium recording,

and kinematic gait analysis in a system that will ultimately enable correlation of cellular level activity with gross level motor function in a way never before possible.

SPINAL CORD CIRCUITRY

Locomotor circuits within the spinal cord are responsible for facilitating motor neuron output to the musculoskeletal system in such a way that their activity produce coordinated, rhythmic patterns of movement. Even the simplest of gaits is a synchronized cycle in which extensor-flexor muscle groups, left-right pairs of limbs, and front-hind pairs of limbs all move in cycle to maintain constant weight support and produce forward, steady propulsion. While spinal locomotor activity is constantly modulated and regulated by supraspinal input from the motor cortex, basal ganglia, and midbrain, it is known that populations of neurons within the spinal cord are capable of autonomously producing alternating left-right limb movements and rudimentary gait patterns. These gait-generating groups of interneurons, termed central pattern generators (CPGs), are located in the central-gray matter of the spinal cord, and their intrinsic ability to create coordinated movement have been the focus of much recent spinal circuit research (Kiehn 2016). Mice display four natural gaits: walk, trot, bound, and gallop. While it is well-established that genetically-driven ablation of specific subsets of CPGs abolish the ability to produce one or more of these gaits, the activity patterns of neural firing and functional connectivity underlying these alterations in gait generation have not yet been fully elucidated.

Similarly undefined are the neural activity patterns and circuit organization underlying chronic pain disorders and spinal cord sensitization. While there is general consensus regarding organization of the normal nociceptive pathways that transmit sensory information from the periphery to the dorsal horn of the spinal cord and ultimately up to the brain, very little is known about how these circuits malfunction and/or maladapt and result in pathologic symptoms of allodynia, hyperalgesia, and spontaneous pain. Furthermore, the specific cellular contributions from the local environment and immune system, such as microglial migration and activation, remain largely unknown. Electrophysiological studies have demonstrated spontaneous, repeated firing activity with the spinal cord dorsal horn in rodent models of neuropathic pain, leading to hypotheses of dysregulated neuronal firing and loss of inhibition as an underlying mechanism of neuropathic pain (West 2015).

GENETICALLY-ENCODED CALCIUM INDICATORS ENABLE IMAGING OF REAL-TIME NEURAL ACTIVITY

Calcium dynamics are a proxy to monitor firing activity in neurons, as action potentials lead to calcium transients in the cytosol through voltage-gated calcium channels. This intracellular rise in calcium levels is reversed following the action potential as calcium is buffered and pumped back into internal stores and the extracellular environment.

Fluorescent genetically encoded calcium indicators (GECIs), such as GCaMP, take advantage of intracellular calcium fluxes to enable real-time, high signal-to-noise,

fluorescence based imaging of neural activity in neurons and other calcium-transient dependent cells. GCaMP is created from a fusion of GFP, calmodulin, and M13, a peptide sequence from myosin light chain kinase (Nakai 2001). GFP is circularly permutated so that the N- and C-termini are fused, creating a new terminus in the middle of the protein (**Fig. 6.1)**. Fused to the new terminus is calmodulin (CaM) and the M13 domain of a myosin light chain kinase. Calmodulin is a symmetrical, hinge-like protein that binds to four calcium ions via E-F motifs. When calcium is present, CaM undergoes a conformational change, and the hinge region is able to bind helical peptide chains on target proteins, such as M13. In the absence of calcium, the circularly permutated fluorescent proteins exist in a poorly fluorescent state due to a water pathway that enables protonation of the chromophore and poor absorbance at the excitation wavelengths. Ca^{2+} binding to the calmodulin moiety results in a structural shift that eliminates this solvent pathway, rapid de-protonation of the chromophore, and bright fluorescence (Wang 2008, Akerboom 2009).

We have incorporated GCaMP and its closely related red-emitting counterpart, RCaMP, into our functional spinal cord imaging protocols, with the ultimate goal of achieving *in vivo* imaging of real-time neural activity, and correlating patterns of activity with sensory, behavior and gait in awake mice.

Preliminary work has focused on *in vivo* imaging of neural activity in Ca^{+}/calmodulin-dependent protein kinase II (CaMKII) neurons, a genetically-defined set of excitatory neurons present in the dorsal horn and previously found to display

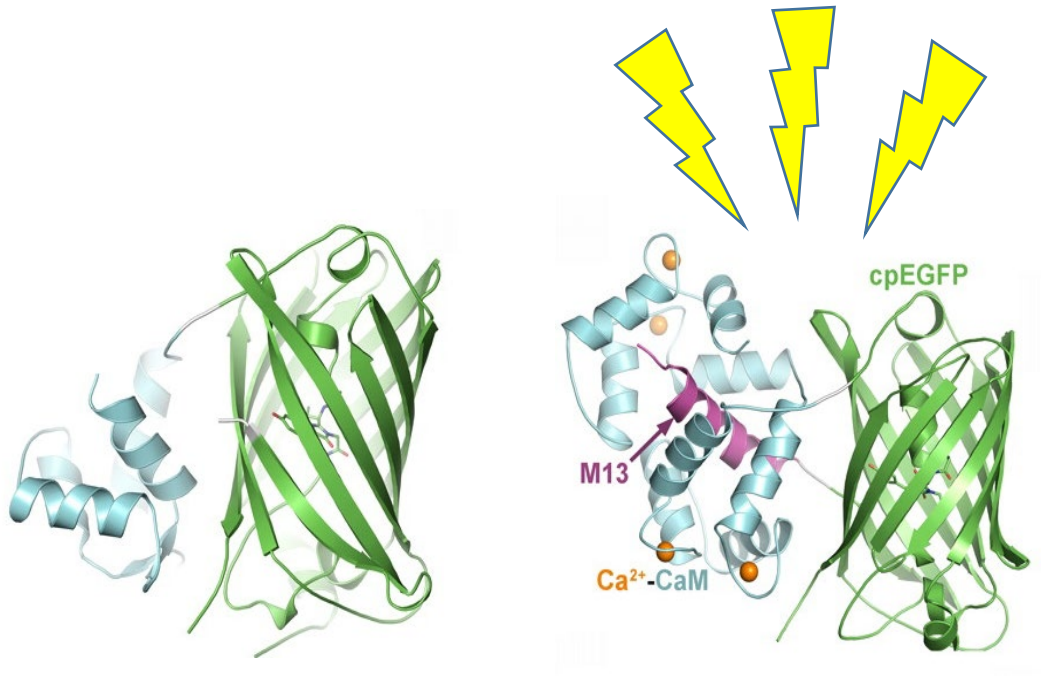

Fig. 6.1 Crystal structure of GCaMP

Left: In the absence of calcium, GCaMP does not absorb excitation light and does not fluoresce

Right: Calcium-binding induces a conformational change enables light absorbance and subsequent fluorescence.

Source: http://www.jbc.org/content/284/10/6455/F1.large.jpg,
Akerboom J, Rivera JDV, Guilbe MMR, etc al. Crystal structures of the GCaMP calcium sensor reveal the mechanism of fluorescence signal change and aid rational design. J Bio Chem 2009: 284(10): 6455-6464.

elevated activity in rodent models of neuropathic pain (Dai 2005). Initial experiments demonstrated the ability to image and record calcium transients in the spinal cord of anesthetized mice. Juvenile transgenic CaMKIItTA-GCaMP6s mice expressing GCaMP in spinal cord excitatory CaMKII neurons, were surgically implanted with imaging chambers and 2PEF imaging was performed in the anesthetized mice directly after surgery. Time-lapse images were obtained during pulses electrical stimulation of the hind paw, and calcium transient tracings were created by graphing change in fluorescence as a function of time ($\Delta F/F$) (**Fig. 6.2**)

Next, calcium imaging was attempted in mouse models of neuropathic pain to explore for alterations in sensory neural activity. Adult transgenic mice expressing GCaMP in spinal cord excitatory CaMKII neurons underwent unilateral SNI, after which they were allowed a period of 5-15 days to recover from surgery and develop signs of neuropathic pain, as assessed by behavior and Von Frey filament test. They were then surgically implanted with imaging chambers in the lumbar spine and 2PEF was performed directly after surgery. Time lapse images were obtained from both the side ipsilateral and contralateral (control) to SNI. Interestingly, calcium transient tracings obtained from spinal cord of mice following SNI revealed abnormal patterns of spontaneous neural firing on the side ipsilateral to SNI. These aberrant discharges are not observed on the side contralateral to SNI (**Fig. 6.3**). These in vivo findings corroborate previously published ex-vivo electrophysiologic studies (West 2015), and represent exciting preliminary findings for further *in vivo* imaging experiments investigating underlying mechanisms of neuropathic pain.

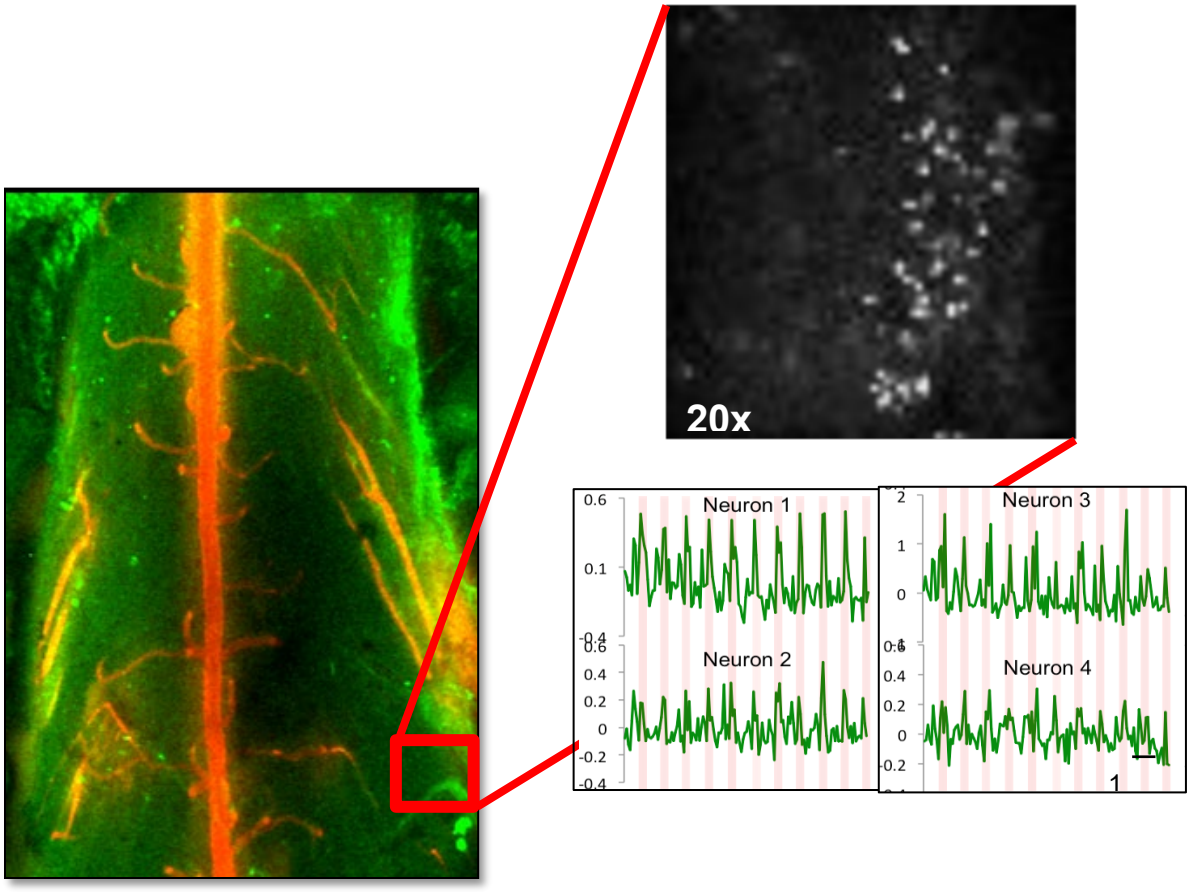

Fig. 6.2 2PEF microscopy of excitatory neural activity

2PEF microscopy of stimulated excitatory neural activity in the spinal cord of an anesthetized CaMKIITA-GCaMP6s mouse (left), GCaMP fluorescence detection from selected region of spinal cord (upper right), and calcium transient tracings (ΔF/F as a function of time) from four individual neurons (lower right).

CaMKII neurons are labeled with GCaMP, vasculature is labeled with Texas Red.

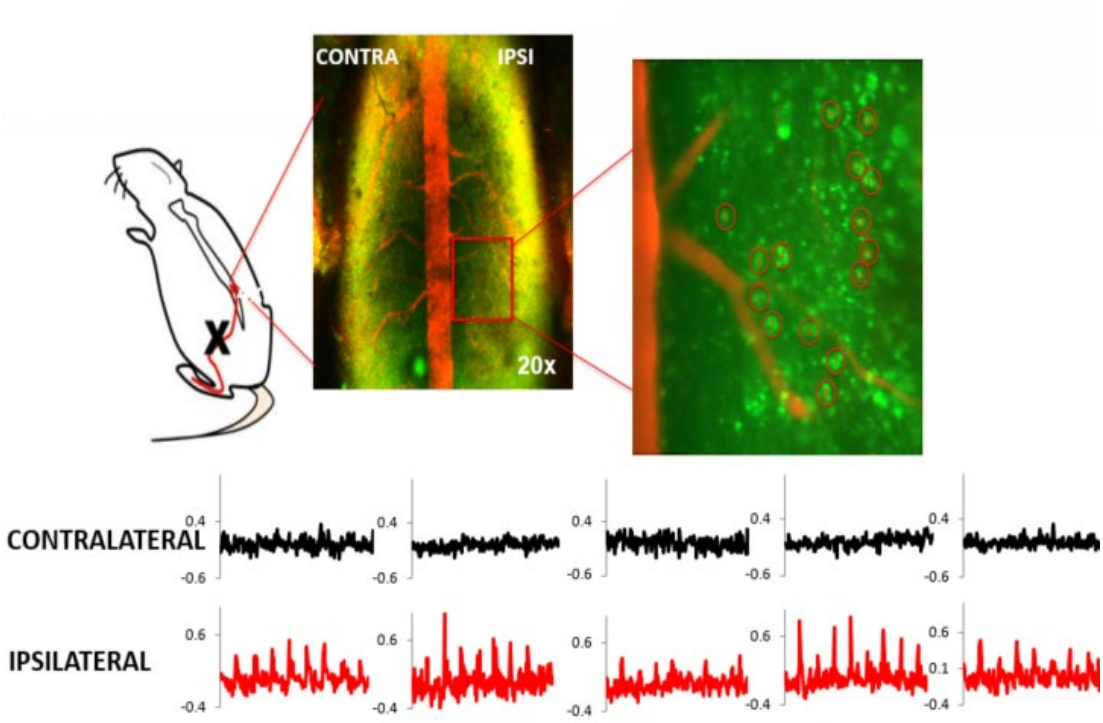

Fig. 6.3 2PEF microscopy reveals altered spinal cord neural activity in a CaMkIITA-GCaMP6s mouse model of neuropathic pain

2PEF microscopy of spontaneous neural activity in a mouse 8 days post SNI demonstrating aberrant spontaneous neural firing patterns on the side ipsilateral to injury. Calcium tracings display ΔF/F as a function of time.

TREADMILL-BASED SYSTEM ENABLES NONLINEAR MICROSCOPY IN AWAKE, LOCOMOTING MICE

In order to fully understand the neural circuits controlling locomotion, one must be able to observe neural firing activity as it occurs in real time and facilitates terminal motor functions such as movement and gait. To achieve this, we have designed a custom wheel-based treadmill on which the mouse stands and runs while spine-fixed under the 2PEF microscope objective (**Fig. 6.4**). The wheel is 25 cm in diameter such that the mouse runs on a relatively flat surface. The wheel was 3D printed from lightweight plastic so the weight of the wheel is similar to that of the mouse. The wheel is mounted on a horizontal rod using roller bearings. By tuning the friction at this junction, the force required to rotate the wheel approximately matches that which the mouse exerts when moving forward, thereby mimicking natural movement forces felt by the mouse. Because the mouse's back moves up and down several millimeters during each stride, we have suspended the horizontal rod on springs with a stiffness chosen so the entire wheel will move down a few millimeters under the force the mouse exerts with each step, about 50% of body weight (Fowler 2009). To prevent the wheel from swinging on the springs, linear bearings restrict drum motion to one axis.

To optimize running performance, mice undergo treadmill acclimation training prior to chamber implantation (see training protocol below). To encourage forward movement and discourage the animal from turning, a small tunnel-like enclosure is placed directly in front of and around the mouse. On either side of the wheel are brackets to hold the spinal cord chamber fixed under the microscope. These brackets are

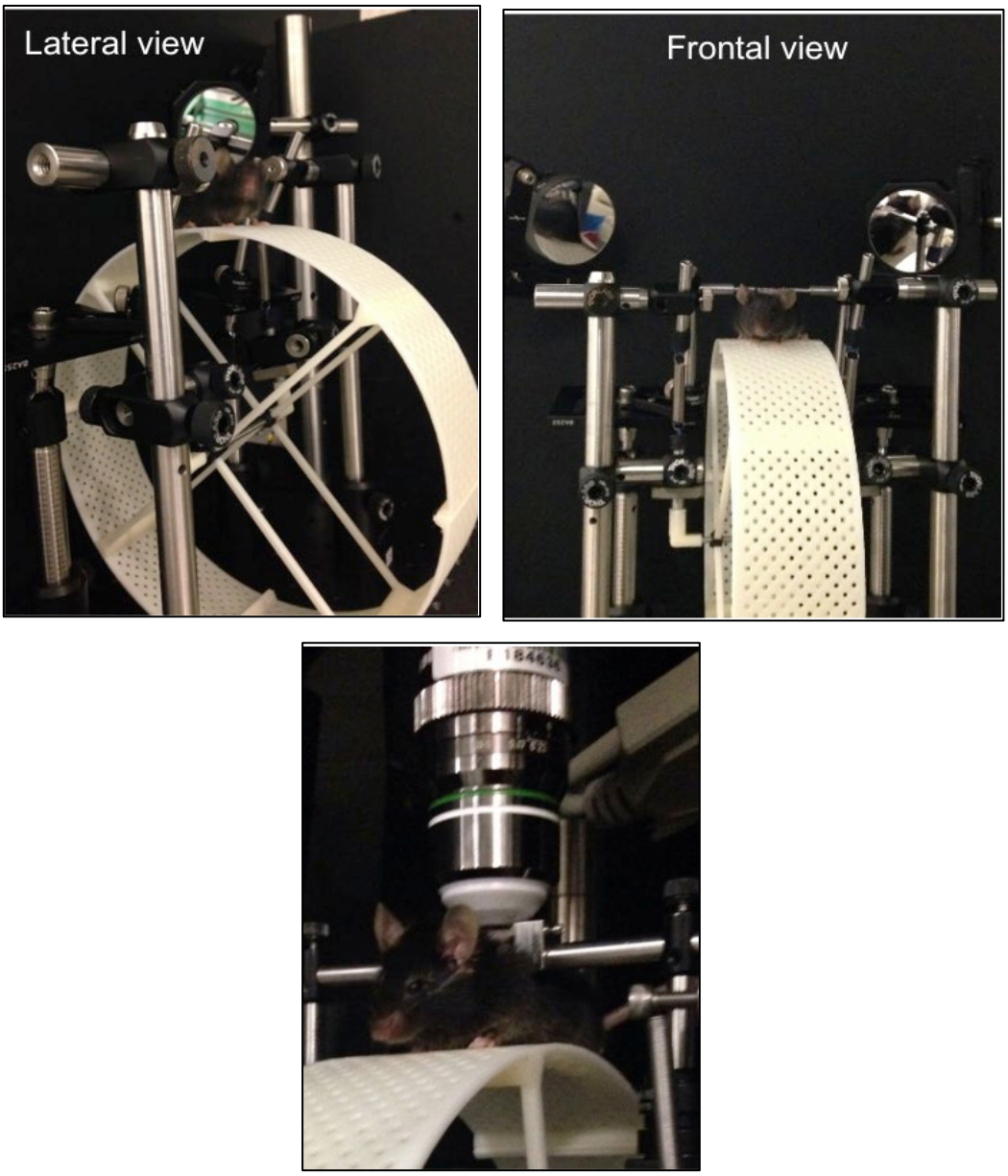

Fig. 6.4 Treadmill system for awake 2PEF imaging

Wheel-based treadmill for in-vivo imaging of awake, running mice (top left). Spine-fixed mouse atop spring-suspended treadmill (top, right). Awake mouse fixed under microscope (bottom).

adjustable up/down, forward/backward, and rotatable along the pitch axis to allow us to tune the configuration for each mouse's size, implant location on the spine, and apparent preferences. The brackets have been machined to articulate perfectly with the chamber to facilitate rapid attachment/detachment of awake mice.

We aim to achieve gait parameters for spine-fixed animals that closely match animals freely moving on the treadmill (previous work showed that treadmill gaits are similar to open field gaits, although mice tend to take smaller strides on a treadmill (Herbin 2015). To achieve this, we have observed gait patterns of several mice when running on the treadmill with and without spine fixation (we lightly hold the mouse's tail when not spine fixed to keep them on the treadmill). We then empirically adjusted the position and angle of the brackets holding the spinal cord chamber, the mass of the wheel, the friction at the roller bearing, and the stiffness of the springs to try to match the spine-fixed and freely-moving gaits.

Mouse Training for Awake Imaging

Mice are acclimated and trained on the treadmill with the goal of imaging awake, behaving animals demonstrating as natural gait and movement as possible. Animals are ultimately spine-fixed under the microscope while able to run freely on the rotating the wheel beneath them. To habituate animals to this imaging approach and ensure that they are in a calm, pain and distress-free state during imaging, we acclimate them with a staged training procedure. First animals that have received chronic spinal imaging implants are acclimated to handling until they comfortably move from hand to hand and

are accustomed to researcher handling (~15 minutes a day for ~2 days). Animals are then placed on the rotating wheel and allowed to learn to run comfortably while being manually held in place by gentle tail tension and/or forceps on their imaging chamber (~15 minutes a day for 3-4 days). This allows the mouse to become comfortable running on the wheel without the physical constraint of being spine-fixed. They then have several sessions of running on the wheel with the spinal cord implant bolted into a support until they calmly switch between moving and stationary states (~20 minutes a day for 3-4 days, then increasing duration to 1 hour over a week) (**Fig. 6.5**). Finally animals are placed in the spine-fixed support atop the treadmill under the 2PEF microscope for imaging.

By the end of training, we observed normal curiosity and grooming behaviors while the mouse is atop the treadmill. Spine-fixed running activity was measured (n=3 mice) in terms of average running speed (0.36 m/s) and fraction of time spent running in a 10 min session (21%) (**Fig. 6.6**). These values are comparable to those for free-running mice (0.43 m/s and 18%). Further, we 2PEF imaged the spinal cord in awake, running mice, and motion artifact was estimated by tracking features in an image stack over time using a cross-correlation approach. During a 100-s running bout, we found that both lateral and axial motion artifacts were about 3 μm, which is comparable to published awake brain imaging results (Dombeck 2007) (**Fig. 6.7**).

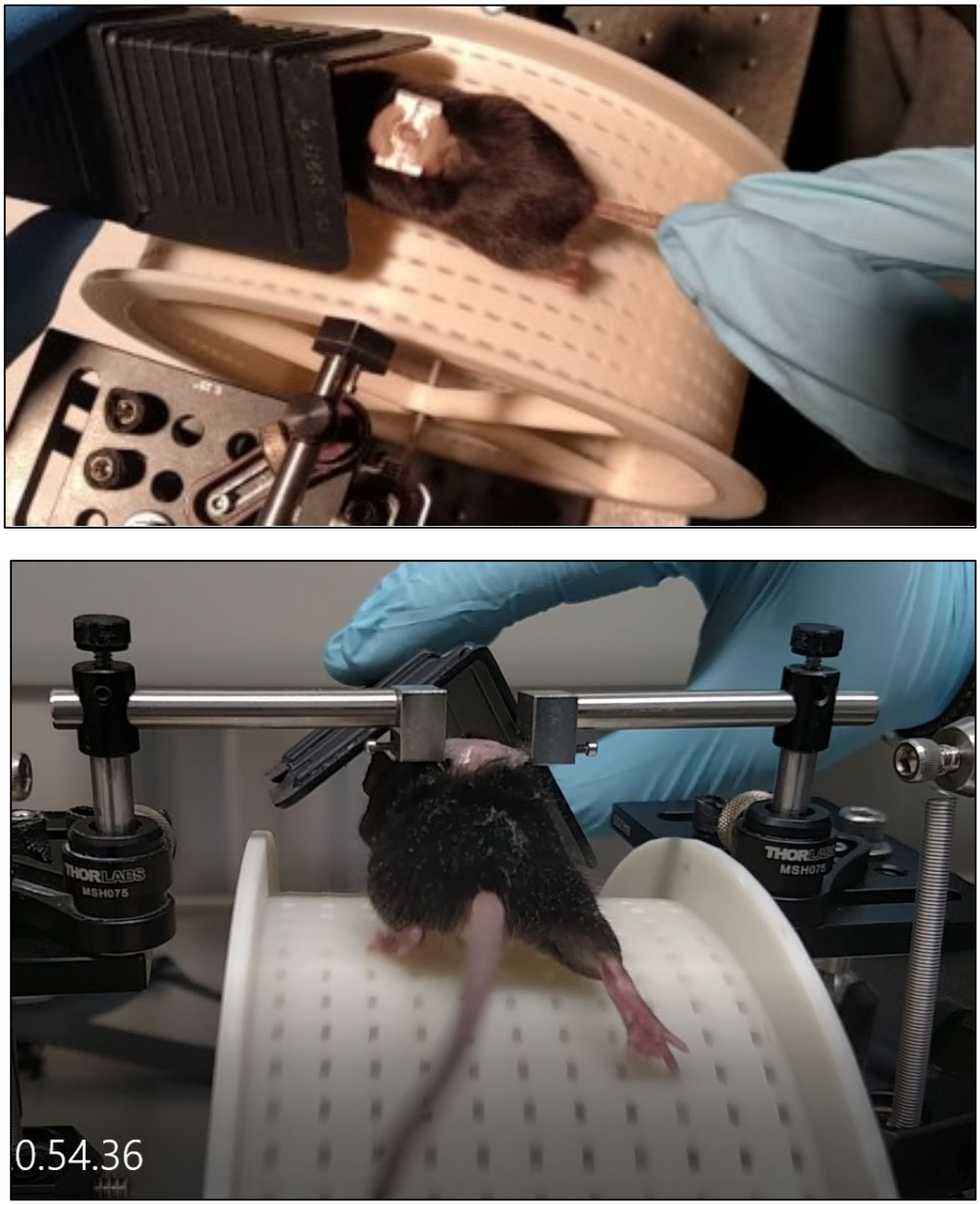

Fig. 6.5 Mouse treadmill training

Treadmill training process includes acclimation to running atop the treadmill with gentle tail traction (above) with eventual graduation to spine-fixation (below).

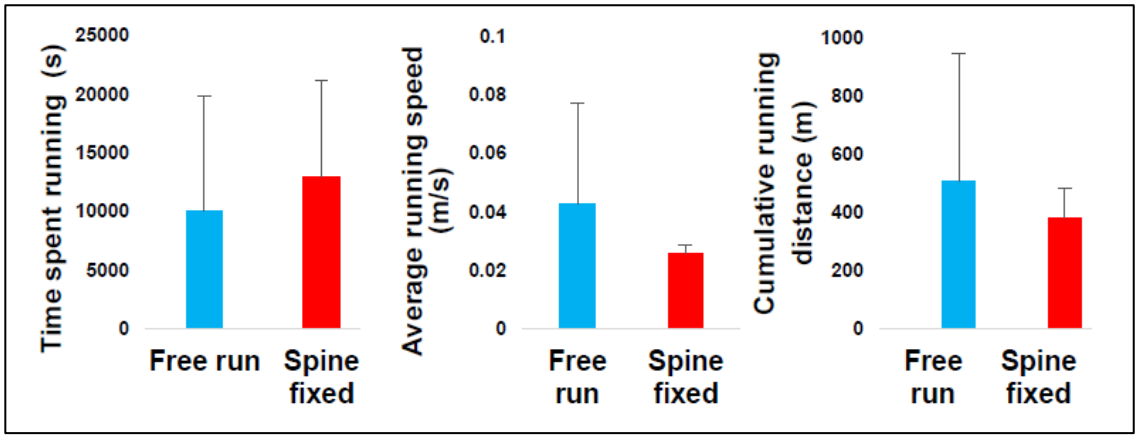

Fig. 6.6 Behavioral parameters in spine-fixed mice

Comparison of time spent running, average running speed, and cumulative running distance in freely running mice compared to spine-fixed mice. Median values with standard error bars provided.

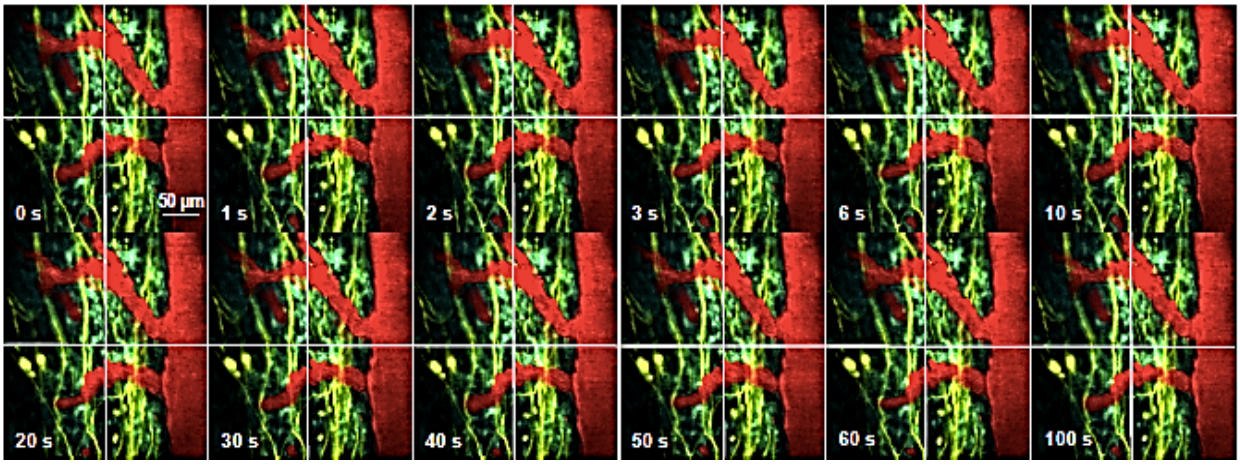

Fig. 6.7 Minimal motion artifact is observed in running mice during 2PEF imaging

Time-lapsed 2PEF images taken over 100 seconds from awake, spine-fixed, running mouse demonstrating minimal motion artifact.

Neurons (yellow), microglia (green), and vasculature (red).

Gait Analysis System

In addition to our custom treadmill, we have designed and built a recording system for capturing video of spine-fixed mice under infrared illumination at 200 fps with four synchronized, 1280 x 1024 8-bit cameras placed in 45° degree angled pairs on either side of the mouse (**Fig. 6.8**). Infrared illuminators allow the mouse to run in visual darkness and doesn't introduce confounding light into the microscope detection optics. Simultaneous imaging from multiple angles will enable acquisition of 3D spatiotemporal position data for regions of interest on the mouse's limbs and body while walking or running on the treadmill.

Efforts are ongoing to design and implement a non-invasive limb tracking and gait analysis system using machine learning algorithms to automatically detect and track the position of paws, limbs, nose, and tail in 3D with high temporal resolution. Support vector machine classifiers will be implemented and trained in order to automate limb tracking, providing detailed kinematic data on limb motion (Machado 2015). By tracking wheel rotation speed, velocity-dependent effects on gait parameters will also be investigated (Neckel 2015). Ultimately, this system will enable comprehensive limb kinematic analysis while visualizing neuronal activity patterns in the spinal cord.

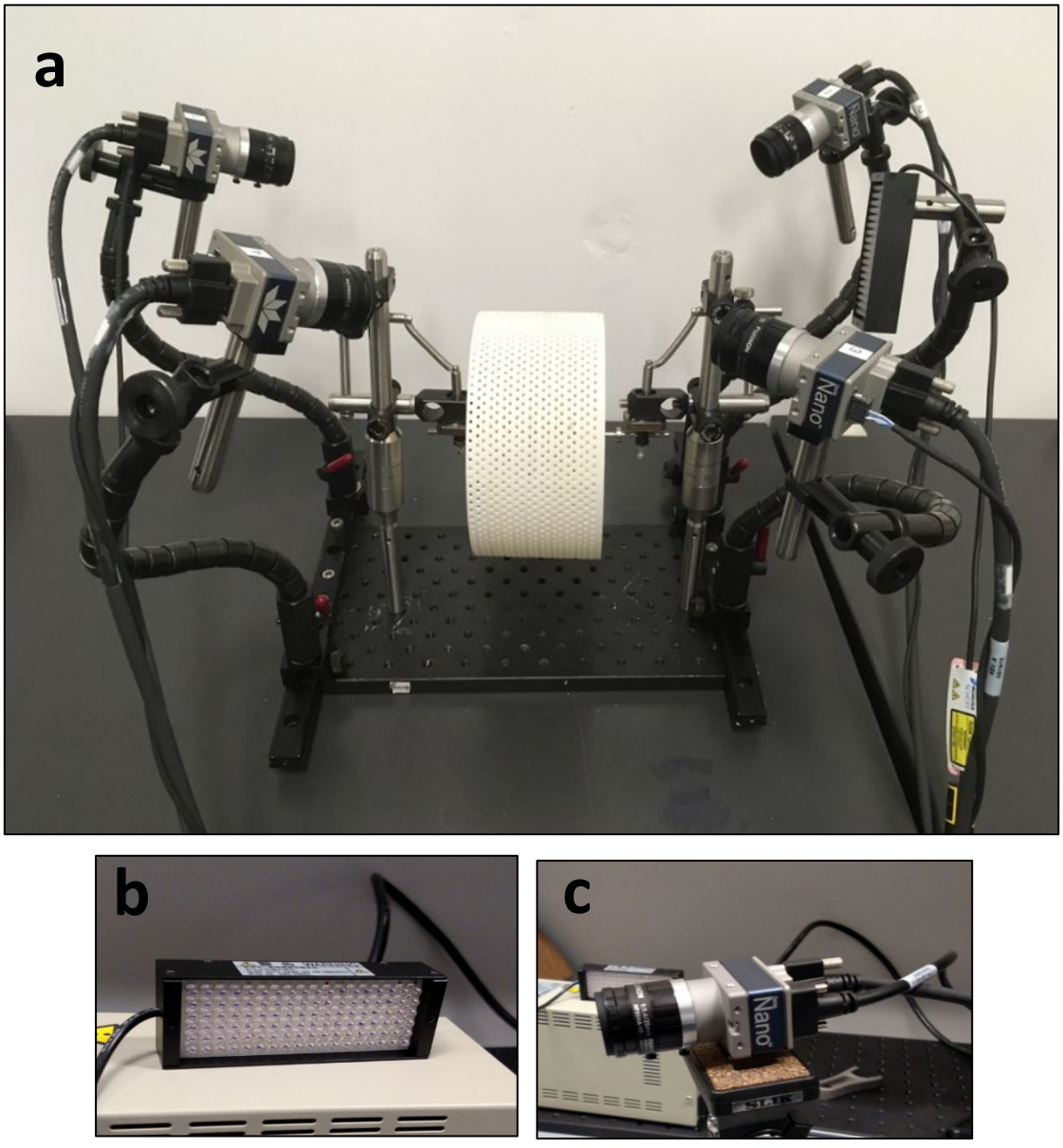

Fig. 6.8 Gait analysis system

(a) Recording system for capturing video of spine-fixed mice during 2PEF imaging. (b) infrared (IR) illuminators and (c) four, synchronizable, 1280 x 1024 8-bit IR cameras capable of 200 fps recording

REFERENCES

- Akerboom J, Rivera JD, Guilbe MM, Malavé EC, Hernandez HH, Tian L, Hires SA, Marvin JS, Looger LL, Schreiter ER. The Journal of Biological Chemistry (2009) 284: 6455–64.
- Broussard, G. J., Liang, R. & Tian, L. Monitoring activity in neural circuits with genetically encoded indicators. Front Mol Neurosci 7, 97, doi:10.3389/fnmol.2014.00097 (2014).
- Crone S, Quinlan K, Zagoraiou L, Droho S, Restrepo C. Genetic ablation of V2a ipsilateral interneurons disrupts left-right locomotor coordination in mammalian spinal cord. Neuron (2008) 60, 70-83, doi:S0896-6273(08)00677-6 [pii]10.1016/j.neuron.2008.08.009 (2008).
- Dai Y, Ogawa A, Yamanaka H, Obata K, Tokunaga A, Noguchi. Ca2+/calmodulin-dependent protein kinase II in the spinal cord contributes to neuropathic pain in a rat model of mononeuropathy. European Journal of Neuroscience (2005) 21:2467-2474)
- Dombeck, D. A., Khabbaz, A. N., Collman, F., Adelman, T. L. & Tank, D. W. Imaging large-scale neural activity with cellular resolution in awake, mobile mice. Neuron 56, 43-57, doi:10.1016/j.neuron.2007.08.003 (2007).
- Fowler, S. C., Miller, B. R., Gaither, T. W., Johnson, M. A. & Rebec, G. V. Force-plate quantification of progressive behavioral deficits in the R6/2 mouse model of

Huntington's disease. Behav Brain Res 202, 130-137, doi:10.1016/j.bbr.2009.03.022 (2009).

- Gangadharan V, Kuner R. Unravelling spinal circuits of pain and mechanical allodynia. Neuron (2015) 87:673-676.
- Herbin, M., Hackert, R., Gasc, J. P. & Renous, S. Gait parameters of treadmill versus overground locomotion in mouse. Behav Brain Res 181, 173-179, doi:10.1016/j.bbr.2007.04.001 (2007).
- Kiehn O. Decoding the organization of spinal circuits that control locomotion. Nat Rev Neurosci (2016) 17:224-238.
- Machado, A. S., Darmohray, D. M., Fayad, J., Marques, H. G. & Carey, M. R. A quantitative framework for whole-body coordination reveals specific deficits in freely walking ataxic mice. Elife 4, doi:10.7554/eLife.07892 (2015).
- Nakai, J., Ohkura, M. & Imoto, K. A high signal-to-noise Ca(2+) probe composed of a single green fluorescent protein. Nat Biotechnol 19, 137-141, doi:10.1038/84397 (2001).
- Neckel, N. D. Methods to quantify the velocity dependence of common gait measurements from automated rodent gait analysis devices. J Neurosci Methods 253, 244-253, doi:10.1016/j.jneumeth.2015.06.017 (2015).
- Wang Q, Shui B, Kotlikoff MI, Sondermann H. Structural basis for calcium sensing by GCaMP2. Structure (2008)16: 1817-27.

- West S, Bannister K, Dickenson A, Bennett D. Circuitry and plasticity of the dorsal horn – toward a better understanding of neuropathic pain. Neuroscience (2015)300:254-75.

CHAPTER 7

THE FUTURE OF MULTIPHOTON IN VIVO IMAGING

Spinal cord research is an area in great need of improved imaging techniques for capturing and interrogating the complex cellular mechanisms underlying spinal cord physiology in health and disease. We have worked to meet that need through the development of a suite of contemporary, cutting-edge optical tools capable of creating a virtual looking glass into the living, functioning spinal cord. These tools not only enable *in vivo* imaging studies of spinal cord disorders never before possible, but also will serve as a foundation for further innovation and technological advancement for years to come.

To date, we have:

- Developed surgical procedures that allow long term optical access in multiple regions of the rodent spinal cord
- Optimized labeling strategies for multicolor fluorescent *in vivo* imaging of cellular interactions
- Demonstrated successful recording of real-time calcium transients and neural activity from populations of sensory and motor neurons in the rodent spinal cord
- Explored and refined established models of SCI and neuropathic pain to make them suitable for serial imaging of axonal dynamics, inflammatory responses, and alterations in neural circuitry
- Designed and custom built a treadmill system on which a mouse can walk and run while spine-fixed under a multiphoton microscope

- Implemented a recording system for capturing video of spine-fixed, running mice from which 3D spatiotemporal positioning of limbs can be measured and ultimately integrated into a comprehensive kinematic gait analysis system

LIMITATIONS TO TWO-PHOTON EXCITED FLUORESCENCE MICROSCOPY IN THE SPINAL CORD

Throughout the projects described in this dissertation, unforeseen biologic and technologic hurdles dictated constant methodological revision and technical optimization. These challenges impacted the feasibility and outcomes of ongoing projects and drove constant technological revision toward better, higher resolution imaging solutions.

A constant challenge to our 2PEF studies was difficulty maintaining optically clear windows in our spinal chamber-implanted mice. The introduction of any blood or injury within the spinal cord brought with it a myriad of blood-derived cells and/or inflammatory mediators, all of which collectively resulted in rapid deposition of fibrin and ultimately fibrous scarring. Coupled with the already dense and highly optically scattering white matter of the spinal cord, any degree of additional reactive tissue between the spinal cord and imaging window completely impeded excitation light from reaching the desired regions of spinal cord unscattered. This manifested optically as poorly resolved images with low signal and high noise components, making observation of cellular dynamics difficult or impossible (**Fig. 7.1**).

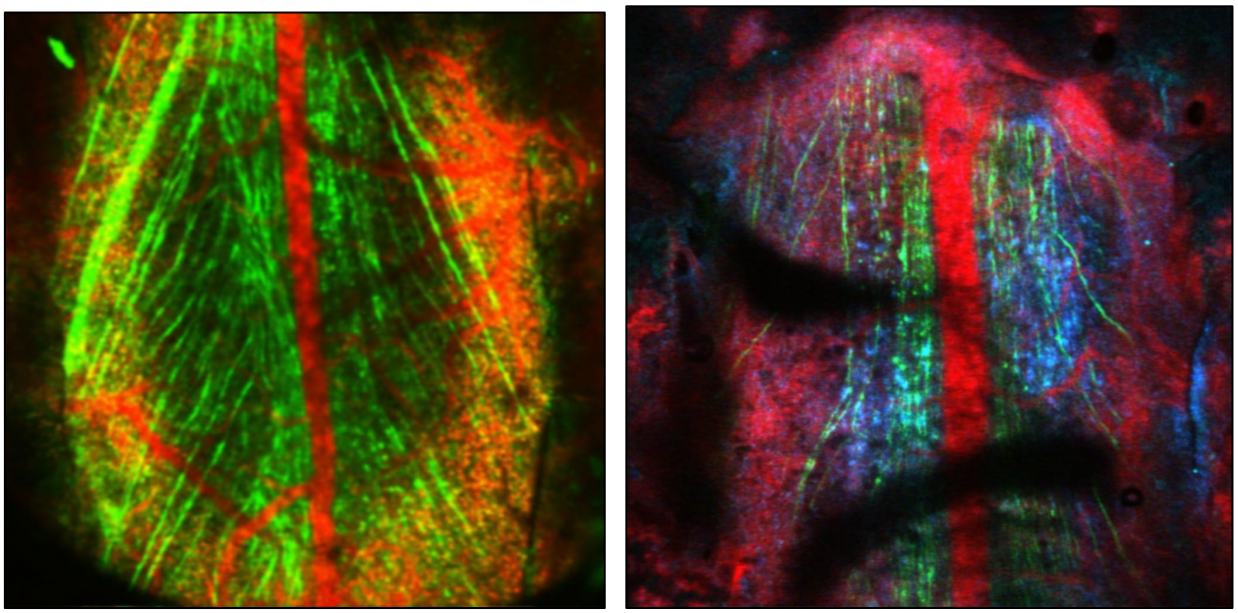

Fig 7.1 Optical impedance in chronically implanted mice spinal cords

2PEF microscopy image from the lumbar spinal cord of different mice obtained 8 and 10 days post imaging chamber implantation.

YFP axons (green), GFP microglia (blue), Texas Red vasculature (red).
4x magnification

Another challenge we repeatedly faced was acute inflammation stemming from chamber implantation surgery. This inflammatory response, although relatively mild with good surgical technique, resulted in microglial influx throughout the imaging window and confounded our ability to quantify the microglial response to SNI in our studies of neuropathic pain (**Fig. 7.2**). This inflammatory response would be expected to subside within weeks of surgery, however, subsequent fibrinous tissue deposition prevented imaging studies past approximately a week after surgery in this particular injury model. We have been working on new surgical techniques that involve using a diamond burr to create a thinned area of bone in the dorsal lamina of the vertebrae instead of performing the traditional dorsal laminectomy procedure. While 2PEF microscopy has not been successful in penetrating the thin layer of bone and optically accessing the underlying spinal cord, newer higher order nonlinear methods such as 3PEF hold much promise for success. This thinned-bone prep would have the added benefit of leaving the spinal cord meninges and BBB intact and unperturbed, thereby minimizing any confounding inflammatory response.

Multiphoton microscopy is a rapidly evolving field, and the recent introduction of higher order non-linear imaging modalities hold great potential to overcome these challenges through their ability to image deeper into tissues with higher resolution for longer periods of time than ever possible with 2PEF.

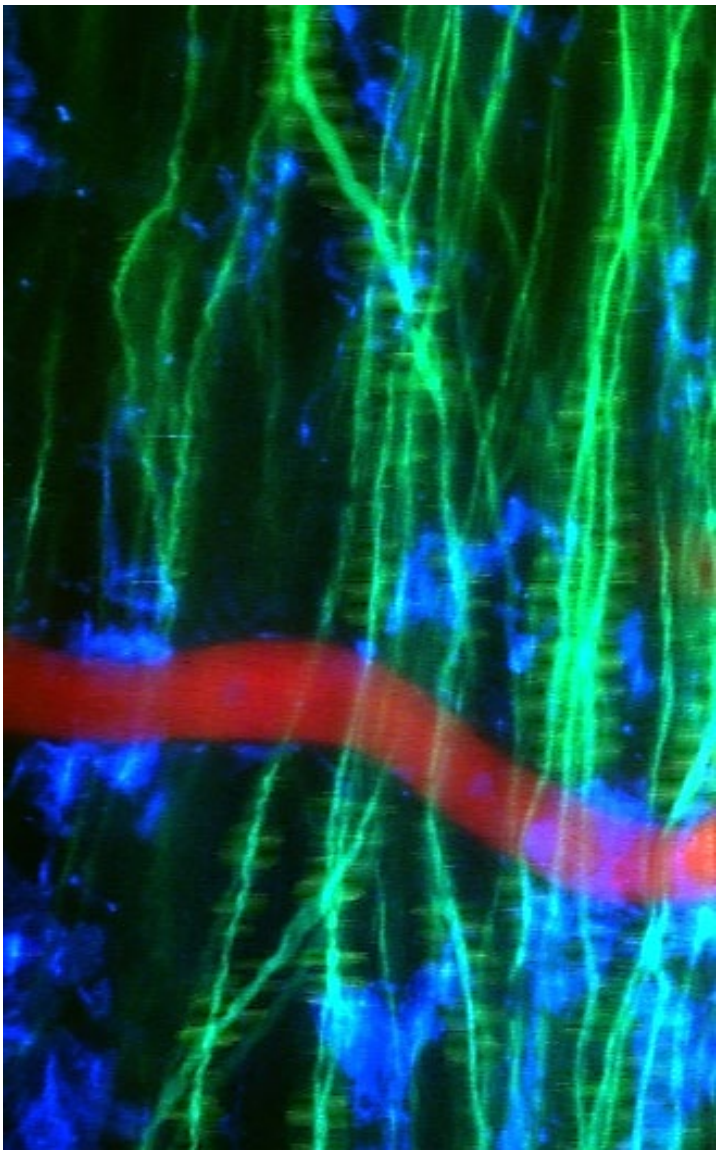

Fig 7.2 Generalized microglial-mediated inflammation following spinal imaging chamber implantation

2PEF microscopy image from the lumbar spinal cord of a mouse obtained 2 days after imaging chamber implantation.

YFP axons (green), GFP microglia (blue), Texas Red vasculature (red).
20x magnification

INTO THE FUTURE: THREE-PHOTON EXCITED FLUORESCENCE MICROSCOPY FOR DEEPER, HIGHER RESOLUTION *IN VIVO* IMAGING OF THE SPINAL CORD

Nonlinear microscopy has become the technique of choice for imaging with sub-cellular resolution deep into scattering tissue in live animals. For any nonlinear optical process, only laser photons that reach the focus unscattered can contribute to the nonlinear effect, so scattered excitation light does not degrade resolution or contrast. In turn, because the signal generation is limited to the laser focus, any signal photons that are detected can be used to reconstruct the image, regardless of their (scattered) path through the sample.

These properties together give nonlinear microscopies a remarkable insensitivity to optical scattering. For deep nonlinear imaging, however, the laser power must be increased exponentially with depth to maintain the signal strength. At the maximal 2PEF imaging depth, the laser intensity at the sample surface approaches the intensity of the unscattered light reaching the focus. In this case, 2PEF is generated from a large volume of out-of-focus structures near the sample surface, producing a background that hides the 2PEF signal from the laser focus. This signal to background limit fundamentally prevents 2PEF imaging at depths of more than about 5 times the attenuation length (depends on absorption and scattering lengths) for the excitation light. In the spinal cord, where the dense, highly-scattering white matter lies superficially on the dorsal surface, this translates into difficulty imaging more than ~150 μm deep. Inflammatory reactions between the spinal cord and imaging window worsen scattering and further prevent successful imaging. Optical impedance through highly-scattering white matter can be

overcome by using longer wavelength light and higher order nonlinear excitation of fluorescent labels.

Three-photon excited fluorescence (3PEF), a nonlinear microscopy method in which three photon are used to simultaneously excite a fluorophore, has been developed by a Cornell collaborator and has shown increased depth penetration in *in vivo* imaging studies of the mouse brain (Horton 2013). Three photon excitation achieves deeper imaging depths due to two effects. First, the longer wavelength excitation light used (1.3 and 1.7 μm for green and red emitting fluorescent species, respectively) is more weakly scattered than the excitation typically used for 2PEF imaging, enabling deeper penetration. Note that it is critical to avoid the strong optical absorption of water at wavelengths between 1.3 and 1.7 μm. Second, the use of a higher order nonlinear excitation process further suppresses the out-of-focal-plane excitation to strongly reduce the fluorescence excitation near the sample surface that ultimately limits 2PEF imaging depths. Already, in vivo 3PEF imaging of neural activity in the brain using GCaMP has been demonstrated (Ouzounov 2017). Recently, we have conducted experiments using a home-built three-photon excited fluorescence (3PEF) microscope to explore the limits of 3PEF imaging of cell structure and neural calcium transients in the spinal cord.

The transition to 3PEM has enabled us to image over longer periods of time after chamber implantation regardless of reactive tissue deposition between the spinal cord and window, thereby addressing many of the technological challenges we've faced in our 2PEF studies. The improved depth capabilities of 3PEF represent another major improvement over 2PEF. In an experiment directly comparing achievable depths in

the same samples using 2PEF and 3PEF, 3PEF successfully imaged spinal cord vasculature with high resolution at depths of nearly 600 um (deep enough to reach motor neuron populations within the gray matter), while 2PEF imaging in the same location only achieved imaging down to 125 um (**Fig. 7.3**). Using 1300 nm light we have successfully three-photon excited green-emitting fluorescent molecules such as GFP and FITC, and similarly, with 1700 nm light we have efficiently pumped red fluorescent species such as RFP and Texas Red (**Fig. 7.4**). Additionally, using transgenic animals and AAV vectors, we have induced neural expression of fluorescent genetically encoded calcium indicators (GCaMP and RCamp) to enable long-term, high signal-to-noise, fluorescence based imaging of real-time spinal cord neural activity.

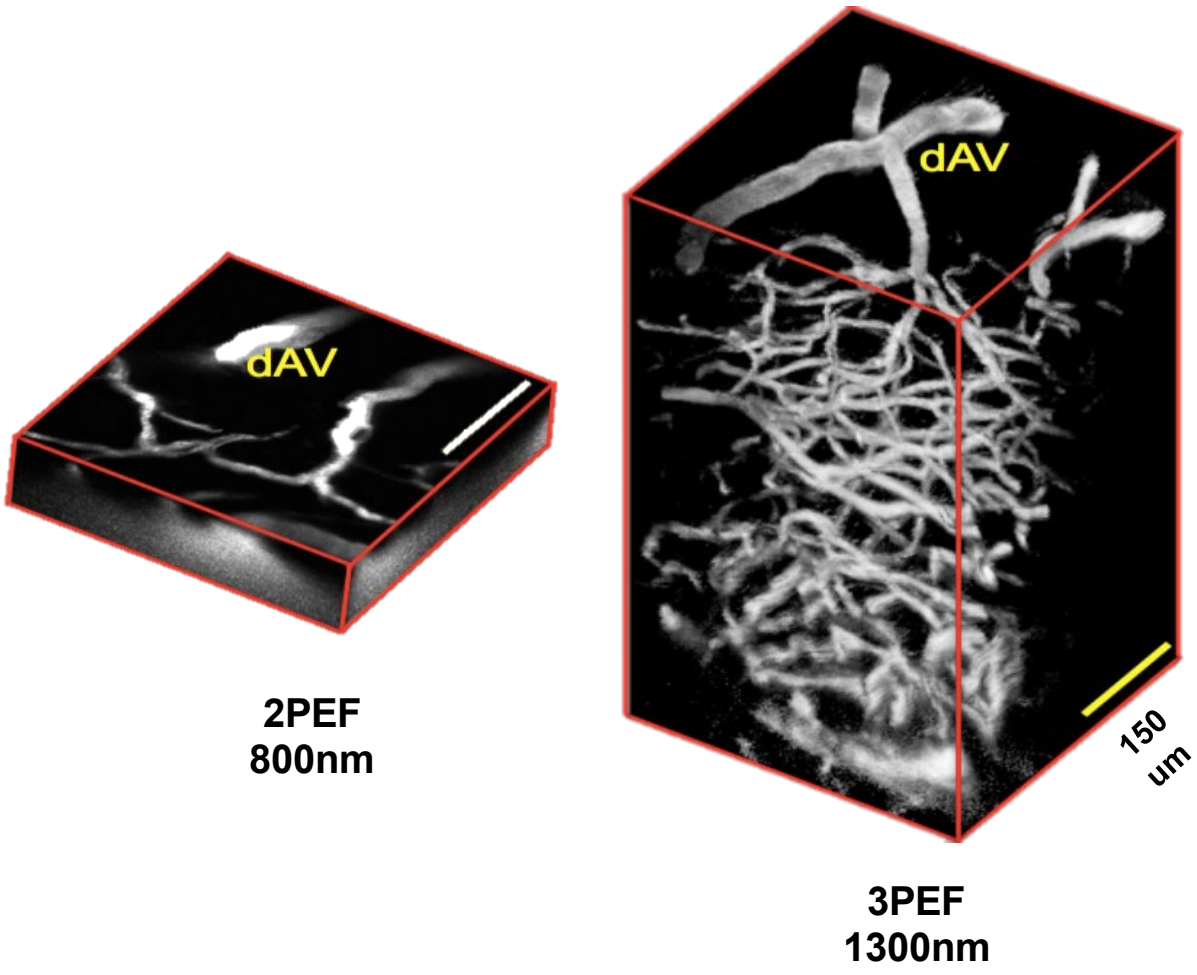

Fig. 7.3 3PEF microscopy enables deeper imaging of the spinal cord

3D reconstructions comparing achievable imaging depths in the same tissue using 2PEF versus 3PEF. 3PEF is able to image to approximate depths of 600 um, which 2PEF only achieves 125 um.

dAV = dorsal ascending venule

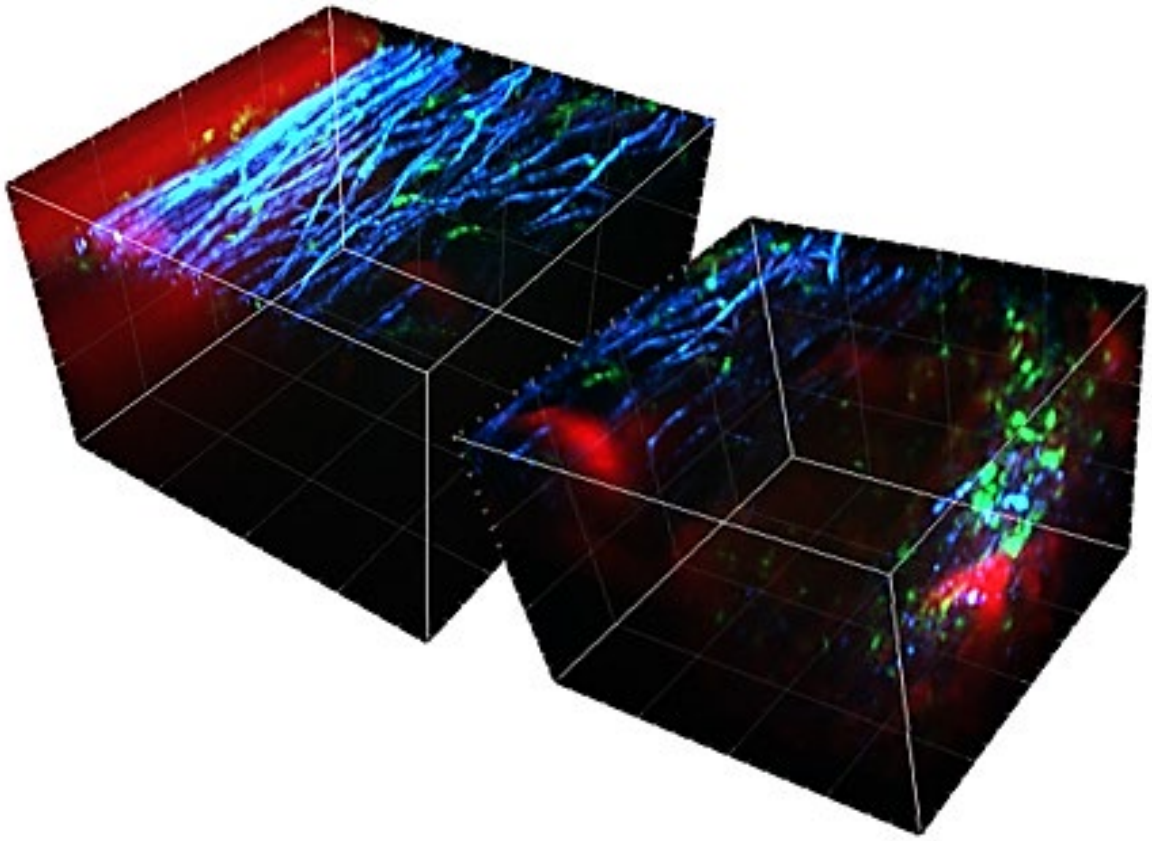

Fig. 7.4 3PEF microscopy enables deeper imaging of the spinal cord

3D reconstructed image stacks demonstrating deep structural imaging using 3PEF in the spinal cord.

YFP axons (blue), GFP microglia (green), FITC vasculature (red).
4x magnification

3PEF Enables Imaging of Neural Activity Deep in the Spinal Cord of Awake Mice

Recent function imaging experiments are exploring CPG circuit activity through the investigation of V2a class of Chx10-expressing neurons, a genetically-defined set of CPG interneurons known to play an important role in locomotor behavior (Crone 2008). Chx10 neurons can be fluorescently labeled by crossing a mouse expressing Cre recombinase under the Chx10 promotor to a mouse with a floxed-stop RCaMP GECI, leading to sustained expression of the calcium indicator in Chx10 cells. The biggest challenge to the work thus far has been difficulty imaging deep enough to see the neurons involved in the coordination of movement, which are located in the central to ventral spinal cord gray matter. Thus far 2PEF has not been successful at reaching these depths, however, using 3PEF we have successfully imaged RCaMP-labeled neurons and their calcium transients up to 0.5 mm beneath the dorsal surface of the spinal cord (**Fig. 7.5**). This is just enough depth to access to the Chx10 cells, which form one of the most superficial of the motor related interneuron classes. The ultimate goal of this work is to determine which Chx10 neurons are activated during different phases of the locomotor cycle and how their patterns of activity change as the animal performs tasks and travels at different speeds.

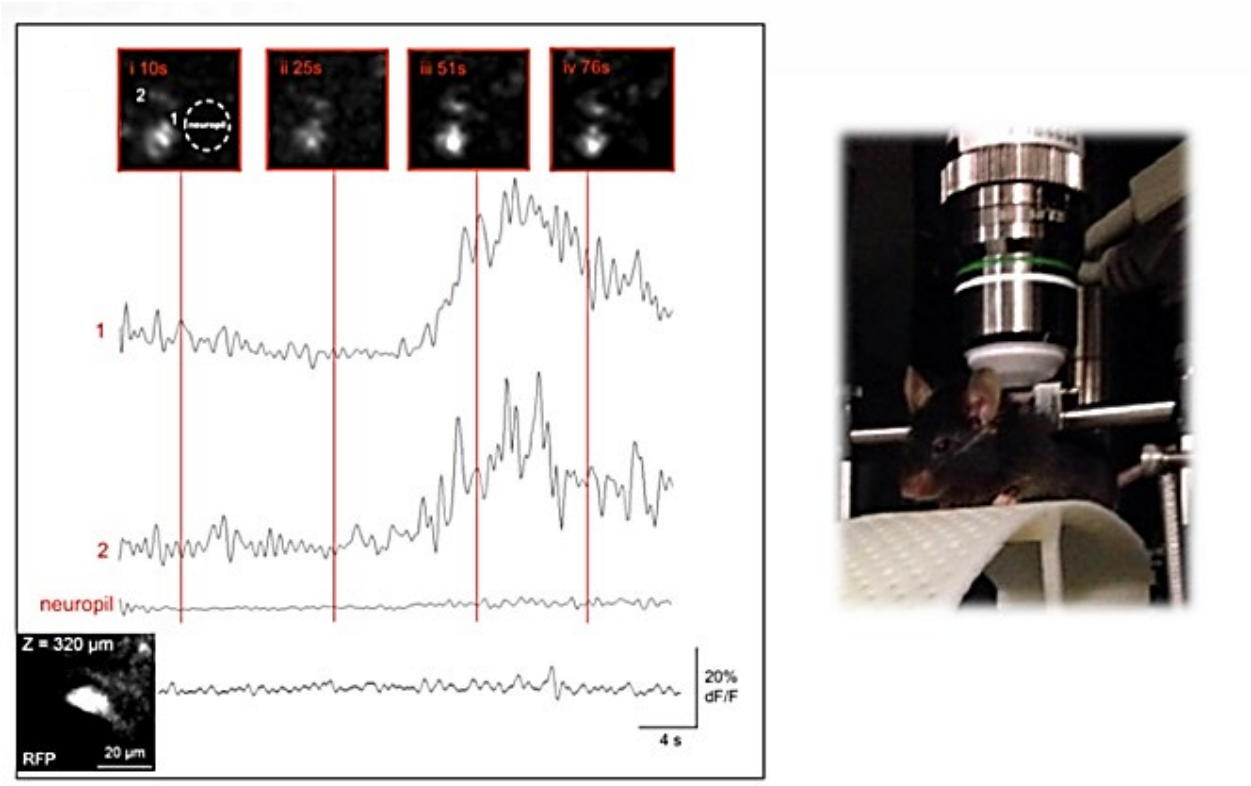

Fig. 7.5 3PEF RCaMP calcium transients in an awake, locomoting mouse

Calcium transients from spinal cord neurons expressing RCaMP in an awake, locomoting mouse. Such transients were not observed in neuropil or red fluorescent protein (RFP) transfected neurons (bottom trace).

The overarching goals to explore cellular responses occurring in the spinal cord in models of injury and disorder and correlate neural firing patterns in the spinal cord with gross motor and sensory function will continue to be investigated as 3PEF imaging brings with it a new level of imaging possibilities. These scientific initiatives, along with several new areas of imaging research, will be explored under the auspices of the new NSF-funded NueuroNex initiative at Cornell. These include studies exploring spinal cord blood flow dynamics, neural activity in the ventral horn, and central pattern generator functions, all of which will be supported by a brand new multiphoton imaging hub and multifaceted faculty collaborative efforts. Together, this new chapter in multiphoton imaging will continue to drive in vivo imaging technology forward, opening the door for future studies investigating all aspects of the spinal cord in health and disease.

REFERENCES

- Horton N, Wang K, Kobat D, Clark C, Wise F, Schaffer C, Xu C. In vivo three-photon microscopy of subcortical structures within an intact mouse brain. Nature Photonics (2013) 7:205-209.
- Ouzounov D, Wang T, Wang M, Feng D, Horton N, Cruz-Hernandez J, Cheng Y, Reimer J, Tolias A, Nishimura N, Xu C. In vivo three-photon imaging of activity of GCaMP6-labeled neurons deep in intact mouse brain. Nature Methods (2017) 14:388-390.